



MINISTRY OF DEFENCE (PROCUREMENT EXECUTIVE)

AERONAUTICAL RESEARCH COUNCIL

CURRENT PAPERS

The Design of High Sensitivity Pressure Transducers  
for Use in Shock-Tunnels

By

*R. O. Goodchild*

and

*L. Bernstein*

*Queen Mary College*

*London.*

LONDON: HER MAJESTY'S STATIONERY OFFICE

1972

£1.35 net



3 8006 10039 3183

CP No. 1219\*

September 1969

The Design of High Sensitivity Pressure Transducers  
for Use in Shock-Tunnels

by

R. O. Goodchild  
and  
L. Bernstein

Queen Mary College  
London.

SUMMARY

The theory of piezoelectricity in so far as it relates to pressure sensing elements is briefly outlined and various configurations are compared. The relative merits of charge and voltage amplifiers are discussed and a practical charge amplifier and charge calibrator are described. Both acoustic and electronic filters are considered and the extent to which a filter affects the useful rise-time of a transducer is emphasised. Several prototype transducers using sensing elements in compression, shear or bending were built and calibrated. A sensitivity of 48.9 pC/torr was achieved using a PZT bimorph disc in bending, this transducer having a natural frequency of 19 kHz. Environmental tests in a shock tube and in the hypersonic nozzle of a shock tunnel are also described.

Some brief comparisons with commercial transducers are made.

---

\* Replaces A.R.C.31 767



## List of Contents

	<u>Page</u>
1. Introduction	1
2. Piezoelectric sensing elements	3
2.1. Some theoretical considerations	3
2.2. Comparison between the various modes	9
3. Electronic amplifying systems	10
3.1. Charge and voltage amplifiers	11
3.2. Elementary charge amplifier design	13
3.3. Calibration of the charge amplifier	14
4. Filters	15
5. Calibration of pressure transducers	17
6. General design features of transducers	18
6.1. Sensitivity	19
6.2. Natural frequency	19
6.3. Acceleration response	21
6.3.1. Transducer mounting	22
6.4. Cross-axis sensitivity	22
6.5. Thermal response	23
6.6. Linearity and repeatability	23
6.7. General mechanical features	24
7. Prototype transducers	24
7.1. Normal compressive mode transducers	25
7.1.1. The type E compression transducer	25
7.1.2. The type F compression transducer	26
7.1.3. The type I compression transducer	27
7.2. Shear element transducers	28
7.2.1. The type G shear-tube transducer	28
7.3. Bimorph disc transducers	29
7.3.1. The type H bimorph-disc transducer	29
7.4. Bimorph beam transducers	30
7.4.1. The type K bimorph-beam transducer	31
7.5. Environmental testing	32



## 1. Introduction

The hypersonic shock-tunnel at Queen Mary College is designed to operate in the reflected shock mode using cold hydrogen to drive shocks in nitrogen. By current standards the tunnel is a relatively low pressure device, the maximum driver pressure being of order 100 atmospheres. The gases are taken from banks of commercial cylinders, and to avoid the inconvenience of frequent bottle changes the driver pressure is usually limited to about 35 atmospheres.

The driver section is about 2.4 m long and 104 mm in internal diameter. The driven section of the shock-tube is some 9.5 m in length and is 76.2 mm square in cross-section. At present the shock-tube is fitted with a  $10^\circ$  half-angle conical nozzle having an exit diameter of 305 mm and various throat inserts are available ranging in diameter from 3.17 mm to 12.7 mm. The hypersonic stream forms a "free jet" in the test section which is a cylinder about 1 m long and 430 mm in diameter. This test chamber is fitted with observation ports and other access ports, one pair of which carries the support for models undergoing test.

Depending upon which nozzle throat insert is in use, pitot pressures in the range 5-100 torr and static pressures in the range 0.05-1 torr are to be expected (Bernstein, 1963) with a running time between 1 and 2 ms when the tunnel is operated in the tailored-interface mode.

These constraints led to specifications being formulated for two types of transducer to be used in the hypersonic working section, one to cover each of the above ranges. Both types were to be capable of measuring any pressure within the design range to within about 1% and the response times were to be as low as possible, and preferably less than 50  $\mu$ s (i.e. 5% of available test time). Transducer size was not considered to be of paramount importance in the early stages, but the need for later miniaturisation was to be borne in mind during design. A sensing face diameter of 15 mm and an overall length of 25 mm were considered as reasonable maxima for prototype gauges.

No pressure measuring systems satisfying these requirements are commercially available. Several workers (Edwards, 1958; Lederman & Visich, 1965; Martin et al, 1962; Pierce, 1964; Macdonald & Cole 1963) have published information on transducers of their own design but in most cases they either do not meet the above specifications or insufficient details have been released to enable the designs to be adopted. Some comparisons between the transducers described in Section 7 and other designs are made in Section 8 and Fig.29.

An investigation of the pressure sensing devices available when this study began showed that while it may well be possible to achieve the required response time using strain gauge, inductance or capacitance sensors, piezo-electric materials\* have the distinct advantages of being self-generating rather than passive devices and they also have a relatively high sensitivity.

---

\* Piezo-resistive materials which have recently evolved as a product of semi-conductor technology may also be suitable.

In such materials a change in the mechanical stress distribution gives rise to a change in the electric polarisation which may be detected as an apparent redistribution of charge. Clearly the stress distribution in any sensing element will depend not only upon the magnitude of the load applied, but also upon the manner of its application and upon the size and shape of the sensing element. Accordingly a theoretical study was undertaken to determine the most suitable configurations. Several modes were considered; in particular the compressive mode with the stress either co-linear with or perpendicular to the axis of polarisation, the shear mode and two bending modes. Making several fairly realistic assumptions expressions were derived for the sensitivity and natural frequency of elements in each of these modes. These are given in Section 2 where attention is drawn to the product of charge sensitivity and natural frequency as a measure of the mode effectiveness. Several piezoelectric materials are also compared.

To make use of an element in any of these modes it must be incorporated into a practical design. This latter will normally include a casing of some kind together with a diaphragm to provide sealing. In addition if the mode used is force-sensing as opposed to pressure-sensing an "anvil" will be needed to transmit the stress to the element in the appropriate direction. The ancillary parts of a practical transducer may have a major effect on the performance, depending on factors such as mass, stiffness, size and the manner in which the parts are bonded to one another. These effects are difficult to analyse in general circumstances and several prototype gauges were therefore built and tested. The parameters considered most important in defining the performance of a transducer are:

- (i) charge sensitivity to pressure,
  - (ii) natural frequency,
  - (iii) acceleration response and cross sensitivity,
  - (iv) thermal response,
  - (v) linearity and hysteresis,
  - (vi) repeatability from day to day,
- and (vii) a degree of repeatability between nominally identical transducers is desirable from a practical point of view.

In order to investigate the behaviour of the transducers in relation to these features and having regard also to the specifications laid down earlier it is clearly necessary to ensure that the amplifying and recording system should not introduce further, large, unknown errors. Consideration has been given to both voltage and charge amplifying systems and the latter was chosen largely for the practical reasons which are outlined in Section 3.

Transducers normally "ring" at their natural frequency and it is usually necessary to filter the output in some way so that the recorded signal is easily interpreted. The relative merits of acoustic and electronic filtering are discussed in Section 4.

Detailed interpretation of the recorded signal is only possible however when the measuring system has been calibrated. Considerable attention was paid to this topic for it had been reported (Pallant 1966) that different calibration factors were applicable to some transducers depending upon whether

a static or a dynamic calibration had been carried out. It is easily recognised that only the overall calibration of the total measuring system (pressure vs. recorded signal) is necessary in principle, but because in practice the gain of the amplifier and the oscilloscope are adjusted according to the expected magnitude of the transducer output, a more practical system was adopted. This employs a "charge calibrator" which is used in conjunction with a digital voltmeter. An accurately measured charge is thus injected into the system immediately after a transducer output has been recorded. The shock-tube was used to provide pressure steps for a dynamic calibration of the less sensitive gauges and a solenoid-operated semi-dynamic system was used with the high sensitivity gauges. The calibration is discussed briefly in Section 5.

In Section 6 some of the general design features of transducers are considered and in Section 7 some prototype gauges are briefly described and their performances are compared with those expected under calibration conditions. Some preliminary measurements made in their design environment are also described.

Finally in Section 8 the results are briefly assessed in relation to the aims of the project.

## 2. Piezoelectric sensing elements

### 2.1 Some theoretical considerations

Piezoelectricity is the name given to the property possessed by some materials which exhibit a change in electrical polarisation when undergoing a mechanical strain. When parts of the surface are plated with conducting material this change manifests itself as a potential difference across the plated parts. The important parameters are the mechanical stress  $T$ , the strain  $S$ , the electric displacement  $D$ , and the electric field strength  $E$ .

Assuming a linear relationship between the electric displacement and the stress which causes it, we may combine this "piezoelectric property equation" with that for a dielectric material relating  $D$  to  $E$  to give

$$D_i = d_{ijk} T_{jk} + \epsilon_{ij}^T E_j \quad \dots\dots(1)$$

where the superscript  $T$  denotes that the dielectric permittivity  $\epsilon_{ij}$  is to be evaluated at constant stress.

For a material which obeys Hooke's Law it may be shown that including the effect of the electric field on the strain, the latter is given by

$$S_{ij} = s_{ijkl}^E T_{kl} + d_{kij} E_k \quad \dots\dots(2)$$

It is then possible to show that for weak electro-mechanical coupling the voltage generated is

$$V = Q/C_o = - \frac{1}{C_o} \int_B (d_{ijk} T_{jk}^o \bar{E}_i) dB \quad \dots\dots(3)$$

where  $C_0$  is the capacitance,  $Q$  the apparent charge,  $T_{jk}^0$  the stress distribution in the electrically free element and  $\bar{E}_1$  is the field produced by unit applied voltage to the mechanically free element, the integral being taken over the volume  $B$  of the element. Thus  $T_{jk}^0$  and  $\bar{E}_1$  may be obtained as solutions of a purely elastic and a purely electrical problem.

When the element is essentially a thin plate, that is when the dimension  $t$  in the  $x_3$  direction normal to the conducting plates is small, so that  $\bar{E}_3 = 1/t$ , equation (3) simplifies to

$$V \left\{ \frac{\epsilon_{33}^T A}{t} \right\} = - \frac{1}{t} \int_B (d_{3jk} T_{jk}^0) dB \quad \dots(4)$$

where  $A$  is the plated surface area.

Because it simplifies the problem considerably and applies closely to most cases of present interest, equation (4) will be used throughout the remaining discussion. The general approach will be to insert  $T_{jk}^0$  as the solution of the purely elastic problem in order to determine  $Q$  and  $V$ . Usually of course these solutions of the elastic problem will themselves be approximations. In particular it is usual to assume that the material is isotropic which is not justifiable for piezoelectric materials, and in addition some of the stress components will often be neglected. There are thus two fields of approximation; one involved in the derivation of the piezoelectric equations (3) and (4) and the other connected with determining the mechanical stress. In so far as we seek to compare elements of different configuration, these approximations are not serious.

Before examining different element configurations, we may note that the performance of an element depends directly upon the magnitude of the piezoelectric constants  $d_{ijk}$ . Although a very large number of materials are piezoelectric those  $d_{ijk}$  most readily available and having significant values of  $d_{ijk}$  are quartz, Rochelle salt and a variety of ceramic materials based upon barium titanate or lead-zirconate-titanate (PZT). Other properties are also important. Account must be taken of the relative permittivity, the natural time constant of the material which has a direct bearing on the low frequency characteristics, the elastic constants and the density which determine the natural frequency of the element, and the change of piezoelectric constants with temperature.

The material properties must be referred to a specific set of axes which avoid ambiguity, such as crystallographic or polarisation axes and care must be exercised regarding the orientation of this set to those used in the stress analysis. In this work transducer axes refer to those used in the stress analysis which do not necessarily coincide with the crystallographic or polarisation axes. It is very common to find, particularly in commercial literature, that a 'restricted tensor notation' is employed. The relation between the two notations is given by Mason (1947). In this notation equation (4) becomes:-

$$V \left\{ \frac{\epsilon_{33}^T A}{t} \right\} = Q = - \frac{1}{t} \int_B (d_{3n} T_n) dB \quad \dots(5)$$

where the  $x_3$ -direction is normal to the plated surfaces.

Quartz is commonly found in two forms, alpha-quartz and beta-quartz. The former is more widely used. Rochelle salt is rhombic in structure and the crystallographic axes of this and of quartz are discussed by Cady (1964). Although barium titanate and lead-zirconate-titanate exist in crystalline form, they are usually used in ceramic form. Combined with a porcelain-type clay the mixture is fired. The random orientation of the crystals results in no net piezoelectric effect. However after being machined, the ceramic is placed in a high intensity electric field while at the same time it is heated above its Curie temperature and then allowed to cool slowly. The applied field reorients a significant proportion of the crystals so that their axes are aligned more or less parallel. The specimen is thus polarised and exhibits the piezoelectric effect. It is conventional to choose the  $x_3$ -axis in the direction of polarisation, and the ceramic has properties axi-symmetric about this axis.

Of these materials Rochelle salt has found little use in measuring instruments. It is affected considerably by both humidity and temperature and its properties appear to vary not only from one sample to another but also to depend strongly on the stress level (Cady, 1964). Since linearity and repeatability are desirable features of a transducer Rochelle salt may be dismissed as a sensing element material for high accuracy instruments.

Quartz has found a somewhat greater use in commercial instruments than ceramics. It has a lower temperature sensitivity than ceramics and a very high resistivity thus giving it an inherently long time constant which permits static calibration. It exhibits linearity over a very wide range of stress levels. The ceramics have considerably higher sensitivity but suffer from the defect of being pyroelectric. A large amount of commercial research has been applied to quartz transducers. The high sensitivity demanded in the present application has led to attention being concentrated on ceramic materials rather than quartz. Clearly the basic approach is similar for all piezoelectric materials, but detailed design of both the transducers and the associated electronic circuits is affected by the choice of sensing element materials. The manufacturers usually refer to the ceramic materials by code letters. Throughout this design study improvements were being made in the lead-zirconate-titanate (PZT) based ceramics and the latest, PZT-5H, is about twice as sensitive as the earlier PZT-5A which is itself some two or three times more sensitive than barium titanate. Moreover the material time constant of PZT is considerably larger than that of barium titanate. Because of these advantages PZT has been used as the sensing element in all the prototype transducers described later.

Some of the properties of quartz, barium titanate and PZT are listed in Table 1.

The transient response of a transducer is chiefly governed by its natural frequency. The overall construction of the transducer will clearly play a large part in determining the natural frequency, but because of the number of variables involved it is difficult to generalise. The natural frequency of the piezoelectric sensing element is obviously of some relevance, so as a first step in comparing the various sensing modes we shall consider the natural frequency  $f_0$  of a number of vibration modes for elements of practical configurations. Attention will be drawn later to the way in which loading of the element affects  $f_0$ . The modes of interest involve longitudinal compression waves both parallel and perpendicular to the axis of polarisation, transverse shear waves and vibration in bending.

We consider first the normal compressive mode in which pressure waves

travel parallel to the polarisation axis. The transient response of the element to a step input will depend upon the transit time  $\tau$  of the stress wave through the element and upon the way in which the wave is reflected from the end face of the element. When the element is "backed" by a material of the same acoustic impedance, no reflection takes place, and the full output voltage is reached in time  $\tau$  after which the output remains steady. In this configuration the output reaches its full value for the first time after one quarter of a cycle when the vibration is sinusoidal and this suggests that a natural frequency corresponding to the period  $4\tau$  be used. With a "rigid" backing - that is one for which the step input is totally reflected in like sense - the period is again  $4\tau$ , but for a "free" backing the period is  $2\tau$ . The latter is the value usually quoted in manufacturers' literature because they have in mind the more common application as electrical oscillators when mechanical loading is kept to a minimum. However for the present application a value of  $f_0 = 1/4\tau$  would seem more realistic. It is not difficult to show that the appropriate velocity  $v$  of wave propagation for this case is given by  $v^2 = 1/(\rho s_{33}^D)$ .

When used in the transverse compressive mode, a natural frequency based upon the transit time of waves in a direction perpendicular to the polarisation axis is important. This mode is rarely used because the sensitivity is poor. Redwood (1961b) shows that the appropriate wave velocity for this case is given by  $v^2 = 1/(\rho s_{11}^E)$  and it may be argued on physical grounds that the frequency should again be based upon a period of four times the stress wave transit time along the length in the  $x_1$ -direction.

With compression waves the particle displacement is in the same direction as the wave motion. Shear waves are transverse waves however, and the displacement is perpendicular to the direction of wave propagation. For waves travelling parallel to the axis of polarisation, there is only one type of wave because of axial symmetry. For waves moving normal to the polarisation axis there are two types of wave; one in which the displacement is parallel to the polarisation axis, and the other in which it is normal to both the direction of wave propagation and the polarisation axis. The appropriate wave speeds are respectively  $(\rho s_{44})^{-1/2}$ ,  $(\rho s_{44})^{-1/2}$  and  $(\rho s_{66})^{-1/2}$  the external circumstances governing whether these are evaluated at constant field or constant electric displacement. For pressure measurement the load must be transmitted to a shear element by means of an anvil or force transmitter, and the mechanical loading will have a considerable effect on the natural frequency of the transducer as a whole.

The natural frequencies of the anvil itself may also effect the vibration of the transducer as a whole, and in practice it is likely that calculations of the natural frequencies of a shear element transducer will be no more than very approximate. Differences between  $s^D$  and  $s^E$  are not therefore likely to be important.

Lewis (1961) has shown that to a first approximation, the natural frequency of an element in bending is the same as that of a non-piezoelectric material having the same elastic properties. However the readily available results for the vibration of even simple beams and plates all assume an isotropic material. To apply these results we must decide which elastic constants are likely to approximate best the conditions within the element. The configurations of interest are generally thin plates or beams polarised

in the thickness direction ( $x_3$ ). The restoring forces in bending are tensile forces within the "plane" of the element and the appropriate elastic constant would thus be  $s_{11}$ . Comparison of this case with that in which compressive waves are propagated in the  $x_1$ -direction suggests that the elastic compliance should be evaluated at constant electric field, so that the appropriate wave velocity is given by  $v^2 = (1/\rho s_{11}^E)$ .

We now proceed to a consideration of a variety of ceramic element configurations, in particular those illustrated in Fig.1. We assume throughout that the polarisation axis is in the  $x_3$ -direction. The sensitivity to both a uniform pressure loading over one face and to a point force are of interest because even though our present application is to pressure measurement it may be necessary for practical reasons to load the sensing element indirectly, as in the case of shear modes. The capacitance  $C_o$  has some bearing on the design of the amplifier and this is also examined.

As a simple illustration of the application of our previous results we examine the configuration of Fig.1(a), in which a thin plate of thickness  $t$  is subject to a uniform pressure  $p$  in the  $x_3$ -direction. Neglecting lateral stresses as a first approximation the stress field is

$$T_n = 0 \text{ for } n \neq 3 ; T_3 = p \quad \dots\dots(6).$$

Using equation (5),

$$Q = -\frac{1}{t} \int_B (d_{33} T_3) dB = -d_{33} Ap \quad \dots\dots(7).$$

Defining the charge sensitivity to pressure as  $Q_p = Q/p$  and that to force as  $Q_F = Q/F$ , we arrive at

$$Q_p = -Ad_{33} \quad \text{and} \quad Q_F = -d_{33} \quad \dots\dots(8).$$

We may note that in this direct compressive mode (as distinct from bending)  $Q_F$  depends only upon the piezoelectric constants of the material and not upon the dimensions of the element. Since

$$C_o = \epsilon_{33}^T A/t \quad \dots\dots(9).$$

we obtain the voltage sensitivity to pressure  $V_p$  and to force  $V_F$  as

$$V_p = td_{33}/\epsilon_{33}^T \quad \text{and} \quad V_F = \frac{td_{33}}{A\epsilon_{33}^T} \quad \dots\dots(10).$$

For this configuration we see that  $Q$  and  $V$  are respectively proportional to the area and the thickness of the element, so that it would appear that the element should be made as large as possible to give maximum sensitivity. We shall see later that  $Q_p$  is somewhat more important than  $V_p$  and in addition increasing the thickness lowers the natural frequency.

In a practical transducer the area  $A$  will be limited by the allowable overall size. It is possible to increase the effective area by "stacking" a number of plates one above the other and connecting them in parallel. The voltage sensitivity remains as given by equation (10) but  $Q_p$  will be multiplied by the number of plates in the stack. However the natural frequency of the stack is that of a single element divided by the number of plates. Thus the

product  $Q_p f_o$  remains unchanged when a number of identical elements are stacked, and this suggests that this product is a useful measure of the mode effectiveness. (It is analogous to the gain-bandwidth product which governs the performance of some electronic amplifying circuits.) The natural frequency for this mode as suggested earlier is given by

$$f_o = \frac{1}{4t \sqrt{(\rho s_{33}^D)}} \quad \dots (11)$$

so that for this configuration

$$Q_p f_o = \frac{Ad_{33}}{4t \sqrt{(\rho s_{33}^D)}} \quad \dots (12)$$

This expression must be used with some care. It applies for a stack of n identical elements cascaded in an appropriate fashion, so that for an overall thickness nt the charge sensitivity to pressure is proportional to n. Consequently we may decide upon an overall thickness consistent with the desired natural frequency and increase  $Q_p$  by building this overall thickness from as many elements as is practical.

In a similar manner one may determine the sensitivities, static capacitance and natural frequencies for the other configurations shown in Fig.1. The results are summarised in Tables 2 & 3. The latter table has been drawn up using the piezoelectric constants for PZT-5A and the dimensions of the elements are expressed in units such that each dimension is of order unity. This makes immediate comparison easy.

One or two remarks concerning some of the modes are in order here.

The plate undergoing transverse compression is similar to that in direct compression but  $d_{31}$  replaces  $d_{33}$  thereby reducing the sensitivity by a factor of two or three. Consequently it has found little use although a variation consisting of a thin-walled tube, polarised radially, could prove useful.

A shear stress  $T_5$  on the plate produces a field in the  $x_1$ -direction. We see from Table 3 that for ceramics  $Q_F$  for the shear mode is higher than for the direct compressive mode because  $d_{15}$  is somewhat greater than  $d_{33}$ . It is not possible to assess the sensitivity to pressure since some means of transmitting the pressure as a tangential force is required. Again the thin-walled tube is a useful variation in which the load is applied tangentially to the inner surface and the outer one is fixed. A stack of plates with co-directional polarisation axes, connected in parallel, may also be used in the shear mode. The effects of cascading are analogous to those for the plates in compression.

The bending modes invariably use elements of bimorph construction. These consist of two similar plates with conducting plating on the upper and lower faces, which are connected mechanically and electrically along their common surface. They are polarised in the thickness direction. Applying equation (5) to the simple case of a beam undergoing two dimensional bending we obtain

$$V = \frac{-1}{\epsilon_{33}^A} \int \int_{\text{Area}} \left\{ \int_{-t/2}^0 (d_{31} T_1) dx_3 + \int_0^{t/2} (d_{31} T_1) dx_3 \right\} dx_1 dx_2 \quad \dots (13)$$

Since the simple theory of bending gives

$$T_1(x_1, x_2, x_3) = -T_1(x_1, x_2, -x_3) \quad \dots\dots(14)$$

the voltage generated is zero. This is because the potential difference across the upper plate is equal but opposite in sign to that across the lower plate, so that the voltage developed between the upper and lower surfaces is zero. However by appropriate electrical connection the potential differences may be added, or alternatively by using plates polarised in opposite directions (so that the sign of  $d_{31}$  is changed in one of the integrals of equation (13)) we may obtain an output across the outer faces. These two configurations are known respectively as parallel- and series-connected. It is easy to see that the series-connected configuration, which is the more practical, has twice the voltage sensitivity, half the charge sensitivity and a quarter the static capacitance of the parallel connection.

According to the simple theory of bending, the stress  $T_1$  at a distance  $x_3$  from the neutral axis is related to the bending moment  $M$  and the second moment of area  $I$  of the cross section by

$$T_1 = Mx_3/I.$$

For a simple beam of length  $\ell$  and rectangular cross section we obtain for the series connection

$$Q = \frac{3d_{31}}{t^2} \int_0^\ell M(x_1) dx_1 \quad \dots\dots(15)$$

According to a well known theorem in the theory of simple bending the integral in equation (15) is proportional to the difference in slopes between the two ends of the beam. The end fixing should therefore be such as to make this difference a maximum. A beam built-in at both ends would have zero sensitivity. For this configuration we only evaluate the sensitivity to force since the beam is not a practical shape for the direct measurement of pressure.

A bimorph disc may however be loaded directly by pressure so that  $Q_p$  can be calculated. Using the values of circumferential and radial stress given by Roark (1954) the sensitivities have been derived and together with the natural frequencies these are listed in Tables 2 & 3 for various kinds of loading. Again the clamped edge case gives zero sensitivity.

## 2.2 Comparison between the various modes

In order to make some comparisons of the various modes we shall make use of Table 3. Anticipating the conclusions of Section 3 we shall use the charge sensitivities rather than the voltage sensitivities for comparison, discussing the direct pressure sensing modes first. At first sight it would appear that the mode with the highest charge sensitivity-natural frequency product is the only one that need be considered, but with the limitations imposed by transducer size it is often not possible to obtain a sufficiently high sensitivity using this mode. In such circumstances a mode with a lower value of  $Q_p f_0$  must be chosen and natural frequency sacrificed.

Table 3 shows that the disc (or plate) in normal compression gives the largest value of  $Q_p f_0$  and we have seen that for  $n$  elements having the same overall thickness  $t$  this product is  $n$  times as large. Even so the highest  $Q_p$  obtainable with PZT in this mode is only of the order of several

pC/torr. The modes with the next highest value of  $Q_p f_0$  use the bimorph disc. Although the pinned edge disc is slightly superior from the natural frequency viewpoint, such conditions are difficult to achieve in practice. Charge sensitivities approaching 100 pC/torr would seem to be feasible although the natural frequency would then only be of order 10 kHz. The only other mode which may be used for direct pressure sensing is the plate in transverse compression and we have already noted that this is inferior to the direct compressive mode.

The force-sensing modes should not only be compared with each other but also as regards their suitability for use in a pressure transducer. Such a transducer will usually consist of a diaphragm and an anvil to transmit the load to the element. The mechanical loading on the element will have an effect on the natural frequency which is not easy to determine. A pressure of 1 torr acting on a diaphragm 1 cm in diameter would produce a force of about 0.01 newton. Thus for comparison with the direct pressure sensing modes we shall consider the output of a force-sensing element to a load of 1 cN.

For such a load the output of the two direct modes, compressive and shear, are about 4 pC and 6 pC. The shear mode however, because of its high stiffness could offer a higher natural frequency even with mechanical loading, so it deserves further investigation. The outputs from the bending modes are of order 100 pC, the cantilever being about twice as sensitive as the other configurations.

With these figures in mind we now proceed to a brief discussion of electronic amplifying systems.

### 3. Electronic amplifying systems

For the measurement of transient pressures it is common practice to use a transducer in conjunction with a cathode ray oscilloscope (C.R.O.), the display being recorded photographically. In order to do this an amplifier with special characteristics is necessary to couple the transducer to the C.R.O. Two aspects are of particular importance: the effect of the capacitance of the connecting cable and the input impedance of the amplifier which largely determines the low frequency response characteristics of the system and thus has a direct bearing on the possibility of static calibration.

In order to discuss the matching of the transducer to the amplifier it is convenient to use the equivalent circuit concept. One common form of the equivalent circuit of the piezoelectric element "as seen from the outside" is that shown in Fig.2(a) where  $C_0$  represents the capacitance and  $R_0$  the d.c. impedance of the element, the voltage  $V$  being that generated on open-circuit.\*

---

\* This equivalent circuit is not to be confused with one which represents the internal behaviour of a piezoelectric element - this is considered in detail by Redwood (1961a)

### 3.1 Charge and Voltage amplifiers

There are two approaches to suitable amplifier design; either voltage or charge amplification may be used. In discussing them we shall need to have particular regard to their performance at low signal levels since this will determine the practical limit of transducer sensitivity. Since the present application is also concerned with the measurement of relatively high speed transients, the high frequency response is also of some importance.

Consider first a voltage amplifier of gain  $-m$  having an input impedance  $R_i$  - the equivalent circuit is shown in Fig.2(a). Assuming an infinite bandwidth and writing the generated voltage as  $V(\omega)$  where  $\omega$  is the frequency, the output voltage  $V_o$  is given by

$$V_o = \frac{-mV(\omega)j\omega\tau}{1 + j\omega\tau} \frac{C_o}{C_o + C_e} \quad \dots\dots(16)$$

where  $\tau = \frac{R_i R_o}{R_i + R_o} (C_o + C_e) \quad \dots\dots(17)$

Thus the effective input voltage to the amplifier is reduced by the presence of the connecting cable capacitance  $C_e$ . Since a typical cable capacitance is of the order of 100 pF/m this may be quite serious for practical cable lengths. A quartz element will typically have a capacitance of about 10 pF and so attenuation factors of ten or more are likely. The capacitance of ceramic transducers is usually an order of magnitude greater than for quartz transducers and the attenuation is correspondingly less.

The low frequency performance depends upon the time constant  $\tau$ . With quartz we may expect the capacitance term to be of order 100 pF so that a time constant of 1 second would require the resistive term to be about  $10^{10}$  ohm. It is relatively easy to achieve a value of  $R_o \gg 10^{10}$  ohm with quartz and using an electrometer valve or an insulated-gate field effect transistor values of  $R_i > 10^{12}$  ohm are readily obtainable. Large time constants are more difficult to obtain with ceramics. It is reasonable to assume for ceramics that  $C_e \ll C_o$  and  $R_i \gg R_o$  so that  $\tau \approx R_o C_o$ . This product is independent of the size of the element and depends only upon the resistivity and permittivity of the material. For barium titanate,  $\tau \approx 100$  second and for PZT it is about 2000 second though for both materials it decreases rapidly with increasing temperature.

A charge amplifier is ideally a d.c. coupled amplifier with capacitive feedback. The equivalent circuit is shown in Fig.2(b). It is similar to that of the voltage amplifier but has a feedback capacitor  $C_f$  and resistance  $R_f$  added. The latter may be either a separate component or the leakage resistance of the capacitor. The amplifier output voltage  $V_o$  is

$$V_o = -V(\omega) \left\{ \frac{mC_o}{C_e + C_o + (m+1)C_f} \right\} \left\{ \frac{j\omega\tau}{1 + j\omega\tau} \right\} \quad \dots\dots(18)$$

where

$$\tau = \frac{C_o + C_e + (m+1)C_f}{\frac{1}{R_i} + \frac{1}{R_o} + \frac{(m+1)}{R_f}} \quad \dots\dots(19)$$

In most amplifiers  $m$  is sufficiently large that  $(m+1)C_f \gg C_e + C_o$ . Equation (18) then reduces to

$$V_o = \frac{-V(\omega)j\omega\tau}{1 + j\omega\tau} \frac{C_o}{C_f} \dots\dots(20)$$

Thus the output varies inversely as  $C_f$  and directly as the product  $C_o V(\omega)$ . This product is the apparent charge given by equation (4), and the charge amplification is  $1/C_f$ .

One of the advantages of this circuit is that the gain is almost independent of cable capacitance, provided that  $mC_f \gg C_e$ . In a practical design it may not be always possible to achieve this, and on the most sensitive ranges, when  $C_f$  is smallest, there will be some dependence on cable capacitance. To obtain high accuracy it is always necessary to calibrate the system: however it is not necessary to calibrate just prior to an experiment in order to determine suitable sensitivities at which to operate the equipment.

In an arrangement for which  $R_f/(m+1) \gg R_i, R_o$  we have from equation (19),  $\tau \approx C_f R_f$ . The time constant is then nearly independent of the cable capacitance and the properties of the transducer. However, this simple circuit does have some disadvantages mainly as regards its drift characteristics and in improving the d.c. stability the low frequency performance may be degraded.

The addition of a biasing resistance  $R_B$ , Fig.2(c), suitably decoupled for low frequencies provides one solution and by careful design a time constant approaching  $(m+1)R_o C_f$  may be obtained. This may be considerably larger than the inherent time constant of the piezoelectric material (so that static calibration is possible).

The performance of an amplifier at low signal level is dependent directly upon the noise generated within the system as a whole. Noise will arise from three main sources; the transducer itself, the connecting cable and the amplifier. Noise generated within the first two of these are indistinguishable from the required signal and some care is necessary in minimising it. Where for example the amplifier is such that a d.c. potential exists at input, a leakage current will flow through the piezoelectric material and this may give rise to noise. A coaxial cable may give rise to noise when it so vibrates that the conductor and inner insulator become separated. Here friction (and perhaps a weak piezoelectric effect) produces a potential difference which leads to charge separation on the conductor and insulator. The charge on the insulator induces one on the inner conductor so that a potential difference is produced between the inner and outer conductors. This source of noise may be reduced by using special graphite filled low noise cables and by ensuring that cable movement is kept to a minimum.

Noise is generated within an amplifier in a wide variety of ways. The subject is a somewhat complex one and is dealt with in some detail by Valley & Wallman (1948) and van der Ziel (1954). When the first stage of an amplifier has a large power gain, the noise generation in later stages may be neglected. It is common practice to represent amplifier noise by equivalent noise generators at the input of the amplifier. A simplified analysis shows that although the overall gain is affected, the relative magnitude of the noise over a given band width is unchanged by feedback. Thus even though cable capacitance barely affects the gain of a charge amplifier, the noise performance is degraded by the additional capacitance. The overall noise

level depends upon the bandwidth of the amplifier, the noise voltage being roughly proportional to the square root of the upper cut-off frequency. It is well known that negative feedback improves the frequency response of an amplifier, and in view of the large amount of capacitative feedback we should expect the upper cut-off frequency to be far higher for a charge amplifier than for a voltage amplifier. While this is true to some extent, the frequency response has to be carefully tailored at high frequencies to ensure stability. The net effect is that while voltage amplifiers typically have upper cut-off frequencies of about 300 kHz, charge amplifiers rarely have a value greater than 150 kHz. The limiting factor in the voltage-amplifier is the electrometer valve in the input stage. Although using insulated gate field effect transistors higher cut-off frequencies may be achieved without lowering the input impedance, the noise performance of these devices is not very good at present.

Thus the charge amplifier has advantages where a long input time constant is required using relatively low impedance ceramic elements. The voltage amplifier is necessary where high frequency performance is of major importance. Although neither system is clearly to be preferred in the present context, the charge amplifier has received more commercial attention because it has definite advantages in fields allied to the present one.

### 3.2 Elementary charge amplifier design

The sensitivity of a charge amplifier is approximately  $1/C_f$ , so that  $C_f$  should be small for high gain. For practical reasons values of  $C_f$  below 10 pF (corresponding to a sensitivity of 100 mV/pC) are rarely used, since stray circuit capacitance which may amount to several picofarads would make the gain unreliable. Where greater sensitivity is required the approach must be to improve the noise level of the charge amplifier and introduce additional voltage amplification stages.

To achieve amplification independent of the cable and sensing element capacitance the open loop gain  $-m$ , of the charge amplifier should be made very large. For maximum sensitivity corresponding to  $C_f = 10\text{pF}$  and for a value of  $(C_o + C_e) = 1000\text{ pF}$  typical of ceramics, the open loop gain would need to be 80dB to give a gain variation not exceeding 1%. This imposes severe stability problems. However in practice the amplifier is used in conjunction with a cathode ray oscilloscope which may well have a variation in its gain of several per cent. Thus calibration must be performed and as we shall see the most convenient way of doing this is to calibrate the amplifying and recording system as a whole just before or just after each pressure measurement. In these circumstances\* a small dependence of the gain on sensing element and cable capacitance is unimportant and in the light of experience it is probably better to restrict the open loop gain to 40dB when stability problems are very much eased since this gain may be obtained with a single stage. It is probable that the frequency response will thus be much improved, since it is not necessary to degrade it to achieve stability. In order to avoid excessive phase shifts the output impedance of the open loop amplifier should be small compared with that of the feedback

---

\* This point was not appreciated initially and the design described could be improved.

capacitance over the required bandwidth. An output impedance of about 100 ohm may be readily obtained using an emitter follower. Where the low frequency response is to be independent of the sensitivity range  $R_f$  may be conveniently changed with  $C_f$  by connecting appropriate values in parallel on the range switch. A maximum pulse droop of 1% over a measuring period of 10 ms requires a time constant of at least 1s. Using the conventional biasing arrangement,  $\tau = R_f C_f$ , so that on maximum sensitivity, when  $C_f = 10$  pF we should need  $R_f = 10^{11}$  ohm. Since it is important that  $R_i \gg R_f$ , the input impedance should exceed  $10^{13}$  ohm, a value which may be realised with electrometer valves or insulated gate field effect transistors.

Since the r.m.s. noise voltage increases with increasing bandwidth, the bandwidth should be kept to the minimum consistent with the required rise-time. This latter is likely to be determined largely by the natural frequency of the transducer, and the bandwidth is conveniently limited by the high-frequency filter which is usually necessary to remove the oscillatory component of the transducer signal (see section 4).

A charge amplifier was built according to some of these ideas and the circuit is shown in Fig.3. The first stage uses an electrometer valve which may be operated from the same power supply as the transistors. The anode load is limited to 150k $\Omega$  by the impedance of the following stage which together with the third stage provides the main amplification. The final stage is an emitter-follower. Because the input grid is not at ground potential a large series capacitance with a high insulation resistance is used. Negative feedback was applied between the emitter of the output transistor and the emitter of the second-stage transistor to overcome a tendency to instability. The components of the feedback network were adjusted on test so that in the range up to 1 MHz the phase shift did not rise above  $100^\circ$ . The nominal sensitivity may be varied in seven switched ranges from 0.1 to 100 mV/pC, the maximum output on each range being limited to  $\pm 2$  volts by the requirements of linearity. The rise-time on most ranges is less than 1  $\mu$ s but it rises with increasing sensitivity and increasing source capacitance, exceeding 5  $\mu$ s only on the two most sensitive ranges with a source capacitance of 1000 pF. The low frequency response is such that a time constant of at least 1s may be obtained on all ranges. The noise level has been very approximately estimated and is less than 0.01 pC referred to the input on the most sensitive range for a source capacitance of 10 pF but it rises to 0.05 pC with a source capacitance of 1000 pF. As suggested earlier limiting the bandwidth reduces the noise level but the situation is a little complicated by the noise introduced by the filter.

### 3.3 Calibration of the charge-amplifier

Although the overall gain of the charge amplifier is substantially independent of the source capacitance, small variations may occur. Moreover the cathode ray oscilloscope which is commonly used to record the transient pressure signal has sensitivity variations from the nominal of several per cent and day-to-day variations of the same order. Consequently it is necessary to calibrate the system. Separate calibration of each item in the measuring system leads to considerable scatter in the points determined for a transducer calibration. This scatter arises from the random errors in the calibration of each item. Clearly this scatter may be reduced by calibrating the 'chain' as a whole.

By applying a suitable voltage  $V_{cal}$  to the system through a series capacitance  $C_{cal}$  a charge input  $V_{cal}C_{cal}$  is simulated. The voltage may be of

any wave form bearing in mind the frequency limitations of the amplifier, but square waves or step functions are most common. The charge calibrator will itself need to be calibrated against an accepted standard and one aim in its design should be that this calibration may be carried out easily and frequently. A second aim is that the calibrator should be so incorporated into the measuring system that the distribution of capacitance in the system is as nearly identical in the calibrate and operate modes as is possible.

The calibrator which has been designed owes much to commercially available instruments but several refinements have been incorporated. It consists of a constant-amplitude square-wave generator which feeds a ten-turn helical potentiometer, Fig.4. The output is taken via a 'monitor socket' to a switching arrangement for connecting the appropriate series capacitor. Values of 10 pF, 100 pF, 1000 pF are used, trimming capacitors enabling adjustment of the values to within 0.1% (the bridge error) using an impedance bridge.

Errors in gain of order  $C_{cal}/mC_f$  may be produced if the calibrator side of the series capacitor is not grounded when the calibrator is off. Accordingly each of the three output channels has to have a set of capacitors so that up to three amplifiers may be calibrated and operated without changing connecting cables.

In its early form the power supply was a mercury cell, but this was found to be subject to as much as 2% variation, so the stabilised power unit supplying the charge amplifier was used. The square wave output is adjusted to 10 volts (with the helical potentiometer set at 10) using a small 50 turn trimming resistance. This is done in the following way. One of the switch positions on the multivibrator - the 'calibrate' mode - enables the output transistor to be switched on continuously, the other transistor being cut off. The output voltage is then measured and adjusted using a digital voltmeter. To ensure that the square-wave and calibrate positions produced the same voltage, the outputs were compared on a d.c. coupled oscilloscope at high sensitivity. A differential amplifier and a 10 volt biasing source were used to keep the trace on the screen. The difference was considerably less than 10mV, corresponding to an error of less than 0.1% for a 10 volt output.

#### 4. Filters

It has been remarked that each transducer will have a natural frequency somewhat lower than that of the element alone. When a step change in pressure is applied to the transducer the latter will 'ring' since the step will include a component at the transducer natural frequency. The amplitude of this oscillatory component is usually comparable with the response to the step input and to facilitate interpretation it is common practice to filter the signal\*. One of two methods is usually employed: acoustic filtering or electronic filtering, though on occasion both may be used.

Since the specification of the pressure measuring system calls for errors of less than 1%, the filter should be such as to reduce the relative amplitude of the oscillatory component to less than 1%. Such a filter will have a rise-time longer than that of the transducer itself and the effect of this on the overall system rise-time will be considered later. Clearly the

---

\* This is not necessary with a 'matched-backing' transducer.

rise-time of the filter alone should be as short as possible consistent with the requirements regarding rejection ratio.

An acoustic filter consists of a cavity and orifice which serves to shield the transducer from the more rapid pressure changes. This effectively limits the rise-time of the applied pressure so that the component it contains at the natural frequency of the transducer is negligibly small and the gauge ringing is minimised. In shock tunnel applications the pressure being measured is often that of a very hot gas, and an orifice and cavity will usually have a sufficiently large thermal capacity to reduce the thermal 'loading' of the transducer to negligible proportions. This may be particularly important when piezoelectric sensing elements are used, since such materials are frequently pyroelectric also, as noted in Section 2.

In many cases where model surface pressures are to be measured, the model size and shape preclude the transducer from being mounted flush with the surface. It is then necessary to use an orifice and a cavity - and perhaps a length of pipe connecting one to the other. Such a filter alters the signals in a complex way. Analysis of the effect for any given orifice/cavity configuration is difficult and at best approximate. This means that for an acoustic filter an exact 'transfer function' cannot be defined and thus the input wave form cannot be reconstructed from the output signal. Moreover it is not a simple matter to adjust the characteristics of the filter to match a given situation.

The major advantages of the electronic filter are that its transfer-function, which is linear, may be accurately calculated, its components are readily altered to match the transducer characteristics and it may be 'switched out of circuit'.

The three forms which have found the widest application are the inductance-capacitance filter, the parallel-tee filter and the cascaded resistance-capacitance filter, see Fig.5.

The basic low pass L-C filter is well known. The inductance and capacitance form the filter thereby determining the frequency scale and a series resistance R provides the damping. The fastest rise-time consistent with no overshoot occurs when the damping is critical, and in this condition the circuit is equivalent to two identical cascaded R-C filters.

The parallel (or twin) tee R-C network has the advantage that the minimum gain and the minimum gain frequency may be independently adjusted. Thus careful choice of components can lead to zero gain at the critical frequency. Although an asymmetrical network provides better rejection, it is usual to use the simpler symmetrical form. Moreover best rejection near resonance is obtained when the parallel resistance is half the series values and the parallel capacitance twice the series capacitances. Such filters easily achieve rejection ratios of 100:1 and may attain 1000:1 with careful design. Only one stage is therefore necessary. However there are some disadvantages. When the signal has components at more than one frequency to be filtered or when the natural motion of the transducer is not strictly sinusoidal, the filter is not ideal. The frequency response of the parallel tee is symmetrical about the resonant frequency, so that components above this frequency are amplified. The gain at frequencies above resonance may be reduced by the addition of a further stage, or stages, such as an L-C filter. Thus the parallel tee is most useful when a signal of one frequency is dominant

with smaller components at higher frequencies. Such responses are characteristic of transducers which are diaphragm dominated.

The multi-stage cascaded R-C filter is widely used. For an n-stage filter the asymptotic slope of the frequency response curve is  $6n$  dB/octave. This is approached quite rapidly. Although the rise time increases with the number of stages there is a decided advantage in using several stages. This is because the basic requirement is for an overall rejection ratio of say 100:1 (40 dB) at a particular frequency, and each stage therefore has a lower RC product the greater the number of stages. This more than compensates for the increase in rise time for several stages as compared to one stage. For example a 4-stage filter has a rise time 0.066 times that of a single stage providing the same rejection ratio. The advantage rapidly diminishes above  $n=4$ .

In most multi-stage filters buffer amplifiers are usually necessary between stages to avoid interference and at input and output in order to match the source and load impedances. Two practical filter circuits are shown in Fig.6.

## 5. Calibration of pressure transducers

In meeting a specification which calls for pressure measurements to within 1%, special attention must be paid to calibration of the transducers. As a general rule the measurement of static quantities may be carried out far more accurately than that of transients. One approach is therefore to design the transducer and measuring system so that it has a flat response from d.c. through the required dynamic range. It may then be calibrated statically - for example using a dead-weight tester in the case of pressure measuring systems - and used dynamically. However the time-constants available with transducers using piezoelectric sensing elements are not really large enough for static calibrations to be made. Another approach is to use a calibrating device which can apply the calibration pressure at varying rates from d.c. through the dynamic range needed. The device itself may then be calibrated statically against a standard. One such device which makes use of the electrostatic attraction that exists between two metal plates having a potential difference between them, has been designed and built at Queen Mary College. It may only be used for transducers having a metal diaphragm, and is limited at present to pressures below about 0.5 torr, though modifications are possible which should increase its range. This is just the range in which calibration pressures are difficult to produce by other means, and although the device has been only partially successful, further development is proposed.

Two other methods are commonly used. In one the transducer is shielded from a vessel containing air at an accurately known pressure by a suitably designed solenoid-operated valve. The small space between the transducer face and the valve is evacuated to a negligible pressure and then the valve is rapidly opened. Opening times of order 1 ms are possible by "over-running" the solenoid (see for example, Pennelegion et al, 1966 and Aronson & Waser, 1963). This method is often referred to as "semi-dynamic" the term "dynamic" being reserved for calibration systems in which the pressure rise-time is substantially less than 100  $\mu$ s.

Such a system is the shock-tube, in which the rise-time for a wall-

mounted transducer depends upon the transit time of the shock across its face. The undisturbed gas pressure  $p_1$  before shock arrival and the shock-wave Mach number  $W_{11}$  must be accurately determined. The pressure rise to which the transducer is subjected is, for shocks of moderate strength given by

$$\frac{\Delta p}{p_1} = \frac{2\gamma}{\gamma+1} (W_{11}^2 - 1) \quad \dots\dots(21)$$

where  $\gamma$  is the ratio of the principal specific heat capacities and is of order unity.

Clearly an error in determining  $p_1$  is directly reflected in a similar fractional error in  $\Delta p$ . Some care must be exercised in examining the effects of errors in estimating the shock Mach number. Thus a small fractional error  $\delta$  in  $W_{11}$  leads to a fractional error in  $\Delta p$  of approximately

$$\frac{2W_{11}^2}{W_{11}^2 - 1} \delta$$

While for shock Mach numbers greater than about 2, the relative error in  $\Delta p$  is only a little more than double that in  $W_{11}$ , at a value of  $W_{11} = 1.5$ , the relative error is four times that in shock Mach number. Thus weak shocks should be avoided unless the shock Mach number can be measured with the necessary accuracy. Among the more important sources of error are the response times of the shock-passage detectors, the gating errors introduced by the trigger amplifiers used to start and stop the chronometer, gating errors within the chronometer, attenuation of the shock strength as it passes between the timing stations, and transducer and shock-detector positioning errors.

The maximum error in  $\Delta p$  may easily reach 4 - 5%, the chief sources of this error being in measuring the shock velocity and comparing oscilloscope traces. The first of these errors may be reduced but two factors should be borne in mind. First the quoted figures are maximum errors; the most probable error is about half this, and the error in the slope of a linear calibration curve will be somewhat less than the individual errors. Secondly where experimental measurements are made using a C.R.O. as a recorder there is little advantage in calibrating to a higher accuracy than that to which the C.R.O. trace may be read.

These errors and other important features of the calibration procedure are to be discussed elsewhere. In calibrating the prototype transducers described in the next section a shock-tube was used with nitrogen in both channel and chamber for the less sensitive transducers and the National Physical Laboratory's semi-dynamic calibrator (Pennelegion et al, 1966) for the two most sensitive which could easily be damaged in the shock-tube environment. Immediately after recording the response of a transducer to a calibration pressure, a known charge was injected into the system from the charge calibrator described earlier, the response being recorded on the same photograph.

## 6. General design features of transducers

Before describing the prototype transducers and their performance we shall examine some of the general features of transducer design bearing in

mind those factors listed in the Introduction by which performance may be assessed.

## 6.1 Sensitivity

The sensitivity required of a transducer depends directly on the minimum signal which may be measured by the charge amplifier to the desired accuracy. In Section 3 we saw that on the most sensitive range the noise level at input to the charge amplifier was 0.01 pC. For pitot pressures in the range 5-100 torr, the greatest sensitivity required is therefore 0.2 pC/torr, while for static pressures in the range 0.05-1 torr, we should require sensitivities of 20 pC/torr.

The pressure is usually transmitted to the sensing element by means of a diaphragm and perhaps also an anvil. This diaphragm has a direct effect on the sensitivity. The load on the sensing element (or anvil) is made up of two parts, the first  $W'_e$  due to the pressure acting directly on the element, and the second part  $W'_d$  due to the reaction by which the element supports the inner edge of the diaphragm, Fig.7. The remainder of the total load  $W$  is supported by the outer casing. Assuming that the stiffness of the diaphragm is low the fraction  $W'/W$  of the total load transmitted to the element varies from 0.25 at  $z = 0$  to 1 at  $z = 1$ , see Fig.7.

Thus for high sensitivity the diameter of the element or anvil should be a large fraction of that of the diaphragm.

When the stiffness of the diaphragm is not low the situation is more complex. Obviously for a very stiff diaphragm, very little of the load is transmitted to the element. A good guide is to make the "point-load" stiffness parameter  $k_p$  of the diaphragm much less than the stiffness parameter  $k_e$  of the element (including the rigidity of the backing)\*. In cases where  $z \rightarrow 1$  this condition is difficult to apply since  $k_p$  depends critically on  $(1 - z)$ , and diaphragm edge conditions are usually uncertain. With comparatively stiff elements, say in the compressive or shear modes, the diaphragm stiffness is unlikely to be significant. Bending elements have comparatively low stiffness, and in these cases it is essential to ensure that the diaphragm stiffness is sufficiently low.

In some cases it may be necessary to minimise the mass loading of the element, so that the anvil must be small. In this case  $z$  will be small, and the response will be "diaphragm-dominated." For such a transducer the transmitted load is 1/4 of the total load when the diaphragm is very thin; for a thick diaphragm it will be very much less.

## 6.2 Natural frequency

The lowest natural frequency of a transducer is the chief factor governing its response time. When the transducer is excited by a step-rise in pressure (e.g. from a shock front parallel to its sensing face), then all its natural modes will be excited. The output will consist of a steady state value plus oscillatory components which may initially be of comparable amplitude, and these oscillations may take many tens of periods to die away to say 1% of the steady state value. Where the shock passes across the sensing face,

---

\* See Notation for definitions of  $k_p$  and  $k_e$ .

the transit time will affect the relative amplitude of the oscillations, but these are rarely so small as to be negligible in shock-tunnel applications.

Some means must therefore be used to limit this "ringing". Three approaches are possible,

- (a) design a transducer which does not ring,
- (b) limit the rise-time of the applied pressure pulse by means of an orifice and cavity so that the natural modes are not excited.
- (c) use electronic filtering to remove the oscillatory components of the response.

The first of these three approaches has been discussed in detail by Edwards (1958). It is only useful where size is not important, since it leads to rather 'long' transducers, but for fast response, the "matched-backing" transducer is unsurpassed.

The other two approaches have been discussed in Section 4, where it is concluded that electronic filtering is superior to acoustic filtering.

Assuming that the signal to be filtered has an oscillatory component at a frequency  $f'_0$  the initial amplitude of which is a fraction  $q$  of the steady state response, then it may be shown that for a 4-stage RC filter having a rejection ratio of 100:1 the rise time is given approximately by

$$t'_r = \frac{0.812}{f'_0} (10q^{\frac{1}{2}} - 1)^{\frac{1}{2}} \quad \text{for } q > 0.01. \quad \dots(22)$$

Taking the transducer rise time as  $1/4f'_0$  we arrive at the approximate expression for the overall rise-time as

$$t_r = \frac{(6.6q^{\frac{1}{2}} - 0.6)^{\frac{1}{2}}}{f'_0} \quad \dots(23)$$

Thus as  $q$  goes from 0.01 to 1 the product  $f'_0 t_r$  goes from 0.25, which is the value for the transducer alone, to 2.45. Hence the useful rise time of a transducer depends not only upon its natural frequency but also upon the relative amplitude of the oscillatory component at this frequency.

The vibrations of the diaphragm may contribute a significant portion of the oscillatory signal unless some care is exercised in design. Supposing that vibration of the element (and anvil) may be neglected, the force transmitted to the element will consist of a steady part  $W'_e$  and a fluctuating part  $W'_d$  due to the diaphragm reaction. In a single-degree of freedom system excited by a step-input, the peak stress is twice its steady state value, with this steady response as the mean of the vibration. By analogy it seems a reasonable inference that the force transmitted to the element will have an oscillatory component of amplitude  $2W'_d$  at a frequency corresponding to the particular diaphragm mode excited.

Where the response is to be "element-dominated",  $W'_d$  should therefore be small, and this corresponds to  $z \rightarrow 1$  which is the same requirement as for high sensitivity. Additionally the diaphragm thickness should be such as to

give a high natural frequency, but its stiffness must be low to meet the requirements of high sensitivity. According to Southwell (1936),

$$f_{\text{diaph.}} = \beta(z) \frac{t}{a^2} \sqrt{\frac{E}{3\rho(1-\nu^2)}} \dots\dots(24)$$

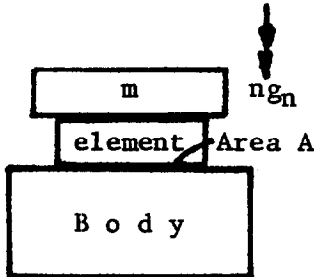
where

z	0	0.1	0.2	0.3	0.4	0.5	0.6	0.7	0.8	0.9
$\beta$	1.93	2.30	2.86	3.70	5.02	7.18	11.2	19.9	44.3	(179)

When the response is not element-dominated, the oscillation modes of the diaphragm are likely to interact with those of the element and anvil. It is not possible to generalise any further and designs must be considered individually.

### 6.3 Acceleration response

One of the most serious problems associated with the measurement of pressure using piezoelectric sensors is that the element responds also to acceleration and vibration. The difference between the two is largely one of the wavelength of the motion. When the wavelength is much longer than a typical dimension of the transducer, the latter undergoes an acceleration; when the two are of the same order, the transducer vibrates. The transducer will respond to an acceleration in any direction, but usually the most important direction is normal to the sensing surface. A convenient measure of the acceleration response is the equivalent pressure causing the same output as an acceleration of one ' $g_n$ '.



We may represent by  $m$  the combined mass loading on the sensing surface of the element due to the pressure plate, diaphragm, anvil and any other attached parts. When the transducer is subject to an acceleration  $ng_n$  as shown, there will be an effective negative pressure  $\Delta p$  on the sensing element given by

$$\Delta p = \frac{mng_n}{A} \dots\dots(25)$$

so that the acceleration sensitivity is  $\frac{mg_n}{A}$  convenient unit being ' $\text{torr}/g_n$ '.

It is thus proportional to the mass/area supported by the element. Although it depends to some extent on the relative areas of element and pressure plate, typical values for brass are:

- 0.15 torr/ $g_n$  for a diaphragm 0.25 mm thick
- 1.0 torr/ $g_n$  for a pressure plate 1.6 mm thick

In addition there is an effect due to the mass of the element itself,

and this may be taken into account by assuming a mass of one half that of the element distributed over its surface.

For a PZT-5 element 1 mm in thickness, the acceleration sensitivity is about  $0.3 \text{ torr}/g_n$ .

The acceleration sensitivities in directions other than normal to the sensing surface depend upon the appropriate element sensitivities in those directions. It is not possible to generalise in this case, but it is clear that in all cases the mass supported by the element should be minimised.

### 6.3.1 Transducer mounting

The way in which the transducer is mounted will have an effect on the acceleration response. Often it is necessary to provide a vacuum seal in the form of a rubber O-ring or washer. When this is mounted 'behind' the transducer, the force on the transducer due to the pressure on its sensing surface can produce significant accelerations. Seals should therefore be mounted in front of a shoulder, with a rigid backing behind the transducer. With pressure transducers located in sting-mounted models, the forces and moments on the model often produce large accelerations. In these circumstances it is necessary to compensate for the acceleration response. This is usually done by having a second element within the transducer as nearly identical in properties and mechanical loading as is possible, but not subjected to the pressure being measured. The difference in output between the two elements then corresponds to the required pressure sensitivity, compensated for acceleration response.

It has sometimes been the practice to remove vibration components by electronic filtering. This is undesirable because the frequencies of such components are often within the dynamic range of interest. With electronic filtering the lowest vibration frequency will determine the upper limit of the usable frequency response, and consequently the effective rise time.

Since these vibration frequencies are usually lower than the natural modes of the transducer, filtering does not allow the transducer to be used to full advantage.

### 6.4 Cross-axis sensitivity

In addition to responding to loads normal to the sensing face, transducers often respond to loads parallel to the diaphragm. Such forces may be applied by vibration of the mounting. Two factors are important in determining the cross-axis sensitivity. The first is the magnitude of the stress in the element induced by a transverse load applied to the transducer case, and this will depend on the way the element is mounted. The second is the element sensitivity in the appropriate mode.

Once the basic sensing mode has been chosen, nothing can be done about the transverse sensitivity. The only way therefore to reduce the cross-axis sensitivity is to reduce the stress in the element caused by transverse loading of the case. This may be partly a question of design, but mounting of the transducer is of some importance. A minimum of rigid contact between the transducer and its mounting should be provided, though some means of positive location is usually required.

## 6.5 Thermal response

In addition to their pressure response, many piezoelectric materials are also pyroelectric. A temperature change within the material is indistinguishable from a pressure change so far as the electrical output is concerned. In addition, the piezoelectric constants themselves change with temperature. (The two effects are related).

Where the temperature of the test gas whose pressure is being measured is high, the heat flux into the transducer may affect the element and consequently the accuracy of measurement. In some transducers it may be possible to use a sufficiently thick diaphragm or pressure plate so that the element is effectively shielded, but in high sensitivity transducers this cannot be done. There is some compensation in that the regions of highest heat flux are usually stagnation regions where less sensitive transducers may be used.

Where transducers cannot be designed with adequate shielding, it is common to avoid direct contact between the hot flow and the transducer by mounting the latter behind a cavity and orifice. The thermal capacity of the gas within this cavity is then low enough for it to be close to the temperature of the surrounding metal. (Where necessary this may be cooled - particularly in continuous flow environments).

The orifice and cavity have a considerable effect on the transducer response characteristics - in particular the effective response time is lengthened.

## 6.6 Linearity and repeatability

The linearity of a calibration is to some extent a matter of convenience and ease of interpretation. If the calibration curve is known over the working range linearity is unimportant. Perhaps this is to state the obvious. But the calibration curve must be known not only for the transducer but for all elements of the measuring system such as the amplifier and C.R.O., and for all combinations of the likely sensitivity settings. The 'convenience' of a linear calibration is now apparent.

There are two aspects of repeatability. The first relates to the consistency of performance of a single transducer (and its associated amplifier) and the second to different transducers of nominally identical construction. If frequent recalibration is to be avoided, the sensitivity should be free of long term and short term variations. It must therefore be insensitive to ambient conditions, - humidity and temperature - and ageing should not affect its important components. The aim should be that the combined effects of non-linearity and ambient conditions, etc. should be less than 1% of the nominal sensitivity.

The similarity in performance between nominally identical transducers is really a reflection of the amount of control the designer actually has over transducer performance. It is unlikely that successive samples of a particular design will have sensitivities and natural frequencies which differ by less than about  $\pm 10\%$  since at present the piezoelectric properties of ceramics vary by up to  $\pm 5\%$ , (though quartz is rather better). From a commercial viewpoint a very large proportion of the transducers built should be usable, so that the design should ensure that those factors which have significant effects are accurately controllable. Where for example the sensitivity depends critically

upon the properties of a glued joint, poor repeatability is likely. One beneficial side-effect of this requirement is that designs are basically simple. However to examine this aspect of repeatability would require at least half a dozen transducers built to the same design, and this was outside the scope of the project.

### 6.7 General mechanical features

Where pressure transducers are to be mounted in a model in the shock-tunnel, or even an ordinary wind tunnel, size is usually of some importance. Moreover it is desirable that the pressure should be "averaged" over as small an area as possible. Frequently it is necessary to use a small hole in the surface of the model, this hole being connected via tubing and perhaps a cavity to the sensing face of the transducer. As we have seen this impairs the high frequency response, and even where it is necessary it is advantageous to have a small cavity and connecting pipe. Since all the transducers to be described were prototypes rather than production models, less emphasis has been placed on reduction in size. However the possibility of later miniaturisation has been borne in mind during their design.

So that a minimum of disturbance to the flow occurs, pressure transducers are mounted flush with the model surface. A positive means of location is therefore required, and this is conveniently provided by a spigot, so that fixing is obtained by clamping it against a suitably machined surface. Where vacuum sealing is needed an O-ring or similar seal may frequently be incorporated around this spigot. The transducer should also be designed as a sealed unit, since leakage will affect the load on the diaphragm. Co-axial sockets are a frequent source of such leakage.

Finally a piezoelectric element is a high impedance device, and consequently a significant e.m.f. may be induced as "pick-up". One way of minimising this pick-up is to have the system electrostatically shielded. So far as the transducer is concerned, the outer case should be of a good conducting material, with good electrical connection between its various parts. It is common practice to use the case as one "side" of the transducer output connection.

## 7. Prototype transducers

In section 2 the relative merits of a variety of piezoelectric element sensing modes were assessed. It was concluded that for direct pressure sensing the normal compressive mode and the bimorph disc in bending were best, while the shear mode and the bimorph beam cantilever were best suited for the force-sensing type of transducer. Fig.8 (a)-(g) shows various ways in which the elements may be incorporated into a transducer in a fairly simple fashion. The first three use elements in the normal compressive mode. Fig.8(a) shows an element used in a "matched-backing" transducer. No transducers of this type were built since they would be too large for the present application. The second and third type differ only in the relative diameters of the diaphragm and sensing element/anvil. Type (b) will be element-dominated while type (c) in which only the central region of the diaphragm is supported, will have its response dominated by the diaphragm.

The most convenient way of using the bimorph disc in bending is shown at (d), the element being centrally-supported. The only other suitable mode uses pinned edge conditions which are difficult to achieve in practice.

A shear tube is shown at (e), and here an anvil is necessary to transmit the pressure. The element is fixed to the case at the outside and to the anvil on the inside of the tube.

The two final configurations shown at (f) and (g) illustrate the bimorph cantilever. The first will produce a diaphragm-dominated response, whereas that at (g) having the diaphragm supported over most of its surface will be element-dominated. Although a diaphragm-dominated response is not usually desirable, in this case type (g) is not necessarily superior because of the low-stiffness of the element.

A variety of transducers has been built and tested to measure some of the more important quantities mentioned in Section 6. The charge sensitivity, the natural frequency and the minimum useful rise time of the less sensitive types have been measured in a shock-tube. The more sensitive transducers were calibrated using the N.P.L. semi-dynamic calibrator since these transducers could easily be damaged in the shock-tube environment (as distinct from the expanded flow in the hypersonic working section for which they are intended). Their natural frequencies were estimated by examining their response to the noise made by knocking sharply together, two pieces of metal, it being ascertained that the particular metal used was unimportant. Although the other parameters mentioned in Section 6 have been taken into account during design, it has not yet proved possible to measure them.

### 7.1 Normal compressive mode transducers

For an element in the normal compressive mode the charge sensitivity to pressure  $Q_p$  is proportional to the sensing surface area and the natural frequency  $f_0$  is inversely proportional to the thickness. Thus optimum performance is obtained by thin discs of large surface area. Although "stacking" plates will improve the sensitivity, only single element transducers have been built so far, mainly in the interest of simplicity in the development stages. The natural frequency of the transducer will be determined not only by the element but also by the backing material, though the effect is rather complex. As in all transducers the mass loading on the element should be kept to a minimum in order to diminish the acceleration responses.

#### 7.1.1 The type E compression transducer

The first compression element transducer designed and built is shown in Fig.9. It uses as the sensing element a cylinder of PZT-5H, 3 mm in diameter and 3 mm thick, so that the basic parameters for the element alone are

$$Q_p = 0.56 \text{ pC/torr} ; f_0 = 320 \text{ kHz.}$$

The transducer case is brass, and the cavity in which the element is mounted is 6.3 mm in diameter and 6.3 mm deep. This diameter ensured that in cementing the diaphragm into place, any cement displaced into the gap between the walls and the element did not glue the element to the walls and hence impair the sensitivity. After soldering the electrical leads to the plated surfaces, the ends were built up with a layer of Araldite about 1.5 mm thick to provide the necessary insulation.

This transducer was shock-tube calibrated, two calibration curves being shown in Fig.11. Some typical output traces are also shown in Fig.10 with and without electronic filtering.

The measured sensitivity is 0.92 pC/torr compared with the figure of 1.35 pC/torr when account is taken of the diaphragm contribution to sensitivity. The difference is probably due to surplus cement on the diaphragm; small amounts will readily alter the effective ratio  $z$  of inner to outer diameter, and this causes large changes in sensitivity. This suggests that cementing is not a good way of attaching the diaphragm.

The linearity appears to be good and is certainly within the limits of experimental error. This gauge has been calibrated on separate occasions, yielding figures of 0.929, 0.914 and 0.925 pC/torr over the range 0-900 torr. These differences are within the experimental error.

From traces such as that in Fig.10, the fundamental resonance appears to be at about 45 kHz with a higher frequency component at about 240 kHz superimposed. Since the diaphragm contribution to sensitivity is some 40%, it is likely that this low resonant frequency is also due to the diaphragm. Assuming a clamped edge the natural frequency of the diaphragm was estimated to be about 100 kHz, but the fact that it is cemented in place probably means that the fixing is not very rigid and in addition the attached mass would have some effect. The low frequency could also be due to a vibration in bending of part of the housing. The high frequency component is probably attributable to the element.

#### 7.1.2 The type F compression transducer

The type F transducer in Fig.12 was designed to offer higher sensitivity and natural frequency than the type E, and also to assess the acceleration compensation technique. The two identical discs of PZT-5H are 6 mm in diameter and 2 mm thick, and they are mounted back-to-back in such a way that the rear disc senses only acceleration. The basic performance parameters of the isolated element are

$$Q_p = 2.23 \text{ pC/torr} ; f_o = 480 \text{ kHz} .$$

The construction technique was similar to that of type E. In an effort to ensure similarity of the two halves, the lead out wires were taken through the clamped rather than the active portion of the rear diaphragm. It had been hoped that the output from each disc could be brought out through its own coaxial socket, but the sockets available at the time were too large.

The results of shock-tube calibration are shown in Fig.14; the lower range calibration from 0-300 torr shows non-linearities of order 2% and an intercept on the charge axis at about 8 pC both of which are at the limit of the estimated experimental error.

The results of three separate calibrations are 3.11, 3.12, and 3.12 pC/torr, which is again some 40% higher than the basic element sensitivity, for similar reasons to those for type E.

The transient responses illustrated in Fig.13 show the major resonant frequency at 64 kHz with a smaller component at half this frequency. The oscillations are far less regular in amplitude than those of type E, and again none of the frequencies corresponds closely to any of those calculated.

The difficulty of assessing accurately the factors which govern the transient response constitutes the major deficiency of the type E and type F transducers. An attempt was therefore made to simplify the design to one

which might allow a closer theoretical examination of the performance.

### 7.1.3 The type I compression transducer

The two compression transducers previously described had their diaphragms cemented in place, and this meant that the gap between the element and case had to be relatively large and so also did the walls of the casing in order to ensure an adequate surface for adhesion. The transducer is thus rather larger than is perhaps necessary. Spot welding would seem to be a suitable method of fixing the diaphragm, but unfortunately facilities were not available. By using the assembly technique to be described, the number of cemented joints was somewhat reduced. After machining the main case, see Fig.15, the diaphragm and pressure plate were made in one piece, the diaphragm being left some 0.3 mm thicker than finally required, but its outside diameter was accurately dimensioned. The upper surface of the case and the corresponding diaphragm surface were tinned with soft solder, any surplus being removed. The two parts were reheated, placed together in a jig and allowed to cool slowly. The edge of the diaphragm was then trimmed in a lathe and the face machined away carefully to leave the desired thickness. The disc of PZT-5H and the backing piece were cemented together and the locking nut and coaxial socket screwed together. The upper surfaces of the latter were covered with Araldite, which was then machined leaving the tip of the pin protruding. The hole in the backing plate was filled with conducting paste and when assembly was complete Araldite was used to fix the locking cylinder in place.

Two examples of this type,  $I_1$  and  $I_2$  were built, using ceramic discs 1 mm thick. The first has a disc 5 mm in diameter giving basic performance figures of

$$Q_p = 1.55 \text{ pC/torr and } f_o = 960 \text{ kHz}$$

The second has a disc of 6 mm diameter, giving  $Q_p = 2.23 \text{ pC/torr}$ .

The results of shock-tube calibration are shown in Figs. 17(a) & (b) for  $I_1$  and  $I_2$  respectively. We consider type  $I_1$  first.

The most noticeable feature is the discontinuity in slope at about 650 torr. The slope of the lower curve is 1.08 pC/torr and that of the upper portion 1.37 pC/torr. The calibration over the range 0-300 torr has a slope of 1.11 pC/torr and an intercept on the pressure axis at about 3 torr. These features are almost certainly due to the transducer being assembled using a "pre-loading" technique. Unless all the surfaces are flat and parallel during assembly there is bound to be some play in the system. This would imply that at low pressures a larger portion of the load is carried by the case than at higher pressures when the play is taken up. The sensitivity would thus increase with pressure level. It is interesting to note that the sensitivity at the higher pressure levels compares well with the expected value.

The natural frequency of the type  $I_1$  is about 40 kHz, very much lower than the theoretical value. The transducer was designed in the hope that only compressive vibrations would be excited. The overall length is about 16 mm, so that a compressive wave would take about 5  $\mu$ s to reach the back (at about 3360 m/s in brass). The corresponding frequency would be 50 kHz. The first two 'cycles' of the response, Fig.16(a), are close to ramp functions which suggest that the initial response is caused by the reflection of compression waves. It seems clear that a detailed investigation into the effects of

backing material is needed.

The responses of the second version  $I_2$ , shown in Fig.16(b) leave much to be desired. In addition to the major component close to that observed for type  $I_1$ , there is a significant component at about 5 kHz with a very irregular form. This again is probably accounted for by the pre-loading. In view of the poor transient response, and the difficulty in interpreting the traces, the calibration is surprisingly linear. However the sensitivity is only 0.66 pC/torr, some 30% of the theoretical value. A substantial portion of the load is carried by the case, and we must conclude that pre-loading during construction is undesirable, except perhaps where facilities for very accurate surface finishing are available.

## 7.2 Shear element transducers

In section 2 we noted that the relevant sensitivity parameter for elements in the shear mode is  $Q_F$  and that this is independent of the size of the element. Consequently the sensitivity of the transducer will be determined by the total load transmitted for a given pressure and this will be directly proportional to the surface area of the anvil which is used to transmit the load.

From a practical viewpoint, the symmetry afforded by using a cylindrical shear tube has considerable advantage over a shear plate which would probably lead to a performance dependent upon orientation. Although the stiffness in shear is high, the natural frequency of the transducer is likely to be governed by the vibrations of the anvil.

### 7.2.1 The type G shear-tube transducer

The basic construction of the type G transducer is shown in Fig.18. The sensing element is a shear tube of PZT-5H the outside diameter of which is 6.33 mm, the length is 6.35 mm and the wall thickness is 0.5 mm. Two versions were built, the main differences being in the materials used and the method of assembly. The basic sensitivity of the element is 584 pC/newton, so that assuming the entire load on the sensing surface of the transducer ( $0.97 \text{ cm}^2$ ) is transmitted to the element, the pressure sensitivity is 7.53 pC/torr.

With type  $G_1$  the anvil was first attached to the element and then the outside of the element was covered with Araldite and the assembly pushed into the case from the front. It was held in place by jigs while the Araldite cured. The diaphragm was then cemented in place using Araldite again. Upon calibration the sensitivity was found to be only about 1 pC/torr. The diaphragm was thereupon removed in a lathe as was also the considerable amount of surplus cement which, as suspected, had found its way between the anvil and the case. A new diaphragm was fixed in place using a conducting paste\* which did not 'run' as readily as Araldite.

Upon recalibration the results of Fig.20(a) were obtained; the two calibration values of 4.94 pC/torr and 5.10 pC/torr are much closer to the theoretical values. There appear to be non-linearities of about 5%, but there was some difficulty in interpreting the traces, a point we shall discuss later with transient response.

---

\* Johnson Matthey type FSP 49.

Because of the difficulties experienced with cementing the diaphragm, a second version was built using a 'spot-welding' technique. Stainless steel was used in place of brass and duralumin. The diaphragm and anvil were first spot-welded together around the periphery of the anvil and then the shear tube was attached. The diaphragm/anvil unit was spot-welded to the case and Araldite was forced between the case and the element. It was difficult to ensure that none found its way past the element to restrict the freedom between the anvil and the case.

The calibration curve for the type  $G_2$  is shown in Fig.20(b). The linearity is somewhat better than that for type  $G_1$  but there is an intercept on the pressure axis at about 20 torr, which suggests a non-linearity below about 100 torr. The measured sensitivity is only 3.03 pC/torr, well below that of type  $G_1$  and this is probably due to surplus cement. The transient responses Fig.19, show that the dominant frequency is rather low, about 20 kHz. It is difficult to see how this arises. The compression wave transit time over 1 cm is about 2  $\mu$ s, so it is not likely to be a compressive vibration. Shear vibration of the element/Araldite layer loaded by the mass of the anvil has an estimated frequency of 50 kHz for the steel anvil of  $G_2$  and about 80 kHz for the duralumin anvil ( $G_1$ ). The only remaining mode would seem to be a bending one in which either the anvil bends or it rotates as a whole under an asymmetric shear load in the element. Since the sensing face of the anvil is somewhat larger than its base, a transverse shock could well excite this mode. One way of resolving this would be to test the transducer with a head-on shock.

A second disturbing feature of the transient responses is that the mean signal level appears to increase with time in some cases. A genuine rise in pressure may be discounted since no other transducers have shown it. Leakage into the case would cause the signal level to decrease and the element would appear to be well shielded from thermal effects. However the acceleration responses of the type G transducer are rather high due to the mass loading of the anvil. The estimated value for type  $G_1$  is about 1 torr/ $g_n$  and that for type  $G_2$  about 3 torr/ $g_n$  compared with 0.1 torr/ $g_n$  for a compressive type loaded by a 0.25 mm thick steel diaphragm.

If the effect is due to an acceleration the characteristic frequency is very low and the most likely source is a longitudinal bending of the shock-tube channel.

### 7.3 Bimorph disc transducers

The charge sensitivity to pressure of the bimorph disc is proportional to the fourth power of the diameter and inversely proportional to the square of the thickness. Thus very high sensitivities are possible using "broad, thin discs". The natural frequency is proportional to  $(t/d^2)$ .

The stiffness at the edge of the centrally supported disc is comparatively low, so that the effect of diaphragm stiffness must be carefully considered. When the element is cemented to the diaphragm, the element will be effectively stiffened and the sensitivity will be reduced.

#### 7.3.1 The type H bimorph-disc transducer

The type H transducer uses a bimorph disc of PZT-5B, 8 mm in diameter and 0.53 mm thick. The basic performance parameters are thus  $Q_p = 47$  pC/torr and  $f_0 = 17$  kHz for the element alone. The design of this transducer, illus-

trated in Fig.21, owes much to an earlier design of Macdonald and Cole (1963). Two models were built. The assembly technique identical for both, is fairly obvious and will not be described.

These transducers were designed for low pressures, well below 100 torr and it was felt unwise to test them in the shock tube where minimum peak pressures of 1500 torr were likely. They were therefore calibrated in the N.P.L. semi-dynamic calibrator, a typical response being shown in Fig.22. The calibration curves of both  $H_1$  and  $H_2$  are shown in Fig.23. When account is taken of the diaphragm loading the theoretical sensitivity is 66 pC/torr. The measured values are 48.9 pC/torr for type  $H_1$  and 59.6 pC/torr for type  $H_2$ . The design appears to use the element to full advantage, at least as regards sensitivity. The linearity is good, but both transducers have intercepts on the pressure axis, roughly 1 torr for the  $H_1$  and 2 torr for the  $H_2$ . Because of the difference it seems unlikely that these could be due to a zero error in the static pressure gauge used with the calibrator; the cause remains undetermined.

The high sensitivity of these transducers enabled their natural frequencies to be estimated somewhat crudely by examining their response to a loud sharp noise. From these responses the natural frequency of type  $H_1$  was found to be 19 kHz and for type  $H_2$  27 kHz. Again surplus cement is likely to account for the difference from the theoretical value, and in this case it would decrease the sensitivity and increase the natural frequency. However type  $H_1$  has the lower sensitivity and the lower natural frequency so this cannot be the whole explanation. Nevertheless it is hoped that improvements in manufacturing technique will produce a transducer with a performance even closer to the theoretical.

#### 7.4 Bimorph beam transducers

With a cantilevered bimorph beam the load is applied essentially as a point load. Were a simple rod to be used as the anvil the fraction  $W'/W$  of the load on the diaphragm that would be transmitted would be little more than 0.25. The larger is the ratio  $z$  of the inner to outer diameters, the larger is the fraction of the total load transmitted to the element. On the other hand the high sensitivity of the bimorph beam element arises from its low stiffness and a stiff diaphragm reduces the transmitted load. Increasing  $z$  stiffens the diaphragm considerably: for example as  $z$  increases from 0 to 0.5 the stiffness increases by a factor of 10, and from 0 to 0.75 by a factor of 100. Thus as  $z$  is increased to improve the sensitivity the effects on diaphragm stiffness must be borne in mind.

Estimation of the natural frequency of the transducer is far from easy. A reasonable assumption is that the natural frequency of the anvil is high enough to be neglected, but even so we have an annular diaphragm and a cantilever beam coupled by the mass of the anvil. From a design point of view it is clear that the diaphragm should be as thick as possible consistent with sensitivity requirements and the mass of the anvil should be small.

The important sensitivity parameter  $Q_F$  for the beam is proportional to the square of the length to thickness ratio. Although it is possible to have bimorph beams made in a wide range of sizes to order, beams are available from stock, chiefly for use in gramophone cartridges. One of these stock sizes was chosen for the type K transducers.

#### 7.4.1 The type K bimorph-beam transducer

Two type K transducers were designed which differed only in the mass of the anvil. They are illustrated in Fig.24. Three versions were built, one of type  $K_1$  and two of  $K_2$  ( $K_{2A}$  and  $K_{2B}$ ). The sensing element is cut from a series-polarised bimorph strip, 1.02 mm x 0.53 mm in cross-section to a length of 9 mm. The element was cemented into a blind hole in a perspex rod 3 mm in diameter, which was then cemented into the case. The active length of the element was 5 mm.

The two anvil types were of the same length and surface area, but more material was removed from type 2 to reduce its mass. The anvil was in each case cemented to a stainless steel diaphragm 0.025 mm thick with Araldite, and this assembly was cemented to the case, the tip of the anvil being at the same time cemented to the element.

The calibration curves shown in Fig.26 were obtained using the N.P.L. semi-dynamic calibrator, typical traces being shown in Fig.25. The low frequency responses of  $K_1$  and  $K_{2A}$  are very poor, the overall time constants being about 50 ms and 20 ms respectively. There was no improvement after careful cleaning of all the electrical connections and it is inferred that some of the internal insulation is imperfect, since the type  $K_{2B}$  using an element from the same batch has a very large time constant.

The linearity of the calibration of  $K_{2B}$  is good but its sensitivity is only 3.55 pC/torr compared with a theoretical value of 65 pC/torr. Since the sensitivity is critically dependent upon the stiffness of the diaphragm, it seems likely that the small gap of 1.5 mm between the anvil and the case has been partially filled with surplus cement.

The low time constants made interpretation of the traces for  $K_1$  and  $K_{2A}$  somewhat difficult but the sensitivities are much higher than the  $K_{2B}$ , being 20.8 pC/torr and 31.1 pC/torr respectively. These are less than half the theoretical values, and the deficiency is probably due to surplus cement. Indeed at an early stage the diaphragm and anvil assembly of  $K_{2A}$  came away from the case revealing a large amount of surplus cement, though this had not adhered to the case. It was repaired using Kodak Eastman type 910 adhesive. This is a contact adhesive which does not 'run' once applied, and it merits attention for future designs.

The natural frequencies were estimated in the same way as those of the type H transducers. The measured value of the type  $K_1$  is 5.5 kHz. The natural frequency of the element alone is about 10 kHz and the value based on the tip stiffness of the cantilever and the mass of the anvil is about 3.2 kHz, somewhat lower than the observed value. However the measured sensitivity is only about one third of the theoretical value, and this is thought to be due to stiffening of the diaphragm by surplus cement. When the natural frequency is computed using the effective stiffness inferred from this measured sensitivity, we obtain 5.5 kHz, the observed value.

Corresponding values for the other two models are

	$K_1$	$K_{2A}$	$K_{2B}$
Measured, $f'_0$ /kHz	5.5	7.2	16
Theoretical, $f'_0$ /kHz	3.2	4.3	4.3
Semi-empirical, $f'_0$ /kHz	5.5	6.2	18

Thus even for the type  $K_{2B}$ , for which the sensitivity is only 5.5% of the theoretical, this semi-empirical value of the natural frequency is quite close to the measured value, supporting the inference that it is due to surplus cement.

### 7.5 Environmental testing

For the less sensitive transducers, that is the compression types and the shear-tube type G, the calibration procedure carried out in the shock tube provides a fairly good test of their likely performance in the environment for which they were designed. The type E transducer was used for a further wide range of measurements in the shock-tube, using both nitrogen and hydrogen to drive shocks in nitrogen. The detailed results produced could be satisfactorily explained in terms of the flow processes known to occur and no further features of the transducer performance were brought to light.

The same transducer was then mounted for pitot pressure measurement in the hypersonic flow formed by expanding the hot nitrogen behind the reflected shock in the shock-tube through a  $10^\circ$  half-angle conical nozzle. The first test indicated an apparent negative absolute pressure after about  $2\frac{1}{2}$  ms of flow! The diaphragm, which was wholly exposed to the hot stagnant gas, was covered with a thin layer of vacuum grease for subsequent tests, and the effect disappeared. The pitot pressure records reflect fairly closely, with a time lag of course, the pressure variations in the nozzle reservoir which were simultaneously monitored with a Kistler 701A quartz transducer, Fig.27. The flow properties inferred from these tests accorded well with theoretical estimates which included an allowance for the flow conicity and boundary layer growth on the nozzle wall.

The sensitivity of the type E transducer is 0.9 pC/torr and in view of the earlier discussion it should not be used for pressure levels below about 1 torr. Used to measure pitot pressure of about 10 torr it was found to be satisfactory, but for pitot pressures of about 2-3 torr the traces were rather noisy.

The type  $H_2$  bimorph-disc transducer was mounted flush with one of the surfaces of a  $25^\circ$  included-angle wedge. This wedge was sting-mounted in the hypersonic stream referred to above, the working-surface being parallel to the sting axis and about 2 cm above the flow centre-line. Tests were conducted at nominal incidences of  $-4^\circ$ ,  $0^\circ$ ,  $4^\circ$ ,  $8^\circ$  where negative values indicate an expansion from the free-stream to the measuring surface. The flow Mach number inferred from the pitot pressure measurements was about 9.1 so that the compression surface had an attached shock.

Again some of the traces, Fig.28, showed an apparent negative absolute pressure during the useful test time. It seemed unlikely that this was a thermal response and vacuum grease used as before failed to alter the effect. The transducer was then recessed from the surface and shielded from the gas pressure by taping a piece of steel shim over the cavity. The model was then tested at incidences of  $-4^\circ$  and  $+8^\circ$  and the results, Fig.28 strongly suggest an acceleration response. At a nominal incidence of  $-4^\circ$  and making an allowance of  $1^\circ$  for the model-offset and flow conicity, the mean incidence of the model is  $17\frac{1}{2}^\circ$  while at the nominal  $8^\circ$ , the centre-line incidence is only  $5\frac{1}{2}^\circ$ . The acceleration signals are in the ratio of about four to one, and it seems plausible that the net lift on the model causes the sting to vibrate in bending. This conjecture is supported by a record taken at a slow C.R.O.

sweep rate which shows a component of the response at a frequency which corresponds closely with that of the bending of the sting-model system in the vertical plane.

When a linear correction for the acceleration response is applied, the resulting pressures, which are in the range 0.1 to 1 torr, agree fairly well with approximate estimates that take some account of the leading edge "strong-interaction" effect but not of any possible vibrational non-equilibrium effects on the nozzle expansion. (The reservoir pressure and temperature were approximately 18 atm and 3700°K.)

## 8. Discussion.

As a general assessment of the prototype transducers described in Section 7 with those available commercially, Figure 29 has been constructed using the parameter  $f'Q_p$  for comparison. It will be appreciated from what has been said earlier that several other factors are also important. In particular linearity, repeatability and an absence of spurious responses are very desirable features of a transducer. Nevertheless Figure 29 is useful for making general observations. The reason that the commercial transducers have lower values of charge sensitivity natural frequency product is that they use as the sensing element, quartz which has a lower sensitivity. Thus in this regard the commercial transducers do not meet the specifications set out in Section 1. Some of the prototype gauges however show considerable promise; in particular types H and I meet the specifications as regards sensitivity and useful rise-time as defined by equation (23).

Most of the commercial gauges shown in Figure 29 use an element in the normal compressive mode\*. The basic design of the type I transducer, which also uses this mode, is felt to be satisfactory and it gives a smaller transducer with a better response than the type E. Major improvements are however required in manufacturing technique; in particular, welding of the diaphragm to the main case should replace cementing. Some doubts remain regarding the linearity at low pressure levels of transducers assembled using a 'pre-loading' technique.

The factors governing the transient response of compression transducers are not fully understood. The uncertainties arise mainly because of the complex wave interactions within the backing material rather than the element, and the type I design lends itself to an investigation of various backing materials and shapes. The sensitivity of normal compressive mode transducers may be increased by stacking several plates appropriately, but the layers of cement used in building the stack should be thin or the natural frequency will be adversely affected.

Levine (1961) has conducted some tests on transducers using acceleration compensation elements. It is important to remember that the compensating element should have a mass loading as nearly identical with the pressure sensing element as is possible. Since it is unlikely that all motions of the transducer will affect both elements equally it may be an advantage to have

---

\* The Kistler 603 uses an element in the transverse compressive mode.

separate output terminals so that different proportions of the signals may be added. In the one transducer built, the type F, this could not be arranged, and it has not yet been possible to assess the compensation aspect of the design. It should also be possible by careful design to arrange that the compensating element reduces the cross-axis sensitivity.

The type G shear-mode transducers have a fairly good sensitivity but a poor transient response. The latter is largely dependent upon the anvil, and this implies lower natural frequencies than compression transducers. Any increase in sensitivity will be outweighed by a decrease in natural frequency and except for special applications it is doubtful whether this design is worth further development.

The bimorph disc and beam are best suited to high sensitivities. From the results presented here for the type H transducer and from those of Macdonald and Cole (1963) the performance of bimorph disc transducers is close to the theoretical. It should not be difficult to make further improvements and introduce acceleration compensation into a smaller transducer. An output socket at the side would aid mounting in slender models.

The bimorph beam is the best known of the bending modes (Martin et al, 1962, Lederman and Visich, 1965). For the transducers described in section 7.4 considerable improvements in manufacturing techniques are required. Because of the loading by the anvil the natural frequency is somewhat lower than that obtainable with the bimorph disc and the acceleration sensitivity is rather high. It would therefore be advisable to incorporate acceleration compensation as in those designs referenced above, bearing in mind that the diaphragm as well as the anvil affects the acceleration sensitivity.

References

- Aronson, P.M. 1963  
Waser, R.H. Pressure pulse generator for the calibration of pressure gauges.  
U.S. Naval Ordnance Laboratory, TR 63-143.
- Bernstein, L. 1963 Equilibrium real-gas performance charts for a hypersonic shock-tube wind-tunnel employing nitrogen. A.R.C. C.P.633.
- Cady, W.G. 1964 Piezoelectricity.  
Dover Publications Inc., New York.
- Edwards, D.H. 1958 A piezoelectric pressure bar gauge.  
Journal of Scientific Instruments, 35 p.346.
- Lederman, S. 1965  
Visich, M. Acceleration compensated low level pressure transducer. N.A.S.A. CR-286.
- Levine, D. 1961 Acceleration-compensating pressure transducers for surface pressure measurements.  
U.S. Naval Ordnance Laboratory Report 6834.
- Lewis, J.A. 1961 The effect of driving electrode shape on the electrical properties of piezoelectric crystals.  
Bell System Technical Journal, 40, pp.1259-1280.
- Macdonald, W.R. 1963  
Cole, P.W. New piezoelectric pressure transducers for aerodynamic research.  
R.A.E. Technical Note IR 23, A.R.C.25056.
- Martin, J.F. 1962  
Duryea, G.R.  
Stevenson, L.M. Instrumentation for force and pressure measurements in a hypersonic shock tunnel.  
Advances in hypervelocity techniques, Edit. A.M. Krill, Proc. 2nd Symposium on hypervelocity techniques, Denver, Colorado, Distrib. by Plenum Press, New York.
- Mason, W.P. 1947 First and second order equations for piezoelectric crystals expressed in tensor form.  
Bell System Technical Journal, 26, p.80.
- Pallant, R.J. 1966 A note on the design and construction of a low-pressure calibrator and a comparison with shock-tube and static calibration methods.  
A.R.C. C.P.947.
- Pennelegion, L. 1966  
Wilson, K.  
Miss Redston, B. The accuracy of pressure transducers when used in short duration wind tunnel facilities.  
A.R.C. C.P.949.
- Pierce, D. 1964 A microsecond response pressure transducer for blast wave measurements. A.R.C. C.P.747.
- Redwood, M. 1961a Transient performance of a piezoelectric transducer.  
Journ. Acous. Soc. Am. 33 pp.527-536.

- Redwood, M. 1961b Piezoelectric generation of an electrical impulse.  
Journ. Acous. Soc. Am. 33 pp.1386-1390.
- Roark, R.J. 1954 Formulae for stress and strain.  
McGraw-Hill Book Co. Inc. New York.
- Southwell, R.V. 1936 An introduction to the theory of elasticity.  
Oxford University Press, London.
- Valley, G.E. 1948 Vacuum tube amplifiers.  
Wallman, H. McGraw-Hill Book Co. Inc., New York.
- van der Ziel, A. 1954 Noise, Prentice Hall, New Jersey.

Acknowledgement

The authors would like to express their gratitude to the Ministry of Technology which supported this work under an extra-mural agreement.

Notation

A	area
a	radius <u>or</u> major radius
B	volume of piezoelectric element
b	width of element <u>or</u> minor radius
C	capacitance
C <sub>B</sub>	decoupling capacitance, see Fig.2(c)
C <sub>cal</sub>	calibration capacitance
C <sub>e</sub>	parallel capacitance across amplifier input (less C <sub>o</sub> )
C <sub>f</sub>	feedback capacitance
C <sub>o</sub>	transducer capacitance
D, D <sub>i</sub>	electric displacement
d <sub>ijk</sub> , d <sub>in</sub>	piezoelectric constants
d	diameter
E	Young's modulus
E, E <sub>i</sub>	electric field strength
$\bar{E}_i$	electric field strength due to unit applied voltage
F	force
f <sub>diaph</sub>	natural frequency of diaphragm
f <sub>o</sub>	natural frequency of piezoelectric element
f' <sub>o</sub>	lowest resonant frequency of transducer
g <sub>n</sub>	standard specific force due to gravity
h	piezoelectric element dimension, see Fig.1
I	second moment of area
i, j, k, l	as suffices 1, 2, 3
j	complex operator = $\sqrt{-1}$
K <sub>e</sub>	stiffness of element
k <sub>e</sub>	= $K_e \left( \frac{3(1-\nu^2)a^2}{4\pi Et^3} \right)$
k <sub>p</sub>	= $\left( 1-z^2 - \frac{4z^2}{1-z^2}(\log z)^2 \right)^{-1}$
L	inductance
l	length of bending element, see Fig.1

M	bending moment
m	amplifier gain <u>or</u> mass
m,n	as sufficies 1,2,...,6
n	amplifier characteristic gain slope <u>or</u> number of stages in filter
p	pressure
Q	electric charge
$Q_F$	charge sensitivity to force = $Q/F$
$Q_p$	charge sensitivity to pressure = $Q/p$
q	fractional magnitude of oscillatory component, see equation 22.
R	electrical resistance
$R_B$	biasing resistance
$R_f$	feedback resistance
$R_i$	input resistance of amplifier on open-loop
$R_o$	transducer d.c. impedance
$S, S_{ij}, S_n$	elastic strain
$s_{ijkl}, s_{mn}$	elastic compliances
$T, T_{ij}, T_n$	mechanical stress (superscript <sup>o</sup> refers to electrically free condition)
t	thickness of element <u>or</u> diaphragm
$t_r, t'_r$	rise time of signal
V	voltage
$V_{cal}$	calibration voltage
$V_F$	voltage sensitivity to force = $V/F$
$V_o$	amplifier output voltage
$V_p$	voltage sensitivity to pressure = $V/p$
v	wave velocity
W	total load on diaphragm
$W'$	load transmitted to element
$W'_d$	diaphragm component of $W'$
$W'_e$	normal force on element } see Figure 7
$x_i$	spatial coordinate
z	diameter ratio of diaphragm = $b/a$
$\beta$	frequency coefficient defined by equation 24
$\epsilon_{ij}$	dielectric permittivity
$\nu$	Poisson's ratio
$\rho$	density
$\tau$	time <u>or</u> time constant
$\omega$	radian frequency

TABLE 1      Properties of Piezoelectric Materials

α - quartz

$$\begin{array}{c}
 \left| \begin{array}{cccccc}
 s_{11} & s_{12} & s_{13} & s_{14} & 0 & 0 \\
 s_{12} & s_{11} & s_{13} & -s_{14} & 0 & 0 \\
 s_{13} & s_{13} & s_{33} & 0 & 0 & 0 \\
 s_{14} & -s_{14} & 0 & s_{44} & 0 & 0 \\
 0 & 0 & 0 & 0 & s_{44} & 2s_{14} \\
 0 & 0 & 0 & 0 & 2s_{14} & 2(s_{11}-s_{12})
 \end{array} \right| \begin{array}{c} \\ \\ \\ \\ \\ \\ \end{array} \left| \begin{array}{ccc}
 \epsilon_{11} & 0 & 0 \\
 0 & \epsilon_{11} & 0 \\
 0 & 0 & \epsilon_{33}
 \end{array} \right|
 \end{array}$$

$$\begin{array}{c}
 \left| \begin{array}{cccccc}
 e_{11} & -e_{11} & 0 & e_{14} & 0 & 0 \\
 0 & 0 & 0 & 0 & -e_{14} & -e_{11} \\
 0 & 0 & 0 & 0 & 0 & 0
 \end{array} \right| \left| \begin{array}{cccccc}
 d_{11} & -d_{11} & 0 & d_{14} & 0 & 0 \\
 0 & 0 & 0 & 0 & -d_{14} & -2d_{11} \\
 0 & 0 & 0 & 0 & 0 & 0
 \end{array} \right|
 \end{array}$$

Rochelle Salt

$$\begin{array}{c}
 \left| \begin{array}{cccccc}
 s_{11} & s_{12} & s_{13} & 0 & 0 & 0 \\
 s_{12} & s_{22} & s_{23} & 0 & 0 & 0 \\
 s_{13} & s_{23} & s_{33} & 0 & 0 & 0 \\
 0 & 0 & 0 & s_{44} & 0 & 0 \\
 0 & 0 & 0 & 0 & s_{55} & 0 \\
 0 & 0 & 0 & 0 & 0 & s_{66}
 \end{array} \right| \left| \begin{array}{ccc}
 \epsilon_{11} & 0 & 0 \\
 0 & \epsilon_{22} & 0 \\
 0 & 0 & \epsilon_{33}
 \end{array} \right|
 \end{array}$$

$$\begin{array}{c}
 \left| \begin{array}{cccccc}
 0 & 0 & 0 & e_{14} & 0 & 0 \\
 0 & 0 & 0 & 0 & e_{25} & 0 \\
 0 & 0 & 0 & 0 & 0 & e_{36}
 \end{array} \right| \left| \begin{array}{cccccc}
 0 & 0 & 0 & d_{14} & 0 & 0 \\
 0 & 0 & 0 & 0 & d_{25} & 0 \\
 0 & 0 & 0 & 0 & 0 & d_{36}
 \end{array} \right|
 \end{array}$$

Polarised ceramics

$$\begin{array}{c}
 \left| \begin{array}{cccccc}
 s_{11} & s_{12} & s_{13} & 0 & 0 & 0 \\
 s_{12} & s_{11} & s_{13} & 0 & 0 & 0 \\
 s_{13} & s_{13} & s_{33} & 0 & 0 & 0 \\
 0 & 0 & 0 & s_{44} & 0 & 0 \\
 0 & 0 & 0 & 0 & s_{44} & 0 \\
 0 & 0 & 0 & 0 & 0 & 2(s_{11}-s_{12})
 \end{array} \right.
 \end{array}
 \begin{array}{c}
 \left| \begin{array}{ccc}
 \epsilon_{11} & 0 & 0 \\
 0 & \epsilon_{11} & 0 \\
 0 & 0 & \epsilon_{33}
 \end{array} \right.
 \end{array}$$

$$\begin{array}{c}
 \left| \begin{array}{cccccc}
 0 & 0 & 0 & 0 & e_{15} & 0 \\
 0 & 0 & 0 & e_{15} & 0 & 0 \\
 e_{31} & e_{31} & e_{33} & 0 & 0 & 0
 \end{array} \right.
 \end{array}
 \begin{array}{c}
 \left| \begin{array}{cccccc}
 0 & 0 & 0 & 0 & d_{15} & 0 \\
 0 & 0 & 0 & d_{15} & 0 & 0 \\
 d_{31} & d_{31} & d_{33} & 0 & 0 & 0
 \end{array} \right.
 \end{array}$$

TABLE 1 (Contd)

Quantity	Units	$\alpha$ -quartz	Rochelle Salt	BaTio <sub>3</sub>	PZT-5A	PZT-5H
E s <sub>11</sub>	10 <sup>-12</sup> m <sup>2</sup> /N	12.77	51.8	8.6	16.4	16.5
D s <sub>11</sub>		12.64		8.3	14.4	14.05
E s <sub>12</sub>		-1.79	15.3	-2.6	-5.74	-4.78
D s <sub>12</sub>		-1.66		-2.9	-7.71	-7.27
E s <sub>13</sub>		-1.22	-21.1	-2.7	-7.22	-8.45
D s <sub>13</sub>		-1.22		-1.9	-2.98	-3.05
E s <sub>14</sub>		4.50		0	0	0
D s <sub>14</sub>		4.46		0	0	0
E s <sub>22</sub>		E s <sub>11</sub>	34.9	E s <sub>11</sub>	E s <sub>11</sub>	E s <sub>11</sub>
D s <sub>22</sub>		D s <sub>11</sub>		D s <sub>11</sub>	D s <sub>11</sub>	D s <sub>11</sub>
E s <sub>23</sub>		E s <sub>13</sub>	-10.3	E s <sub>13</sub>	E s <sub>13</sub>	E s <sub>13</sub>
D s <sub>23</sub>		D s <sub>13</sub>		D s <sub>13</sub>	D s <sub>13</sub>	D s <sub>13</sub>
E s <sub>33</sub>		9.60	33.4	9.1	18.8	20.7
D s <sub>33</sub>		9.60		7.0	9.46	8.99
E s <sub>44</sub>		20.04	79.8	32.2	47.5	43.5
D s <sub>44</sub>		19.91		17.1	25.2	23.7
E s <sub>55</sub>		E s <sub>44</sub>	328	E s <sub>44</sub>	E s <sub>44</sub>	E s <sub>44</sub>
D s <sub>55</sub>		D s <sub>44</sub>		D s <sub>44</sub>	D s <sub>44</sub>	D s <sub>44</sub>
E s <sub>66</sub>		29.12	101	2(s <sub>11</sub> <sup>E</sup> -s <sub>12</sub> <sup>E</sup> )	2(s <sub>11</sub> <sup>E</sup> -s <sub>12</sub> <sup>E</sup> )	2(s <sub>11</sub> <sup>E</sup> -s <sub>12</sub> <sup>E</sup> )
D s <sub>66</sub>		28.58		2(s <sub>11</sub> <sup>D</sup> -s <sub>12</sub> <sup>D</sup> )	2(s <sub>11</sub> <sup>D</sup> -s <sub>12</sub> <sup>D</sup> )	2(s <sub>11</sub> <sup>D</sup> -s <sub>12</sub> <sup>D</sup> )

TABLE 1 (Contd)

Quantity	Units	$\alpha$ -quartz	Rochelle Salt	BaTiO <sub>3</sub>	PZT-5A	PZT-5H
d <sub>11</sub>	10 <sup>-12</sup> m/V or pC/N	2.31		0	0	0
d <sub>14</sub>		0.727	100-300	0	0	0
d <sub>15</sub>		0		242	584	741
d <sub>25</sub>		-d <sub>14</sub>	-53	0	0	0
d <sub>31</sub>		0		-58	-171	-274
d <sub>33</sub>		0		149	374	593
d <sub>36</sub>		0	11.7	0	0	0
$\epsilon_{11}^T/\epsilon_0$		4.52		1300	1730	3130
$\epsilon_{11}^S/\epsilon_0$		4.43		1000	916	1700
$\epsilon_{22}^T/\epsilon_0$		$\epsilon_{11}^T/\epsilon_0$		$\epsilon_{11}^T/\epsilon_0$	$\epsilon_{11}^T/\epsilon_0$	$\epsilon_{11}^T/\epsilon_0$
$\epsilon_{22}^S/\epsilon_0$		$\epsilon_{11}^S/\epsilon_0$		$\epsilon_{11}^S/\epsilon_0$	$\epsilon_{11}^S/\epsilon_0$	$\epsilon_{11}^S/\epsilon_0$
$\epsilon_{33}^T/\epsilon_0$		4.64		1200	1700	3400
$\epsilon_{33}^S/\epsilon_0$		4.64		910	830	1470
Relative density		2.65	1.77	5.55	7.75	7.5
Natural time constant						
25°C	seconds			> 100	> 2000	> 2000
100°C				~ 0.3	~ 1800	> 2000
200°C				~ 0.002	~ 250	~ 1000
Resistivity						
$\sigma_3$ @ 25°C	ohm cm	~10 <sup>14</sup>		> 10 <sup>12</sup>	> 10 <sup>13</sup>	> 10 <sup>13</sup>
@100°C		~10 <sup>12</sup>		> 10 <sup>9</sup>	~ 10 <sup>13</sup>	~ 10 <sup>13</sup>
$\sigma_1$ @ 25°C		~10 <sup>16</sup>	10 <sup>13</sup>	> 10 <sup>12</sup>	> 10 <sup>13</sup>	> 10 <sup>13</sup>
@100°C			2000	> 10 <sup>9</sup>	~ 10 <sup>13</sup>	~ 10 <sup>13</sup>

	$f_o$	$C_o$	$Q_p$	$V_p$	$Q_F$	$V_F$
Disc in Compression, Normal Mode	$\frac{1}{4t\sqrt{\rho s_{33} D}}$	$\frac{\pi d^2 T}{4 t \epsilon_{33}}$	$d_{33} \frac{\pi d^2}{4}$	$\frac{d_{33}}{\epsilon_{33}} t$	$d_{33}$	$\frac{4 d_{33} t}{\pi \epsilon_{33} d^2}$
Plate, Transverse Mode	$\frac{1}{4h\sqrt{\rho s_{11} E}}$	$\epsilon_{33} \frac{T}{t} \frac{A}{t}$	$d_{31} A$	$\frac{d_{33}}{T} t$		
Shear Plate		$\epsilon_{11} \frac{T}{t} \frac{A}{t}$			$d_{15}$	$\frac{d_{15}}{T} \frac{t}{A}$
Shear Tube		$\epsilon_{11} \frac{T}{t} \frac{\pi dh}{t}$			$d_{15}$	$\frac{d_{15}}{T} \frac{t}{\pi dh}$
Cantilever Bimorph Beam, Series Connected.	$0.162 \frac{t}{\ell^2} \sqrt{\frac{1}{\rho s_{11} E}}$	$\epsilon_{33} \frac{T}{t} \frac{b\ell}{t}$			$\frac{3\ell^2}{2t^2} d_{31}$	$\frac{3}{2} \frac{d_{31} \ell}{T \frac{b}{t} \epsilon_{33}}$
Cantilever Bimorph Beam, Parallel Connected	$0.162 \frac{t}{\ell^2} \sqrt{\frac{1}{\rho s_{11} E}}$	$4\epsilon_{33} \frac{T}{t} \frac{b\ell}{t}$			$\frac{3\ell^2}{t^2} d_{31}$	$\frac{3}{4} \frac{d_{31} \ell}{T \frac{b}{t} \epsilon_{33}}$
Pinned End Bimorph Beam Series Connected	$0.454 \frac{t}{\ell^2} \sqrt{\frac{1}{\rho s_{11} E}}$	$\epsilon_{33} \frac{T}{t} \frac{b\ell}{t}$			$\frac{3\ell^2}{8t^2} d_{31}$	$\frac{3}{8} \frac{d_{31} \ell}{T \frac{b}{t} \epsilon_{33}}$
Pinned Edge Bimorph Disc, Series Connected	$0.988 \frac{t}{d^2} \sqrt{\frac{1}{\rho s_{11} E}}$	$\frac{\pi T}{4 \epsilon_{33}} \frac{d^2}{t}$	$\frac{3\pi}{64} d_{31} \frac{d^4}{t^2}$	$\frac{3}{16} \frac{d_{31}}{T} \frac{d^2}{t}$	$\frac{3d^2}{8t^2} d_{31}$	$\frac{3}{2\pi} \frac{d_{31}}{T} \frac{1}{\epsilon_{33}}$
Centrally Supported Disc, Series Connected	$0.732 \frac{t}{d^2} \sqrt{\frac{1}{\rho s_{11} E}}$	$\frac{\pi T}{4 \epsilon_{33}} \frac{d^2}{t}$	$\frac{3\pi}{64} d_{31} \frac{d^4}{t^2}$	$\frac{3}{16} \frac{d_{31}}{T} \frac{d^2}{t}$		

Table 2. Performance Parameters for Various Modes

Table 3. Performance parameters for various modes  
evaluated for PZT-5A

Note:- t, d, l, b, h, A are typically of order unity

t=mm; d,l,b,h=cm; A=cm <sup>2</sup>	f <sub>o</sub> (kHz)	C <sub>o</sub> (pF)	Q <sub>p</sub> (pC/torr)	V <sub>p</sub> (mV/torr)	Q <sub>F</sub> (pC/N)	V <sub>F</sub> (V/N)	f <sub>o</sub> Q <sub>p</sub> (kHz x pC/torr)
Fig.1a Normal compression disc	$\frac{923}{t}$	1181 $\frac{d^2}{t}$	3.92d <sup>2</sup>	3.32t	374	.316 $\frac{t}{d^2}$	3620 $\frac{d^2}{t}$
Fig.1b Plate-transverse	$\frac{70.1}{h}$	1505 $\frac{A}{t}$	2.28A	1.518t			169 $\frac{A}{t}$
Fig.1c Shear plate		1150 $\frac{A}{t}$			584	.382 $\frac{t}{A}$	
Fig.1d Shear tube		3610 $\frac{dh}{t}$			584	.122 $\frac{t}{dh}$	
Fig.1f Cantilever beam, Series Connected	4.54 $\frac{t}{l^2}$	1505 $\frac{bl}{t}$			2.56x10 <sup>4</sup> $\frac{l^2}{t^2}$		
Fig.1f Cantilever beam, Parallel connected	4.54 $\frac{t}{l^2}$	6020 $\frac{bl}{t}$			5.13x10 <sup>4</sup> $\frac{l^2}{t^2}$		
Fig.1g Pinned end beam, Series Connected	12.70 $\frac{t}{l^2}$	1505 $\frac{bl}{t}$			0.641x10 <sup>4</sup> $\frac{l^2}{t^2}$		
Fig.1g Pinned end beam, Parallel Connected	12.70 $\frac{t}{l^2}$	6020 $\frac{bl}{t}$			1.28 x10 <sup>4</sup> $\frac{l^2}{t^2}$	$\frac{5.43}{t}$	
Fig.1i Pinned edge disc. Series Connected	27.7 $\frac{t}{d^2}$	1181 $\frac{d^2}{t}$	33.55 $\frac{d^4}{t^2}$	28.4 $\frac{d^2}{t}$	0.641x10 <sup>4</sup> $\frac{d^2}{t^2}$		928 $\frac{d^2}{t}$
Fig.1i Pinned edge disc Parallel Connected	27.7 $\frac{t}{d^2}$	4724 $\frac{d^2}{t}$	67.1 $\frac{d^4}{t^2}$	14.2 $\frac{d^2}{t}$	1.28 x10 <sup>4</sup> $\frac{d^2}{t^2}$	$\frac{2.71}{t}$	1860 $\frac{d^2}{t}$
Fig.1j Centrally supported disc, Series Connected	20.5 $\frac{t}{d^2}$	1181 $\frac{d^2}{t}$	33.55 $\frac{d^4}{t^2}$	28.4 $\frac{d^2}{t}$			688 $\frac{d^2}{t}$
Fig.1j Centrally supported disc, Para. Connected	20.5 $\frac{t}{d^2}$	4724 $\frac{d^2}{t}$	67.1 $\frac{d^4}{t^2}$	14.2 $\frac{d^2}{t}$			1380 $\frac{d^2}{t}$

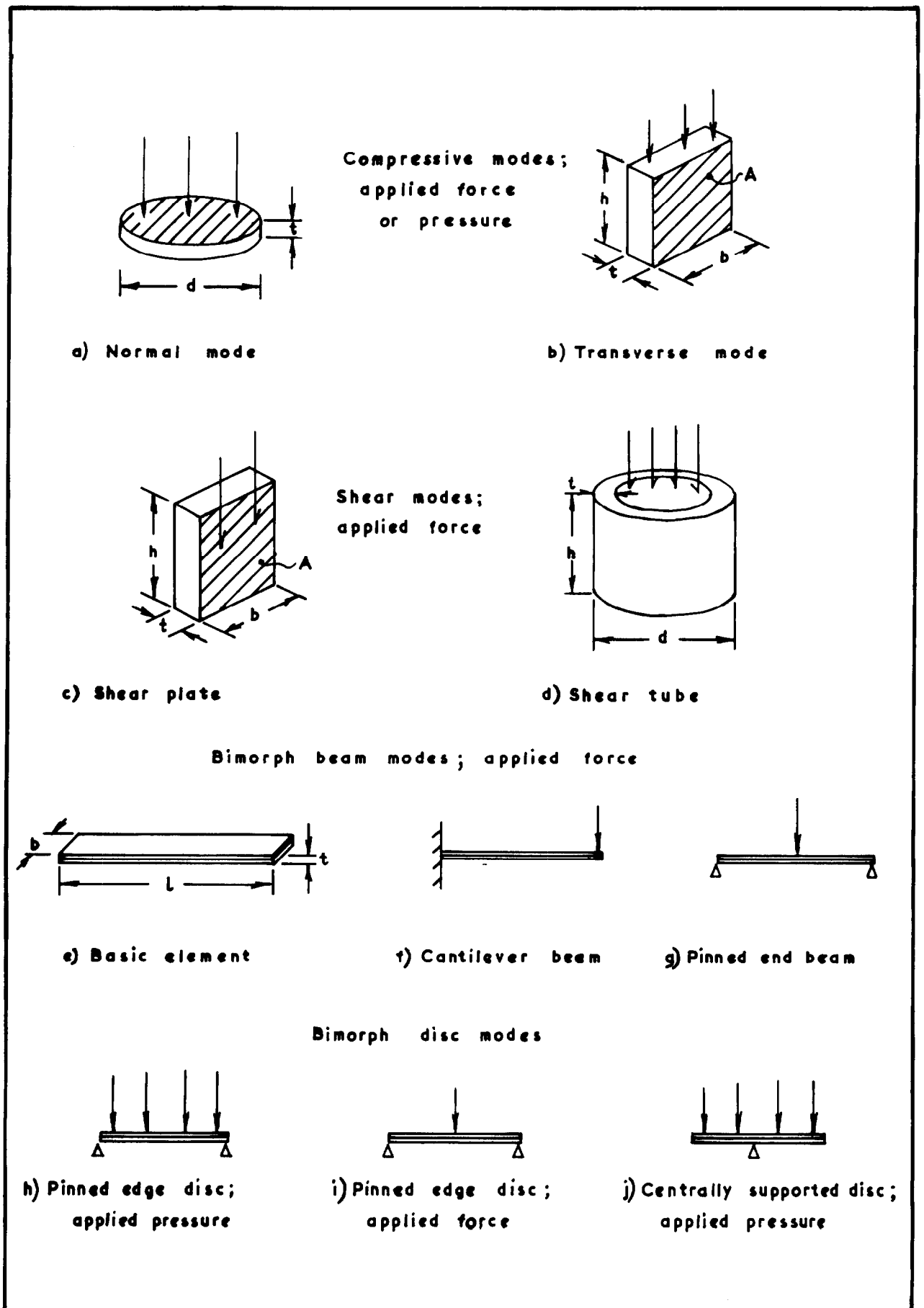
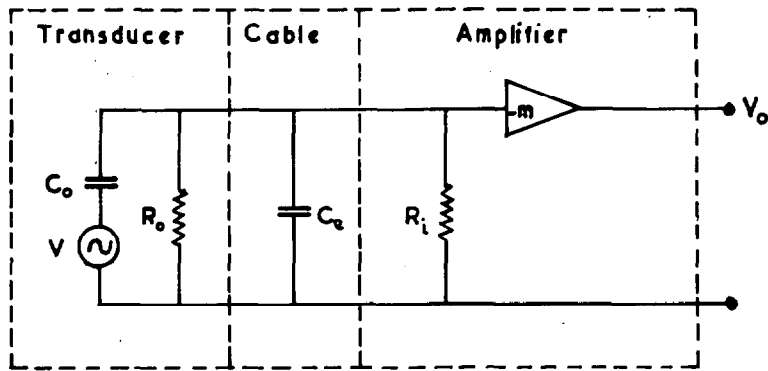
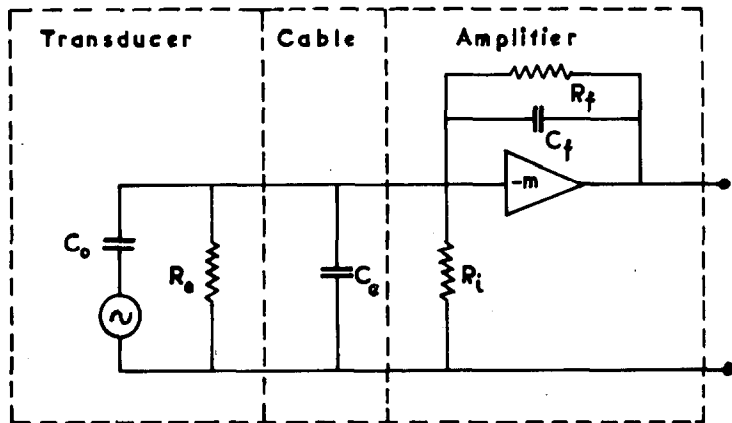


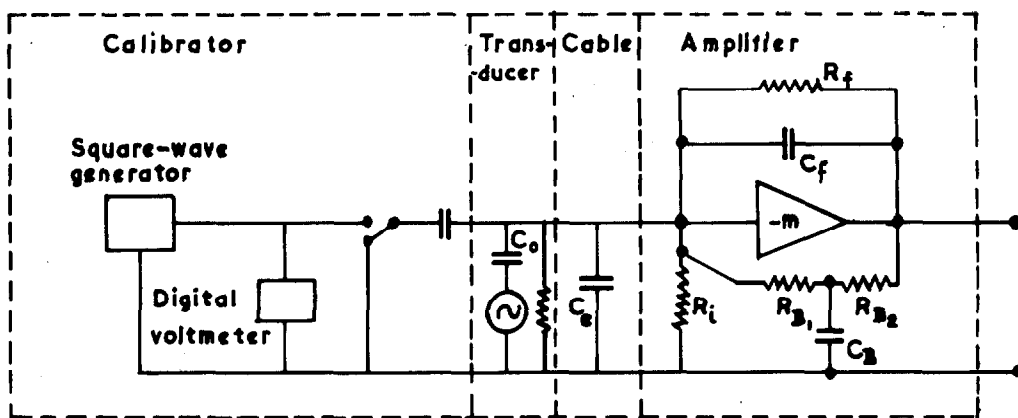
Fig. 1. Basic element sensing modes



a) Voltage amplifier

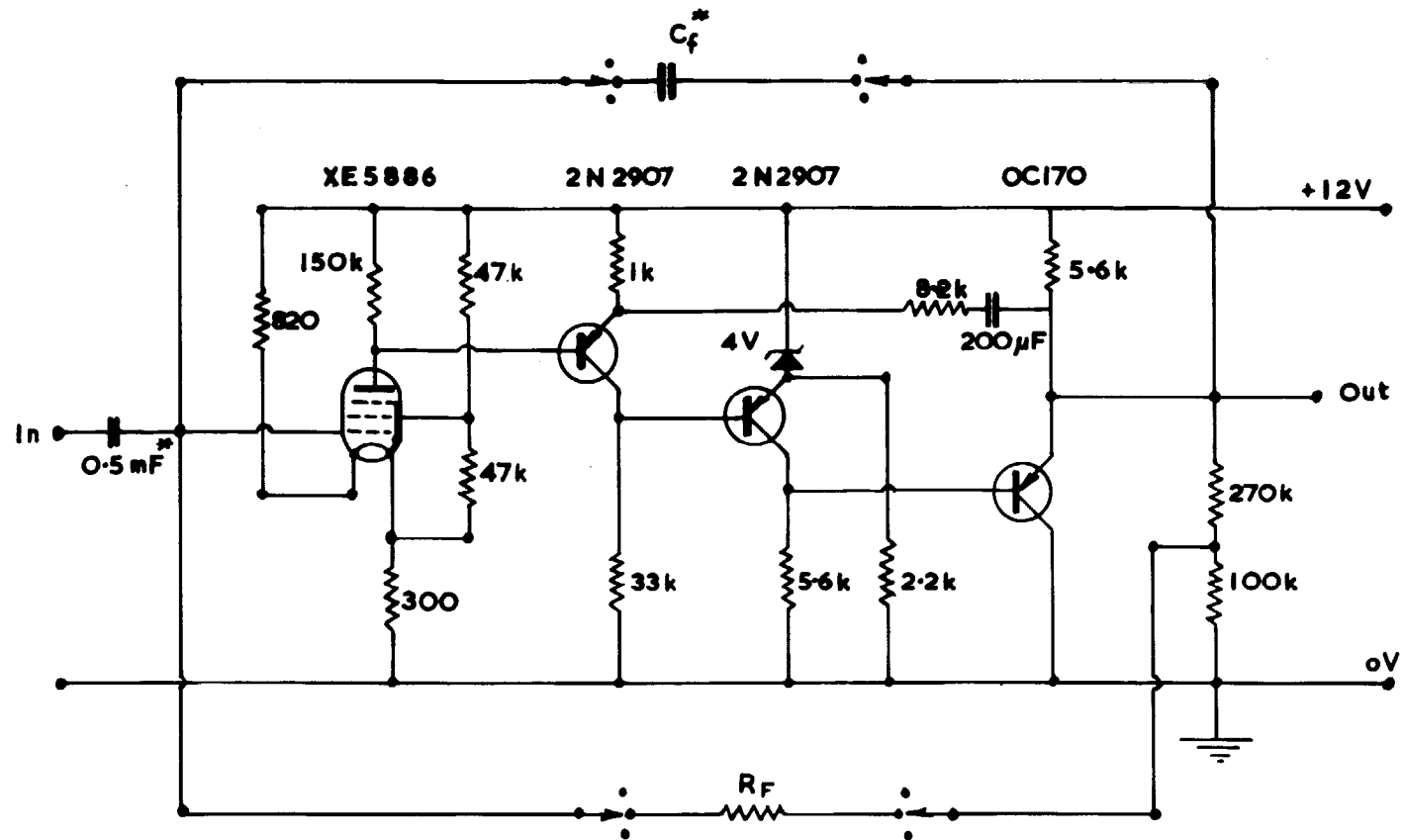


b) Charge amplifier



c) Charge amplifier with calibrator

Fig. 2. Amplifier configurations



\* Polystyrene capacitors

$C_f / \mu\text{F} = 10, 33, 100, 330, 1000, 3300, 10000$

$R_f / \text{ohm} = 10^7, 5 \times 10^8, 10^{10}, 10^{12}$

Fig. 3. Charge amplifier circuit

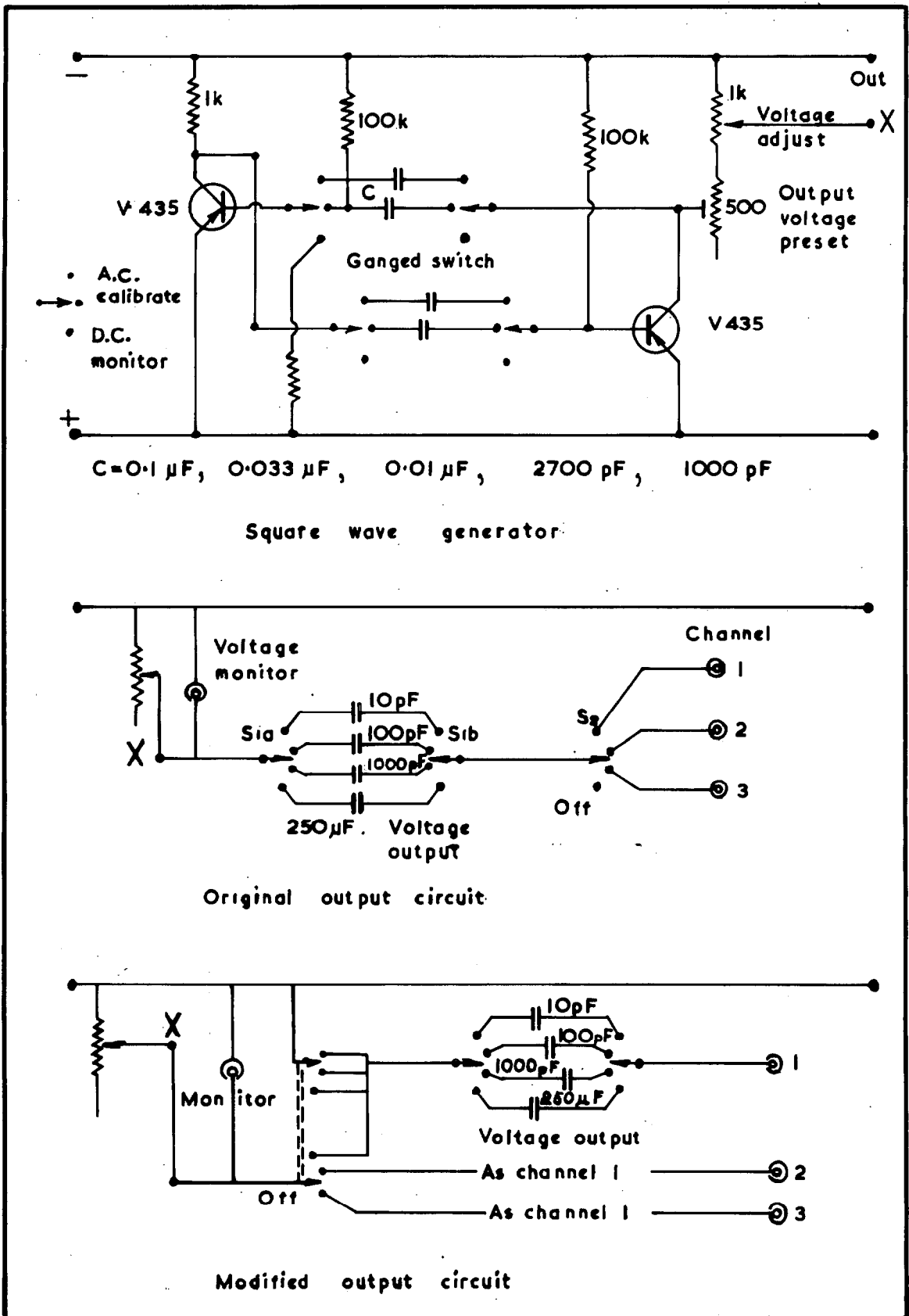
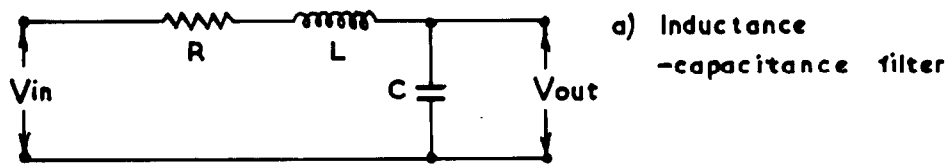
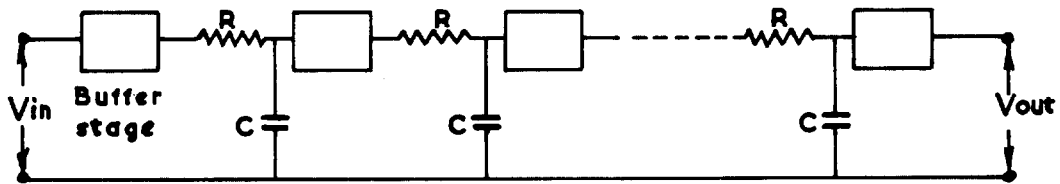


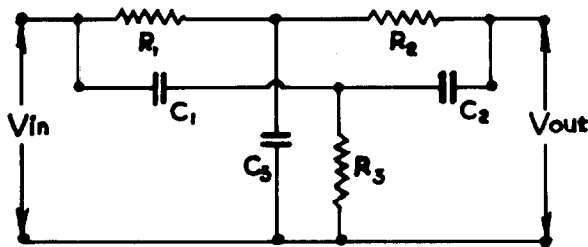
Fig. 4. Charge calibrator circuit



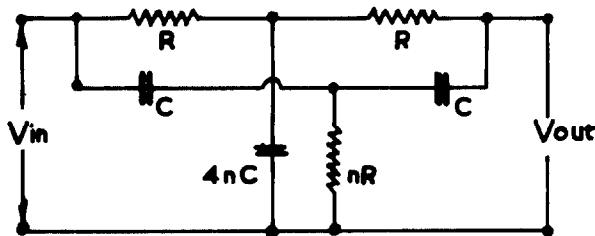
a) Inductance  
-capacitance filter



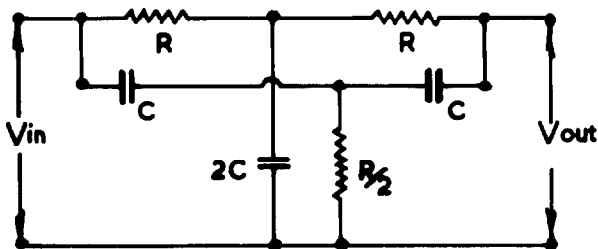
b) Cascaded n-stage resistance-capacitance filter



c) Asymmetric twin-tee  
filter



d) General symmetric  
twin-tee filter



e) Symmetric twin tee  
filter,  $n = \frac{1}{2}$

Fig. 5. Filter circuits

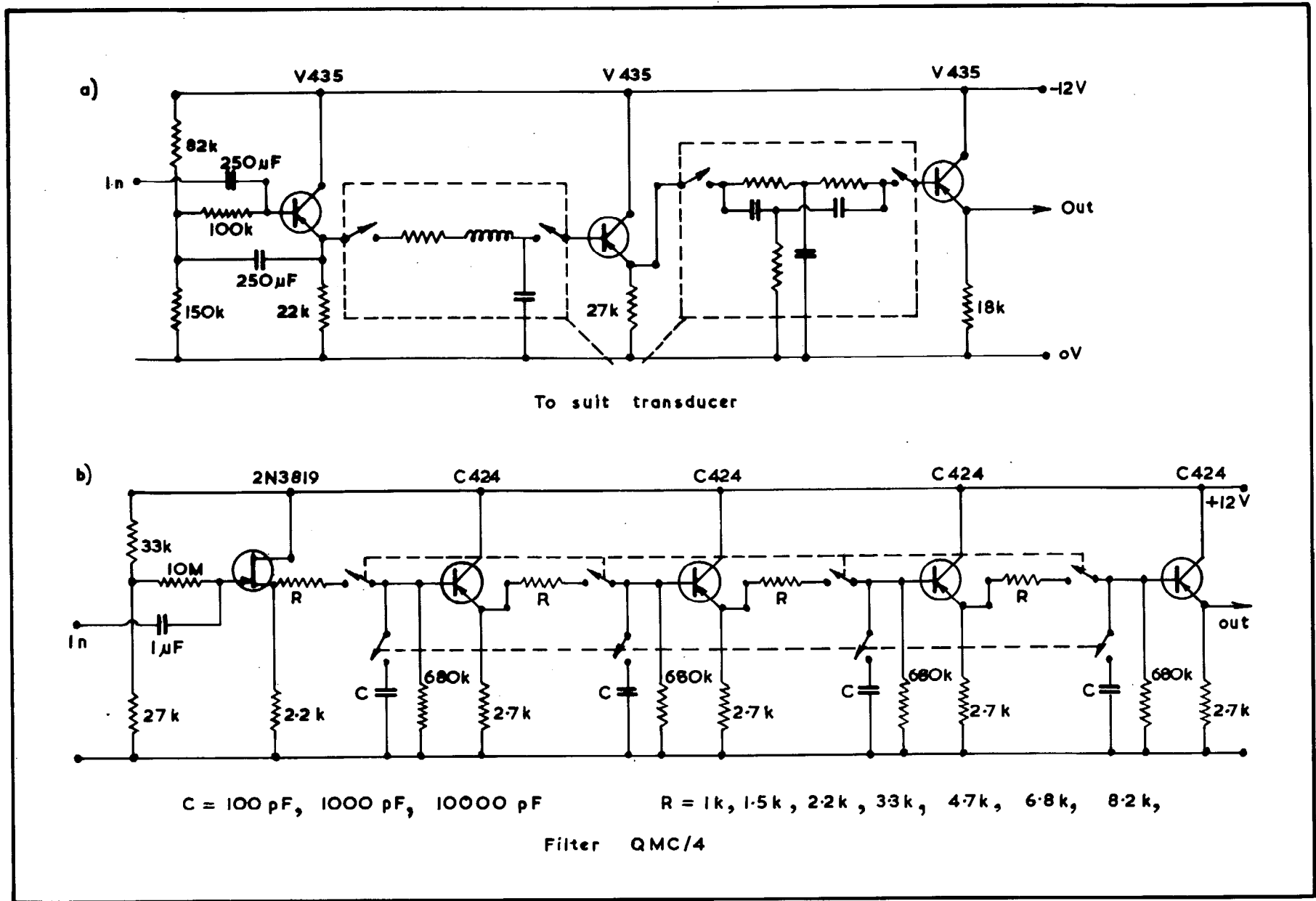


Fig. 6. Two practical filter circuits

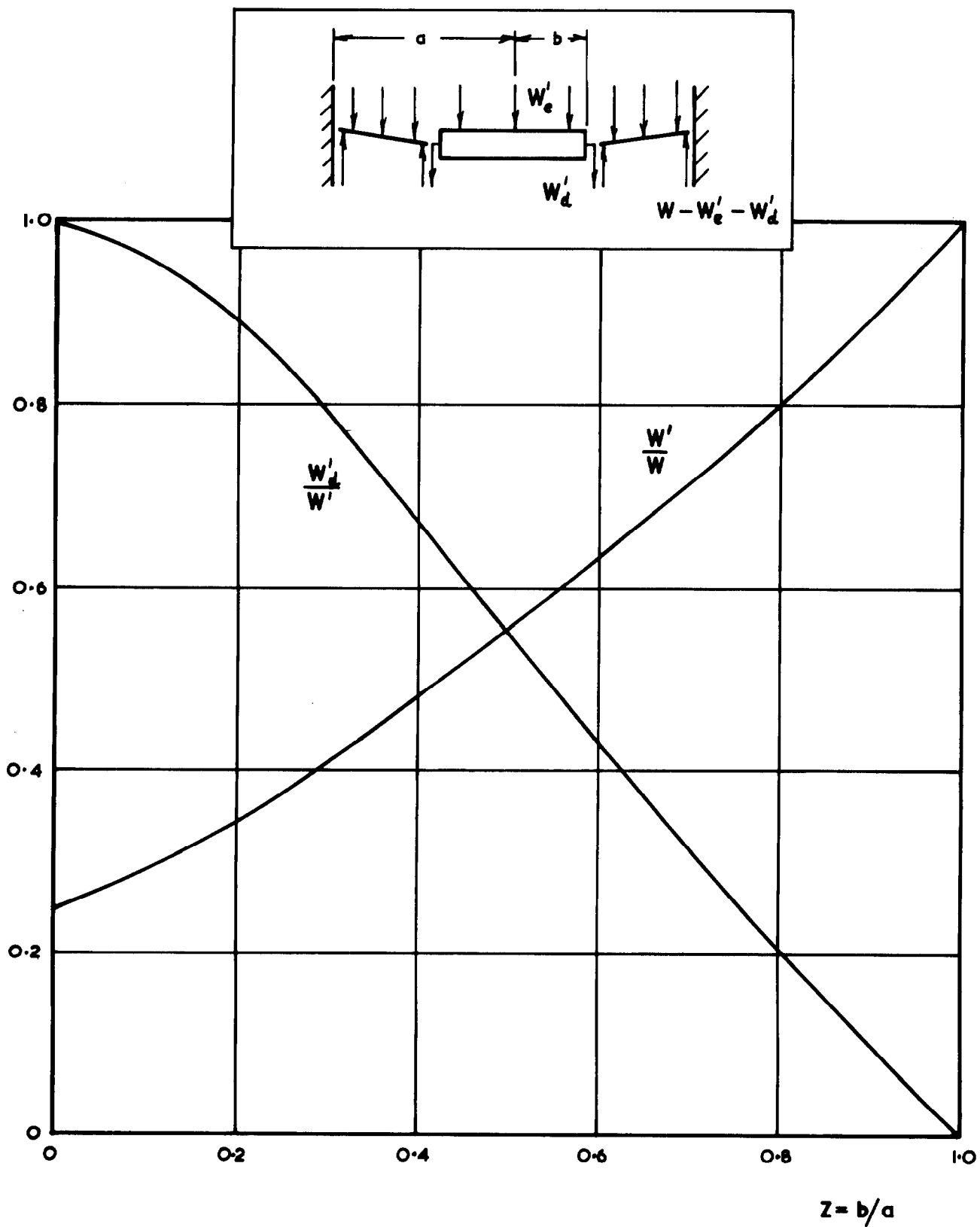
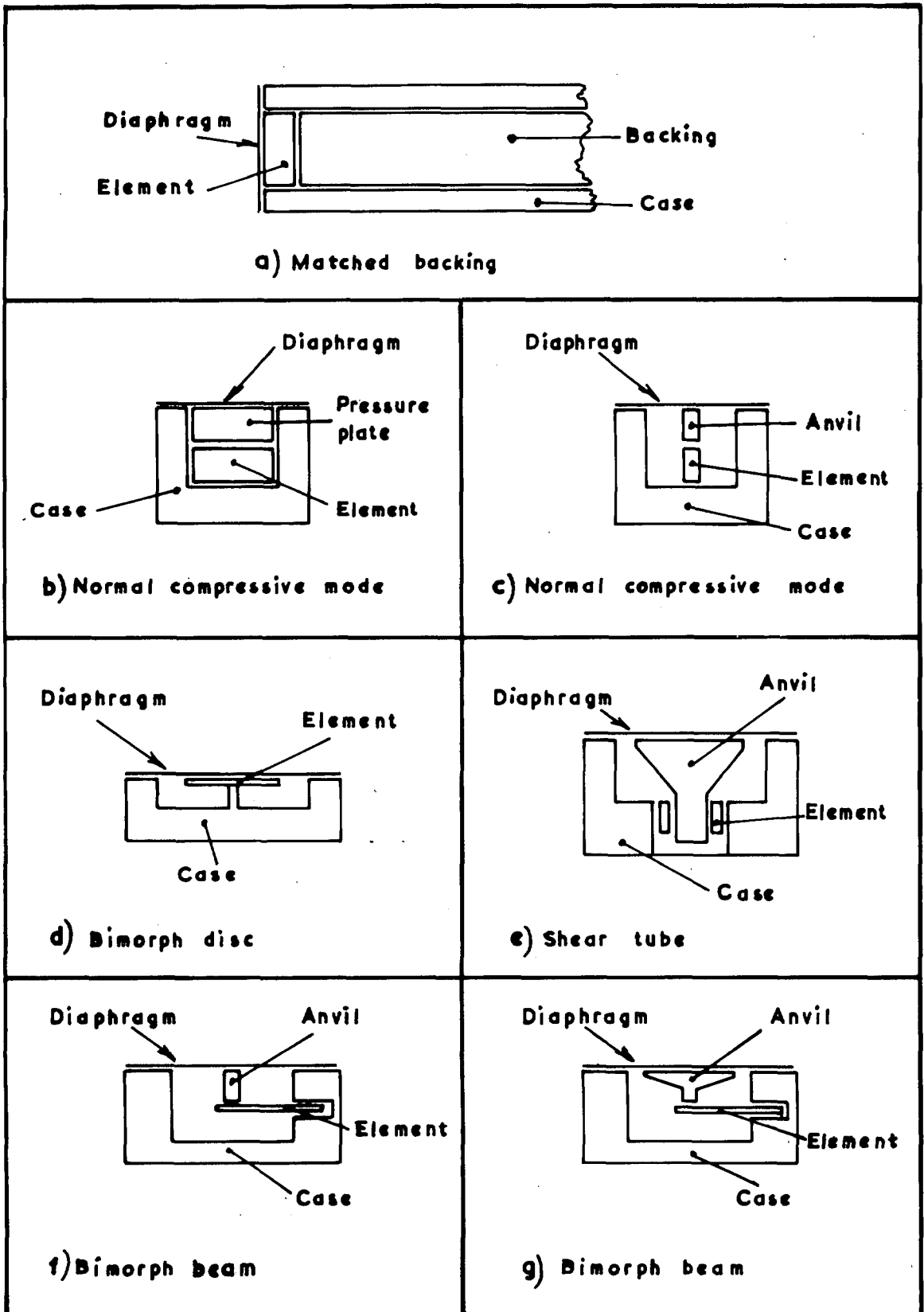
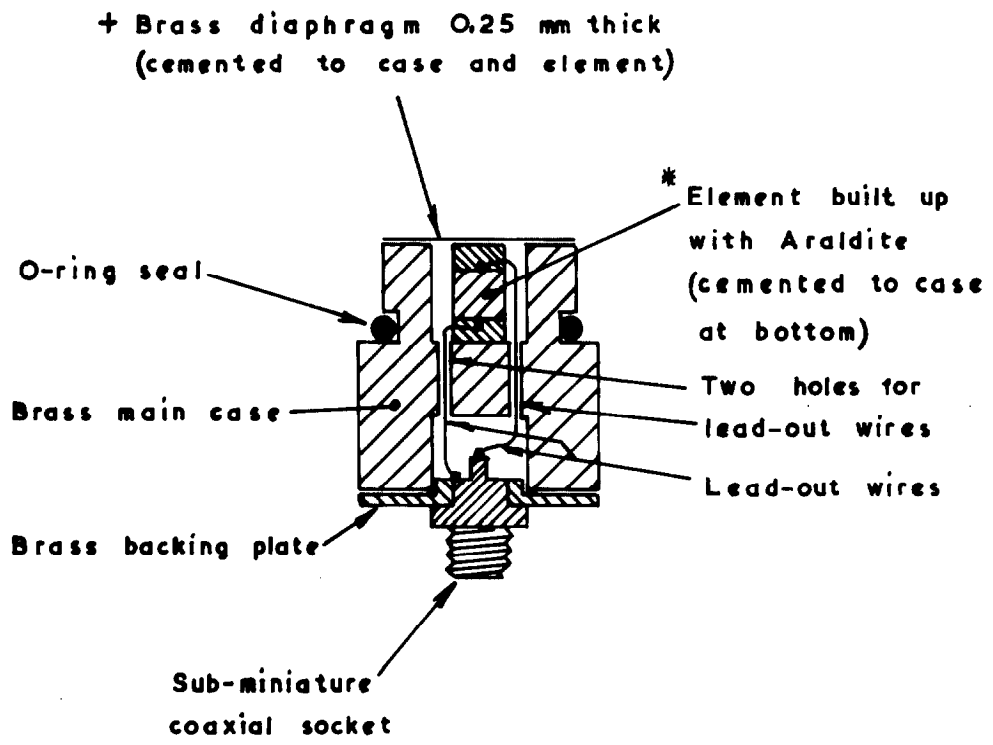


Fig. 7. Diaphragm load transmission factors



**Fig. 8. Basic transducer configurations**



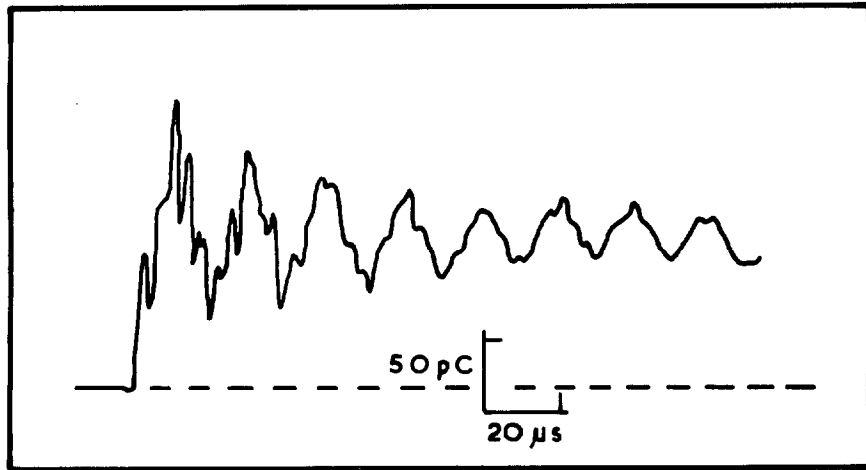
+ Cemented together but small blob of solder used to give electrical connection

\* Element: compression cylinder of PZT-5H 3 mm dia x 3 mm long

1 cm

Fig. 9. The type E transducer

(a)



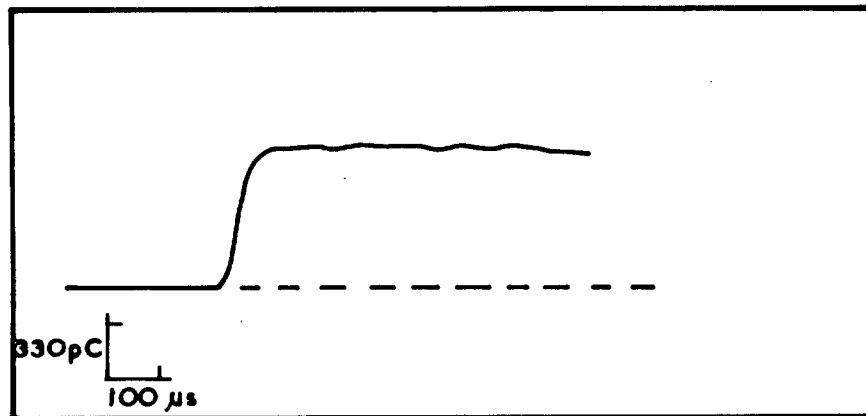
$$W_{11} = 2.52$$

$$p_1 = 20 \text{ torr}$$

$$\Delta p = 125 \text{ torr}$$

No filter

(b)



$$W_{11} = 1.66$$

$$p_1 = 360 \text{ torr}$$

$$\Delta p = 744 \text{ torr}$$

Filter QMC/4, 24 dB/oct,  $f(40 \text{ dB}) = 48 \text{ kHz}$

Fig. 10. Typical traces from type E transducer

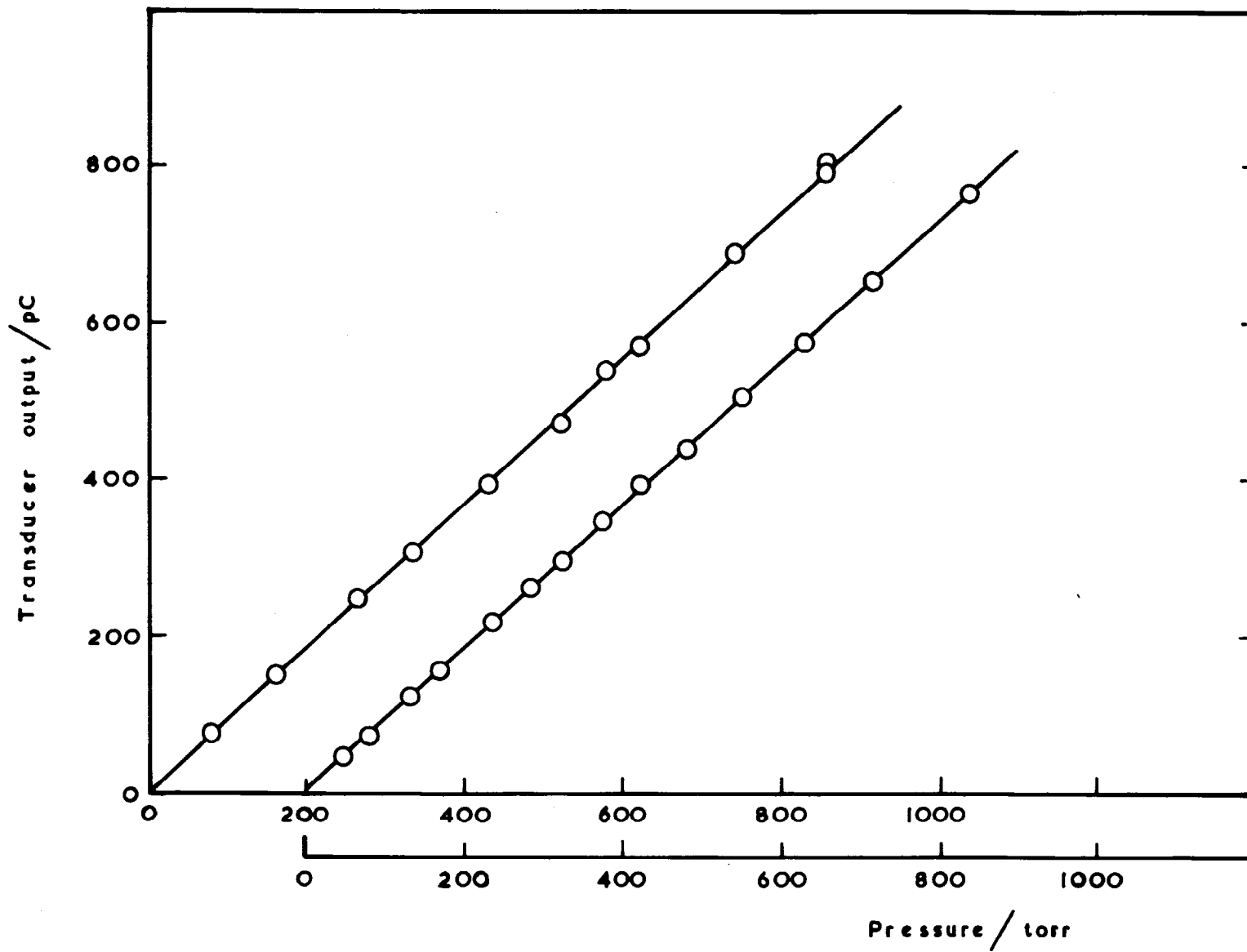


Fig. II Calibration of type E transducer

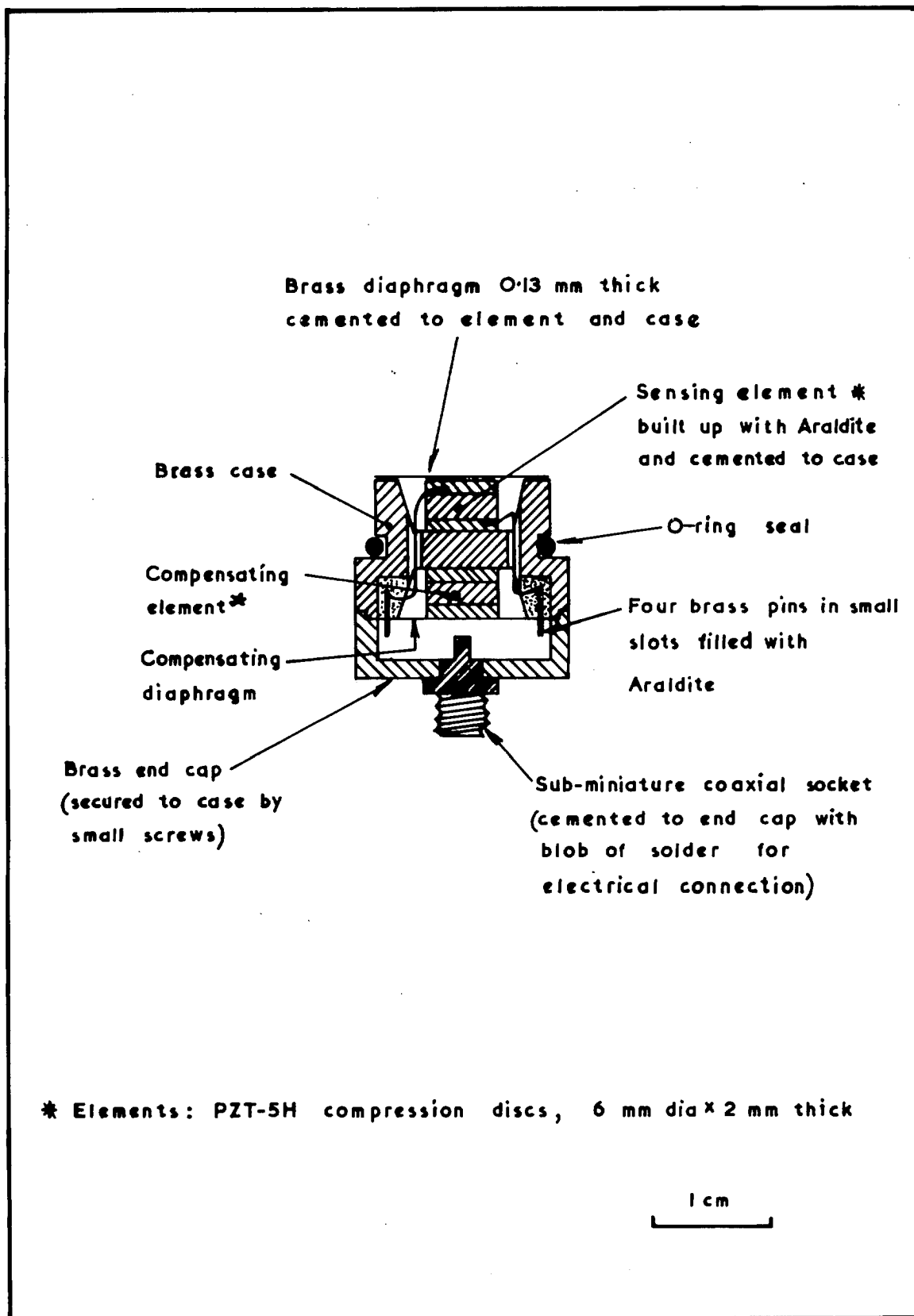
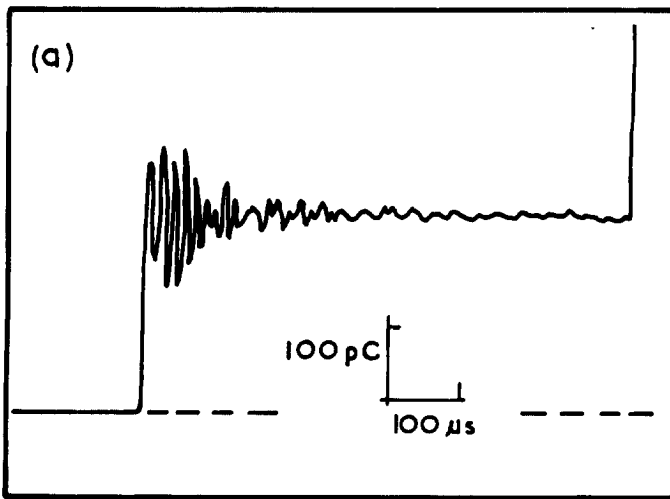
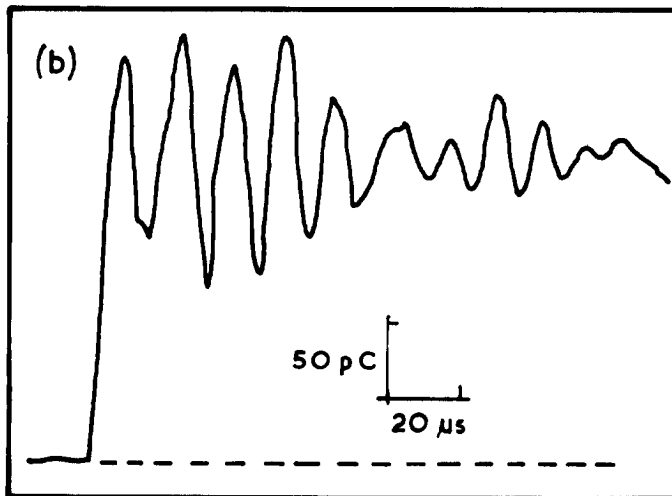


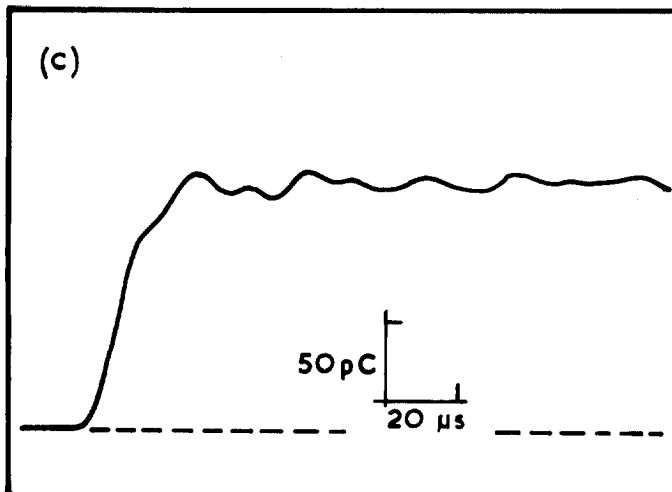
Fig. 12. The type F transducer



$W_{II} = 2.33$   
 $p_i = 17$  torr  
 $\Delta p = 87$  torr  
 No filter



$W_{II} = 2.45$   
 $p_i = 12$  torr  
 $\Delta p = 70$  torr  
 No filter



$W_{II} = 2.45$   
 $p_i = 12$  torr  
 $\Delta p = 70$  torr  
 Filter: QMC/4 24 dB/oct  
 $f(40dB) = 140$  kHz

Fig. 13. Typical traces from type F transducer

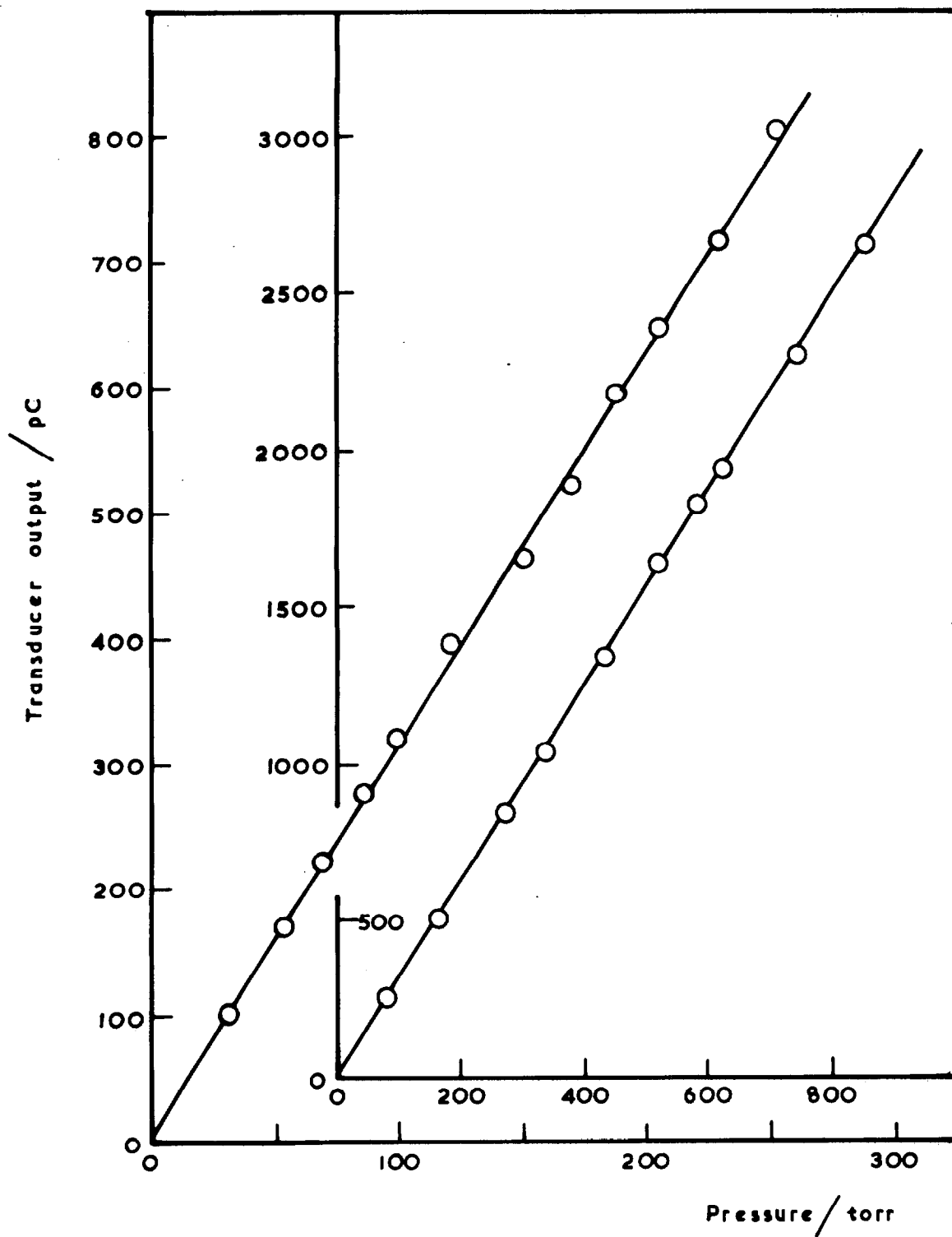


Fig.14. Calibration of type F transducer

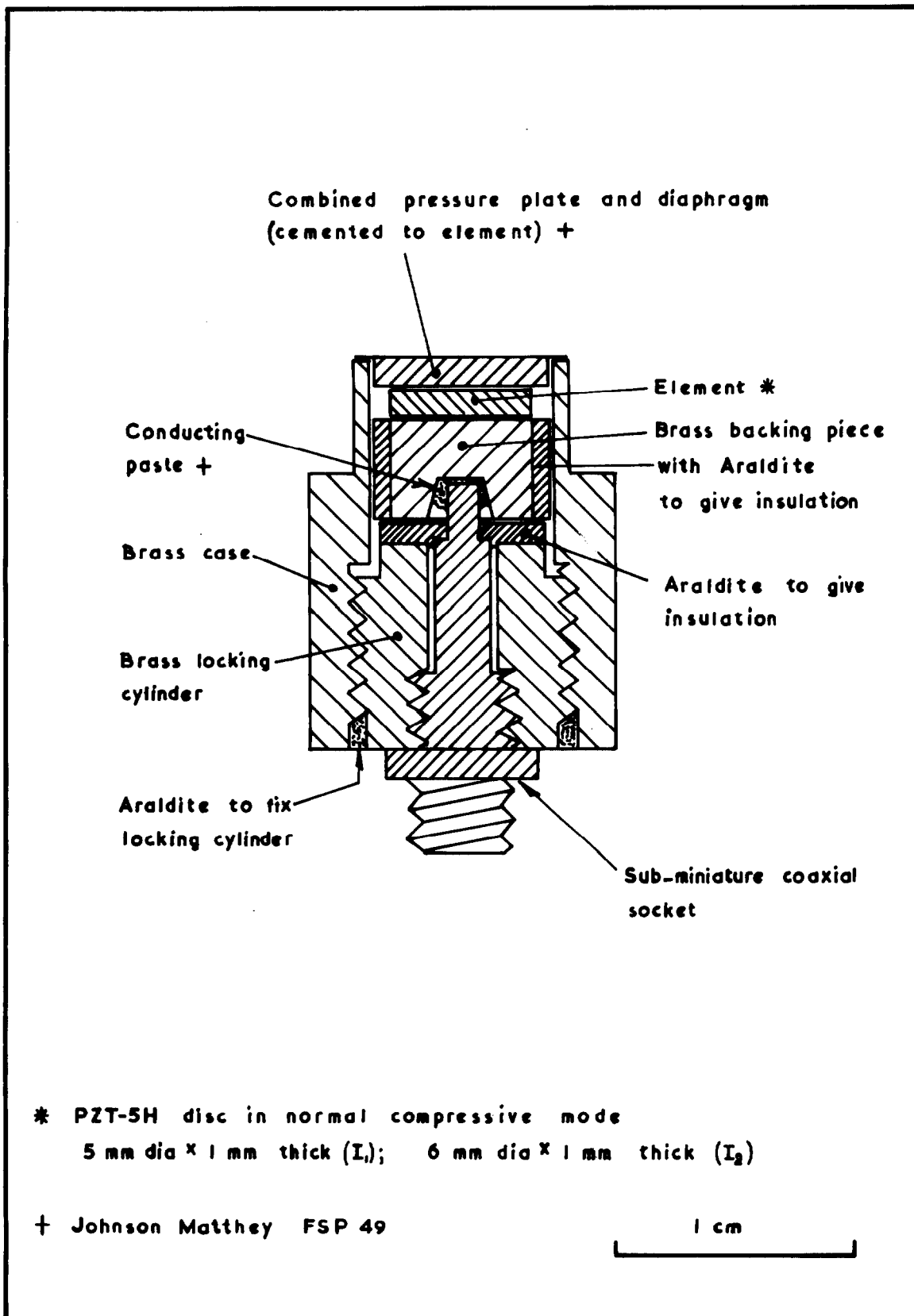
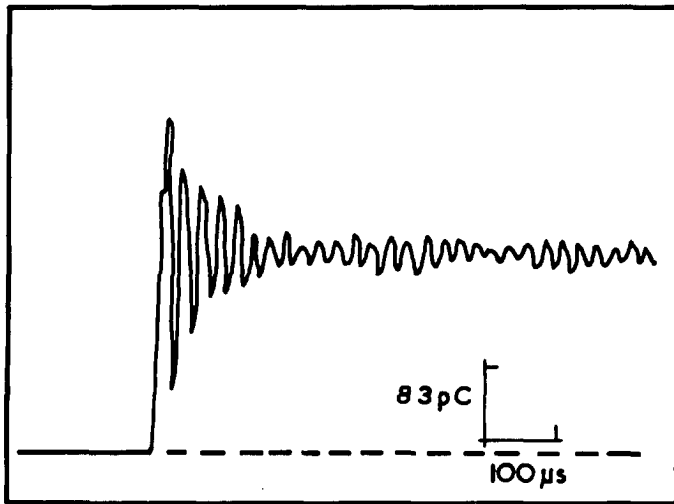
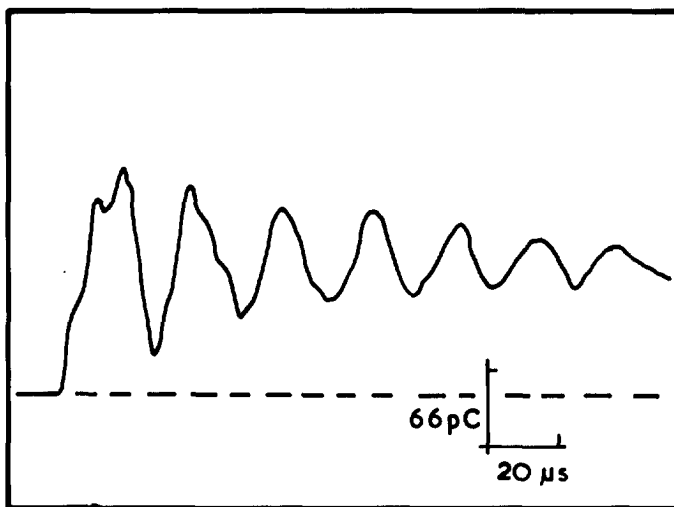


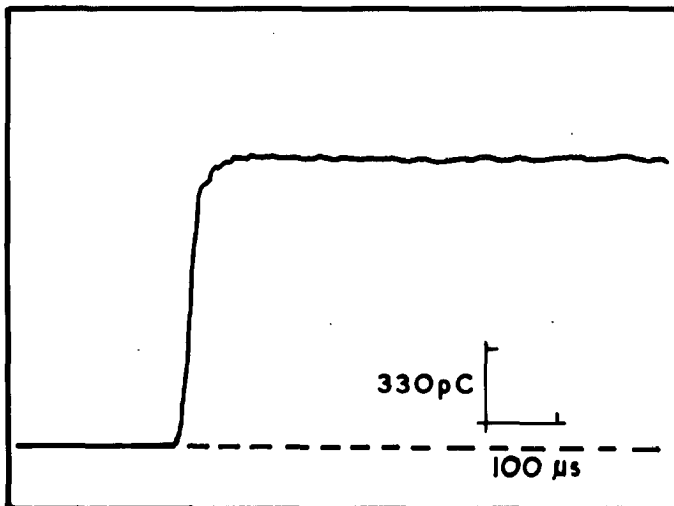
Fig. 15. The type I transducer



$W_{II} = 1.75$   
 $P_i = 120 \text{ torr}$   
 $\Delta P = 288 \text{ torr}$   
 No filter

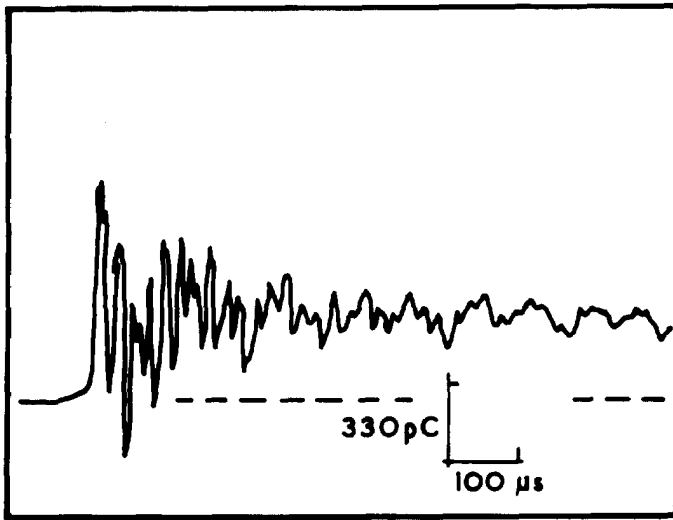


$W_{II} = 2.52$   
 $P_i = 20 \text{ torr}$   
 $\Delta P = 125 \text{ torr}$   
 No filter

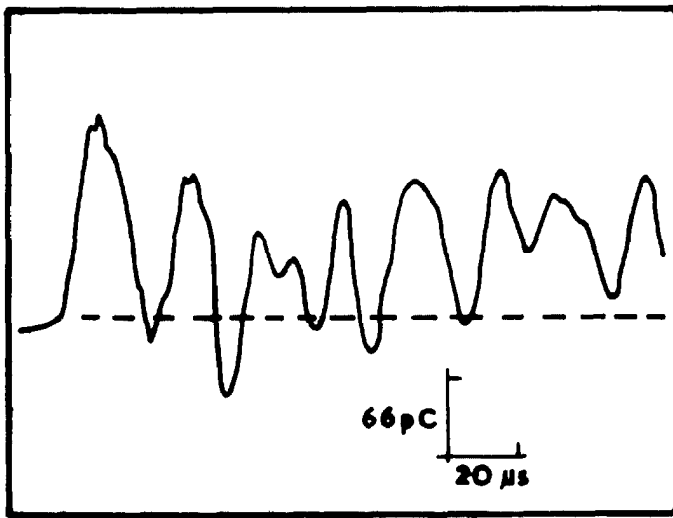


$W_{II} = 1.52$   
 $P_i = 740 \text{ torr}$   
 $\Delta P = 1130 \text{ torr}$   
 Filter QMC 1/E

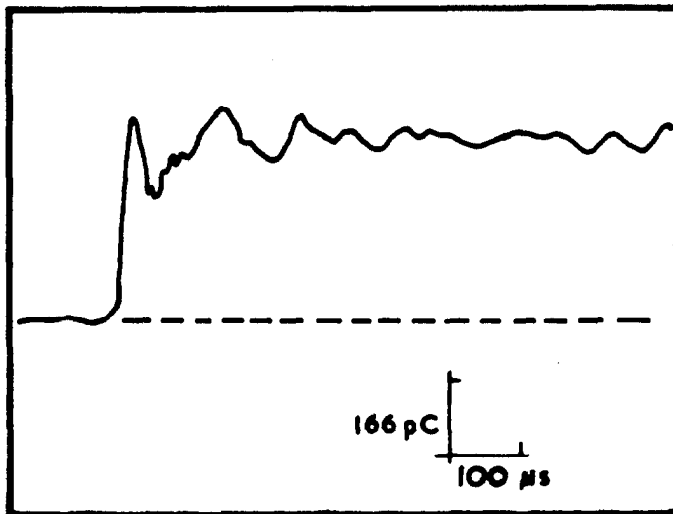
Fig. 16(a). Typical traces from type I<sub>1</sub> transducer



$W_{II} = 2.52$   
 $P_1 = 20$  torr  
 $\Delta P = 125$  torr  
 No filter



$W_{II} = 2.52$   
 $P_1 = 20$  torr  
 $\Delta P = 125$  torr  
 No filter



$W_{II} = 1.71$   
 $P_1 = 280$  torr  
 $\Delta P = 623$  torr  
 Filter QMC 1/E

Fig. 16(b). Typical traces from type  $I_2$  transducer

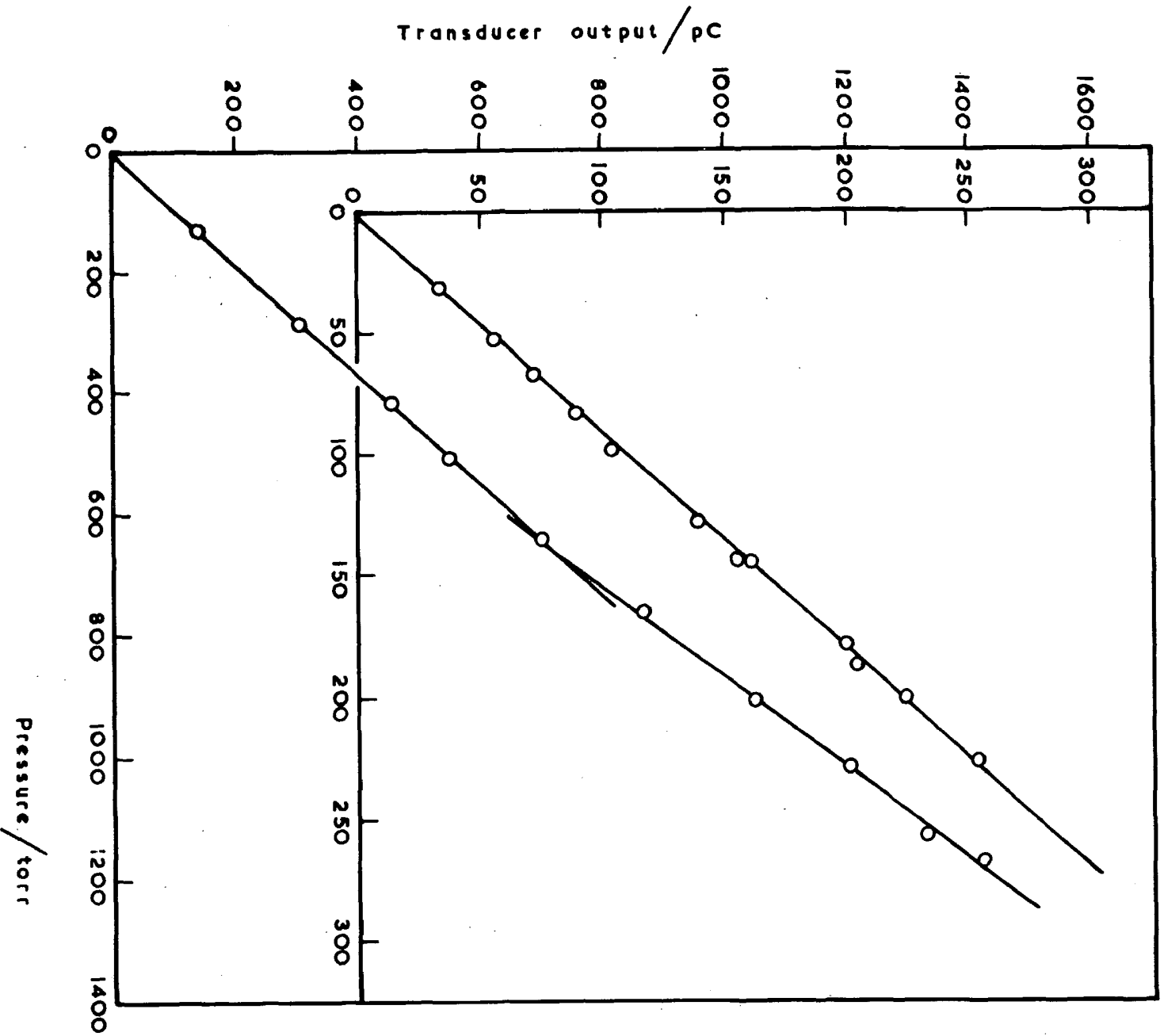


Fig. 17(a). Calibration of type I, transducer

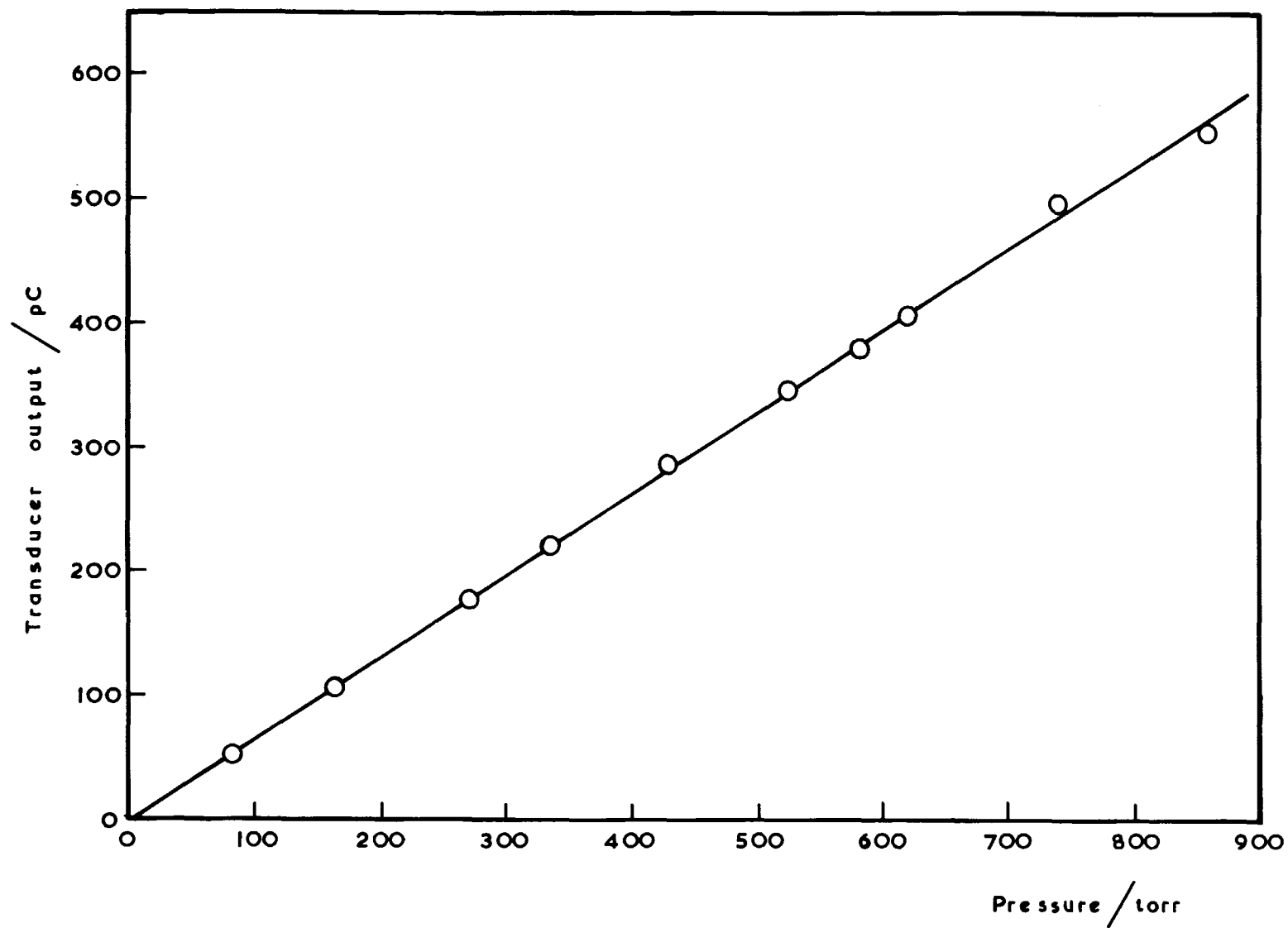


Fig. 17 (b). Calibration of type  $I_2$  transducer

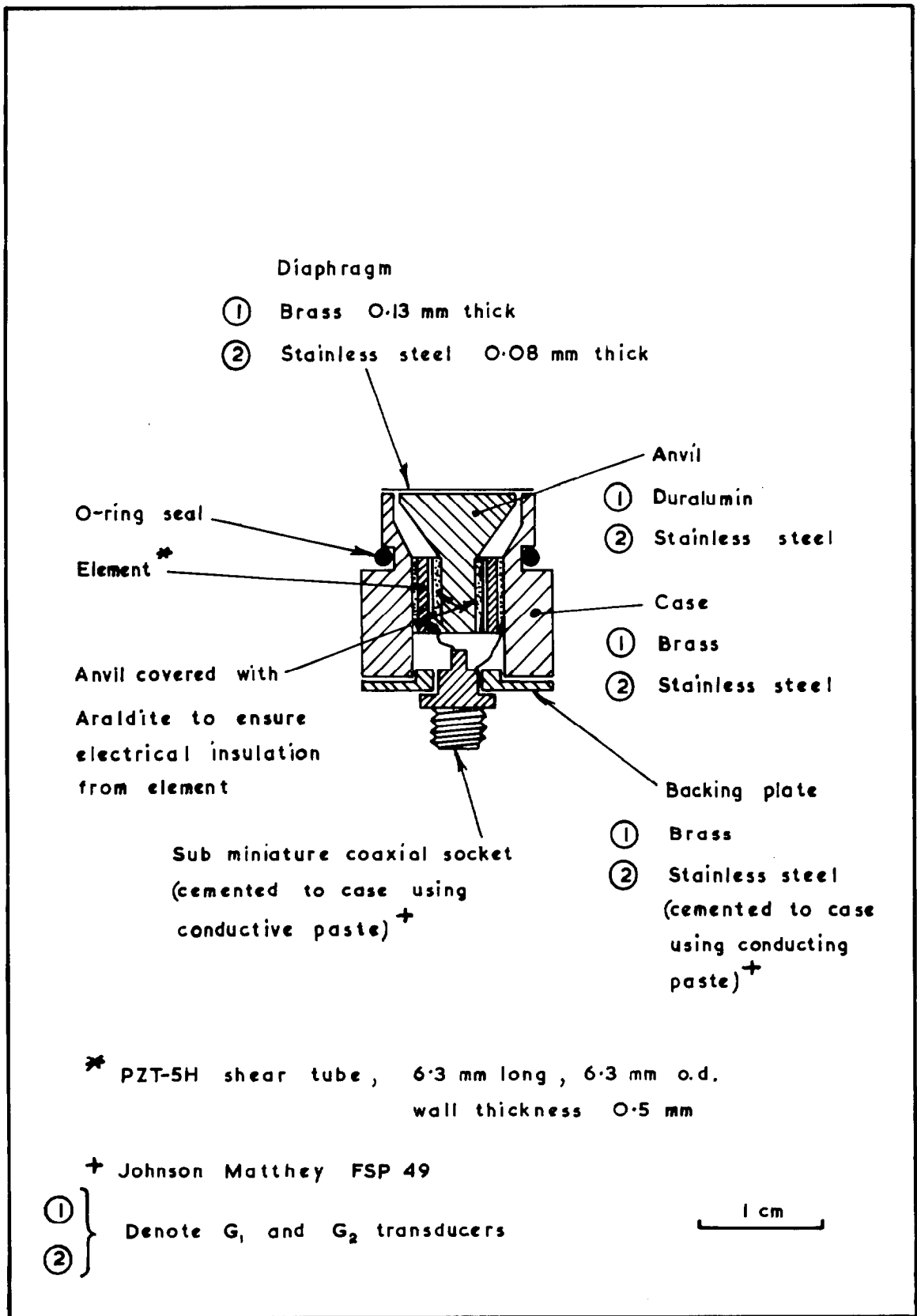
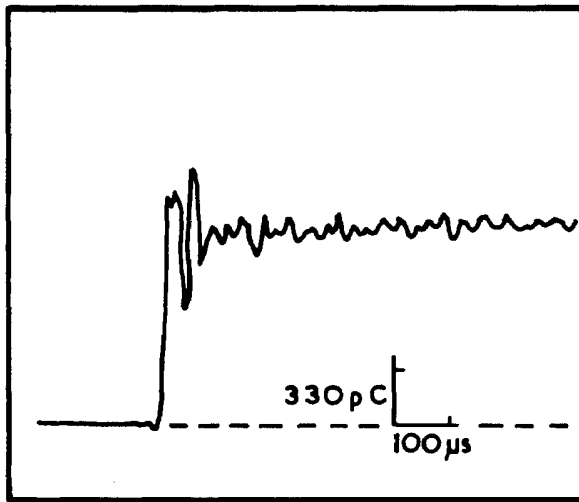
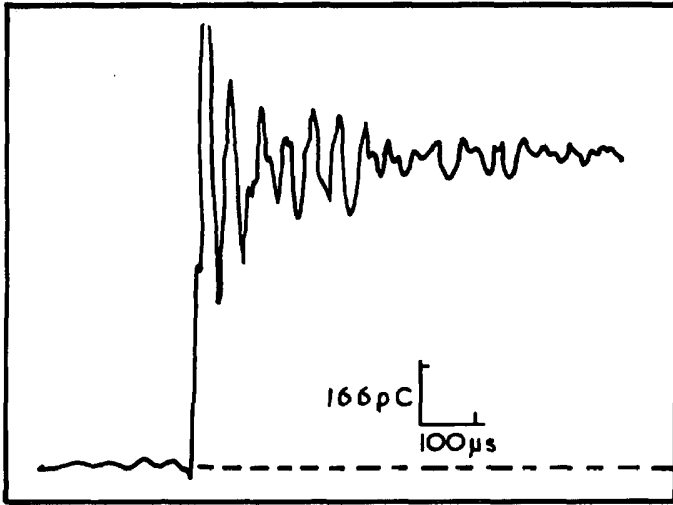


Fig. 18. The type G transducer

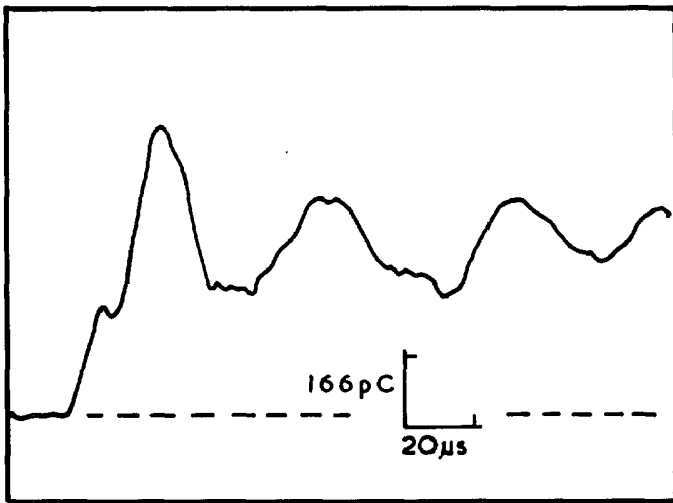


$W_{11} = 1.80$   
 $P_1 = 85 \text{ torr}$   
 $\Delta P = 222 \text{ torr}$   
No filter

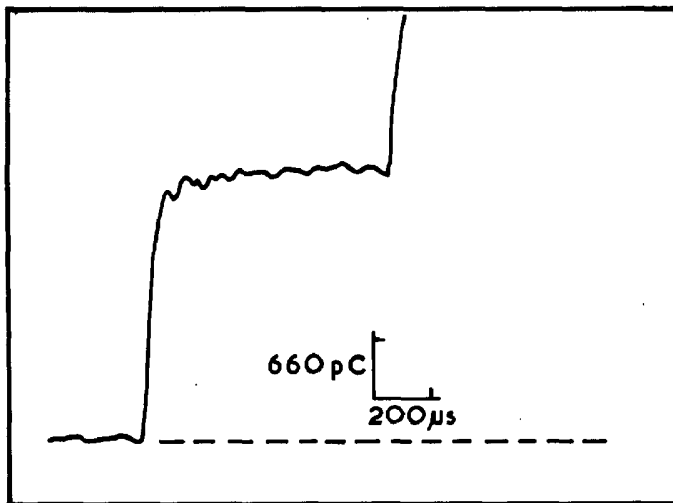
Fig. 19(a). Typical trace from type G, transducer



$W_{11} = 1.75$   
 $P_1 = 120$  torr  
 $\Delta P = 288$  torr  
 No filter



$W_{11} = 2.52$   
 $P_1 = 20$  torr  
 $\Delta P = 125$  torr  
 No filter



$W_{11} = 1.50$   
 $P_1 = 800$  torr  
 $\Delta P = 1180$  torr  
 Filter: QMC/4  
 24dB/oct, f(40dB), 48kHz

Fig. 19(b). Typical traces from type  $G_2$  transducer

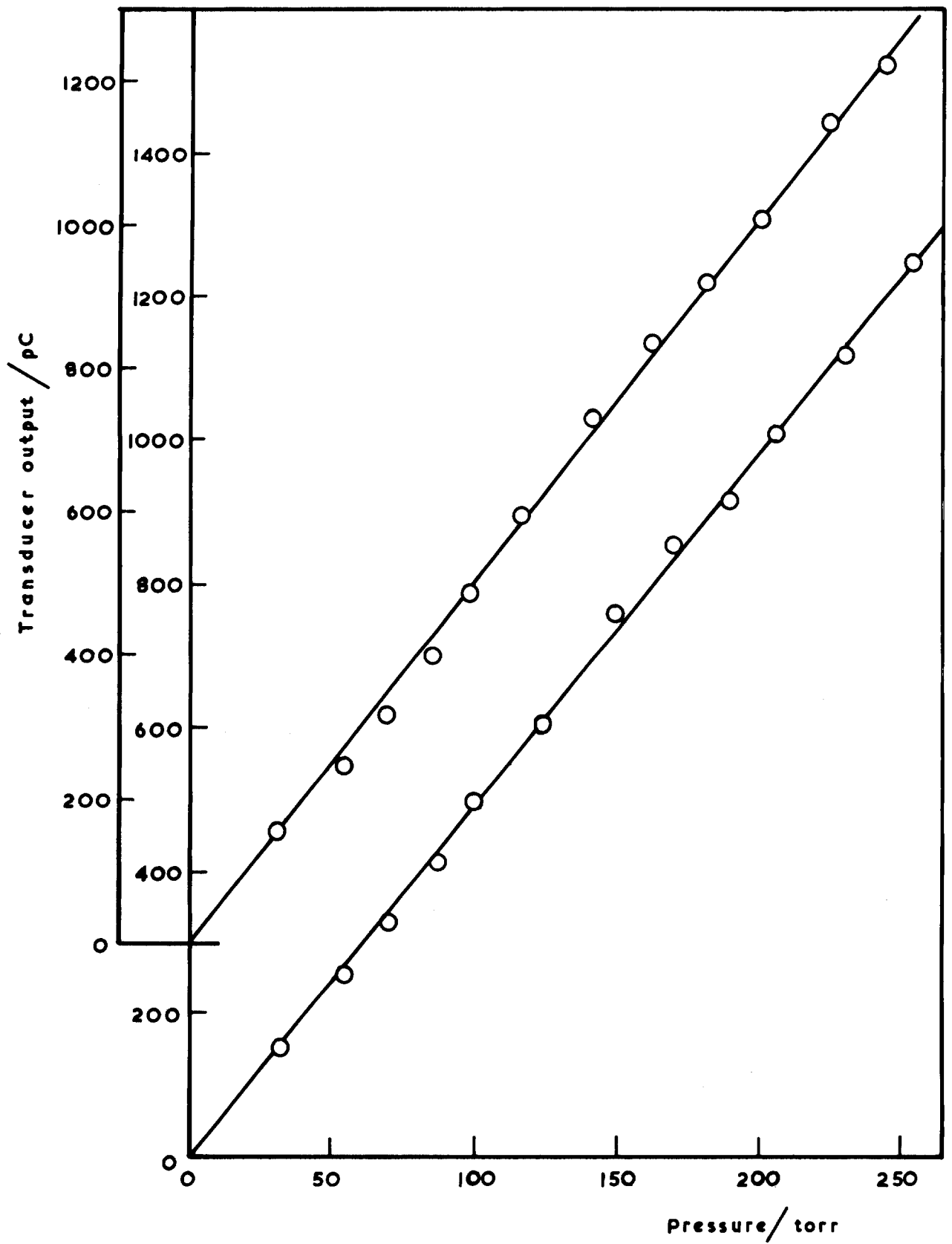


Fig. 20(a). Calibration of type G1 transducer

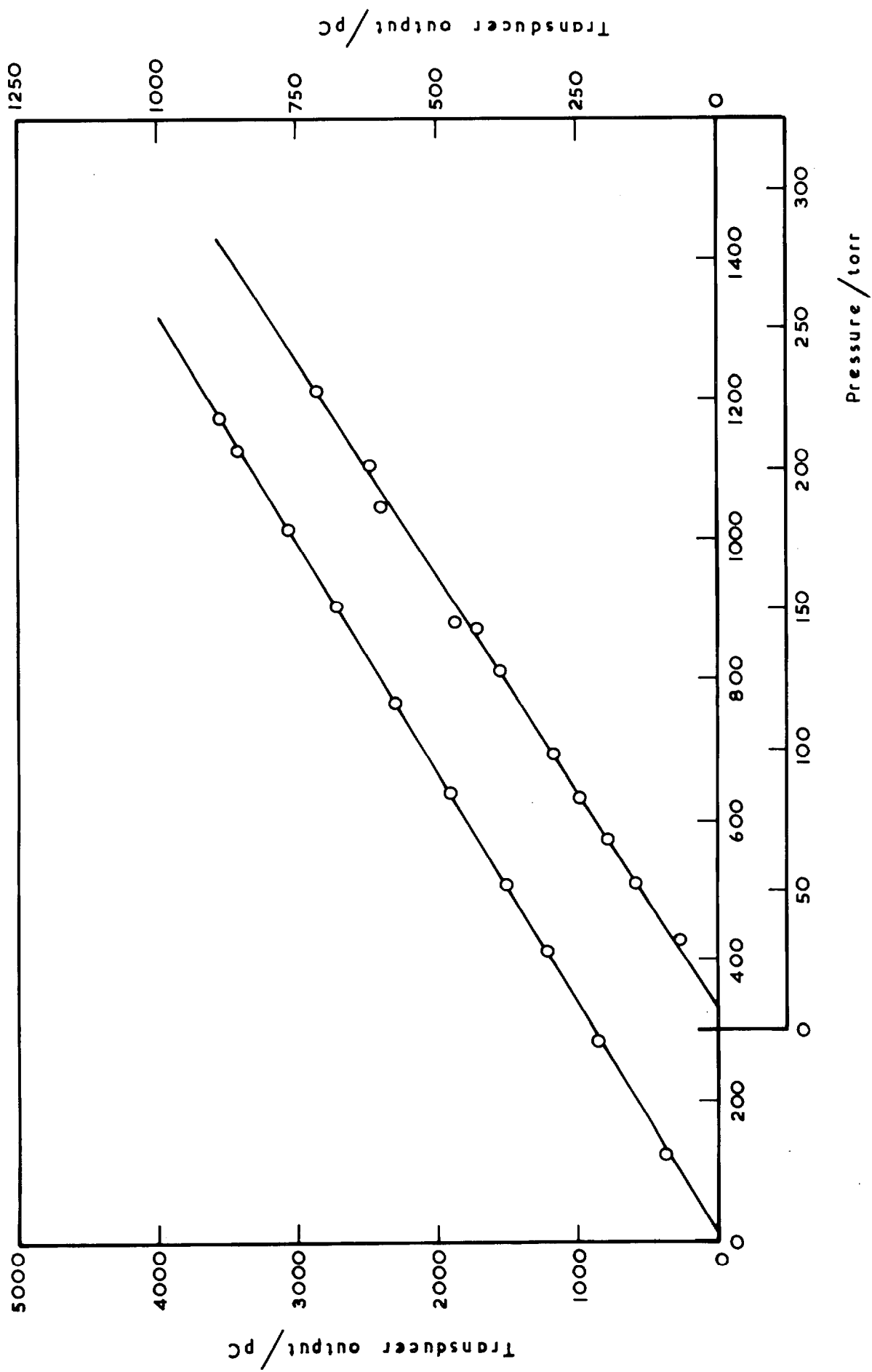


Fig. 20(b). Calibration of G2 transducer

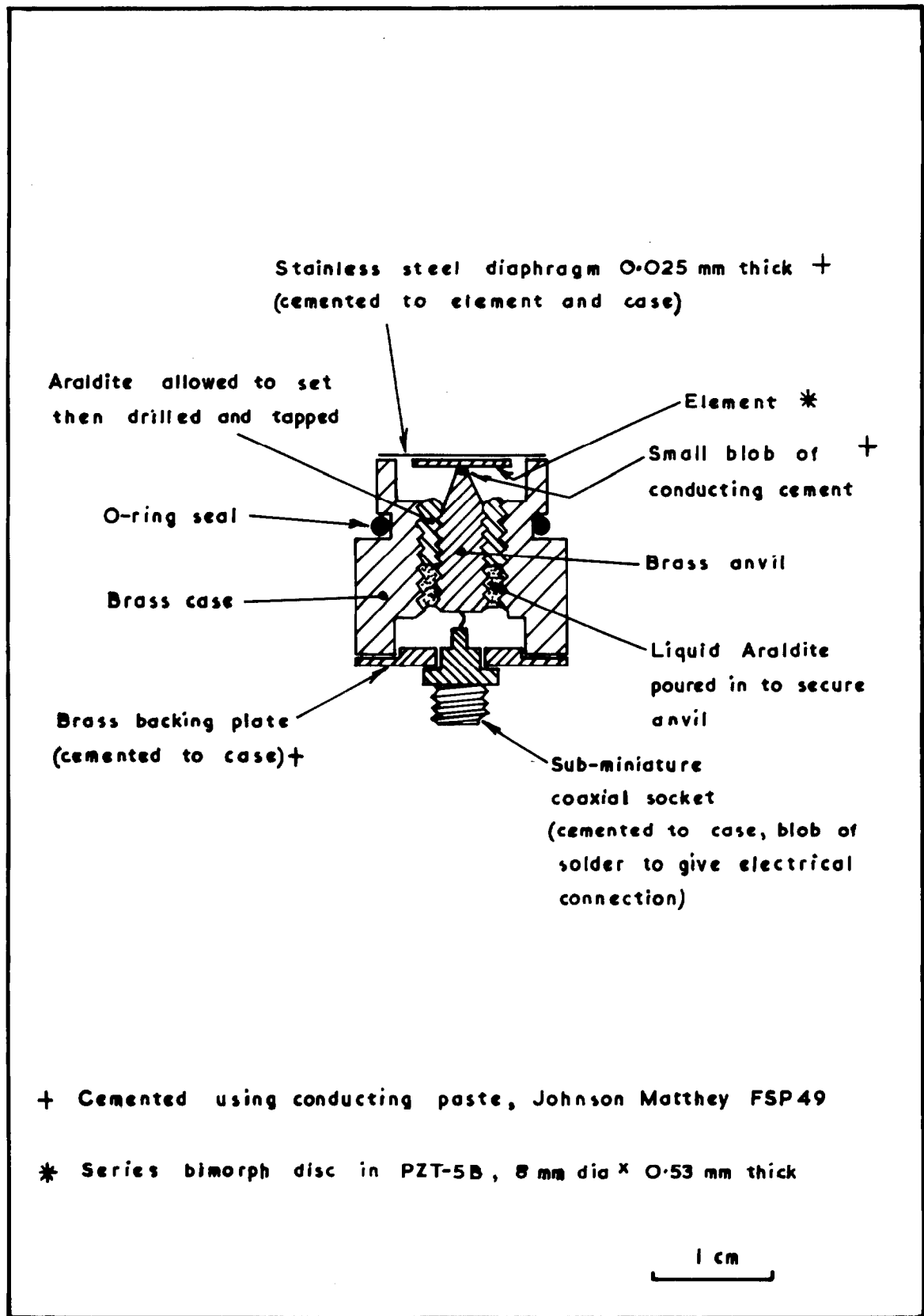
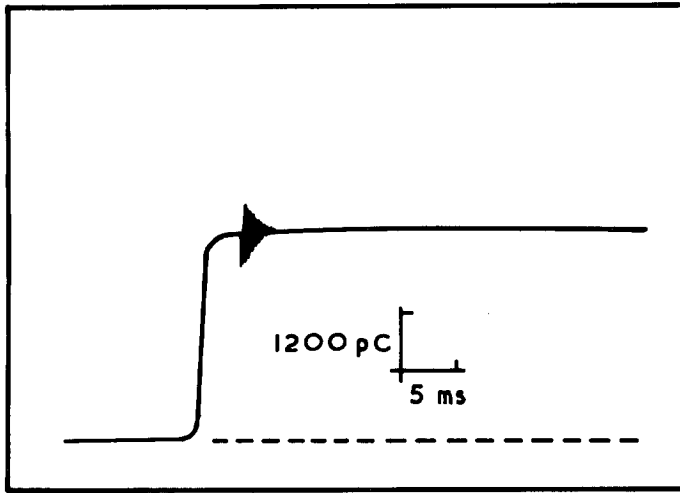
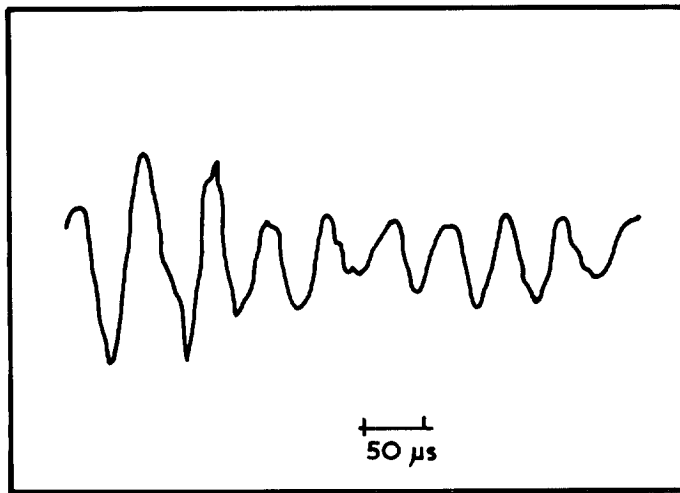


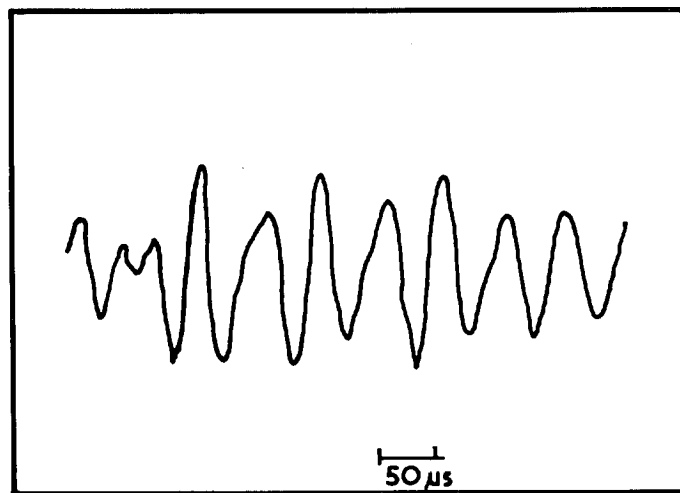
Fig. 21. The type H transducer



$\Delta P = 90 \text{ torr}$   
No filter



Dynamic  
response  
No filter



Dynamic  
response  
No filter

Fig. 22. Typical traces from type H, transducers

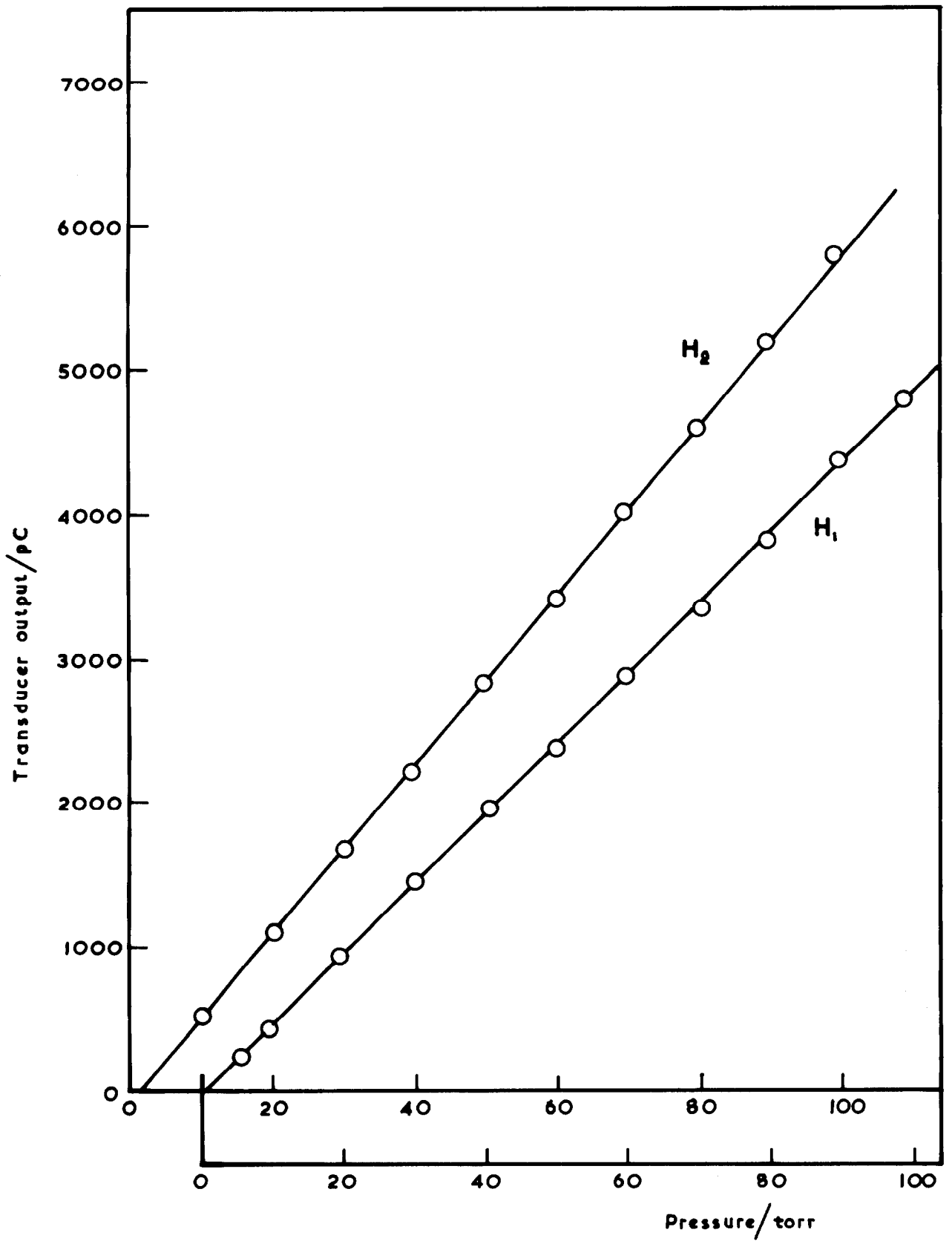


Fig. 23. Calibration of type H transducers

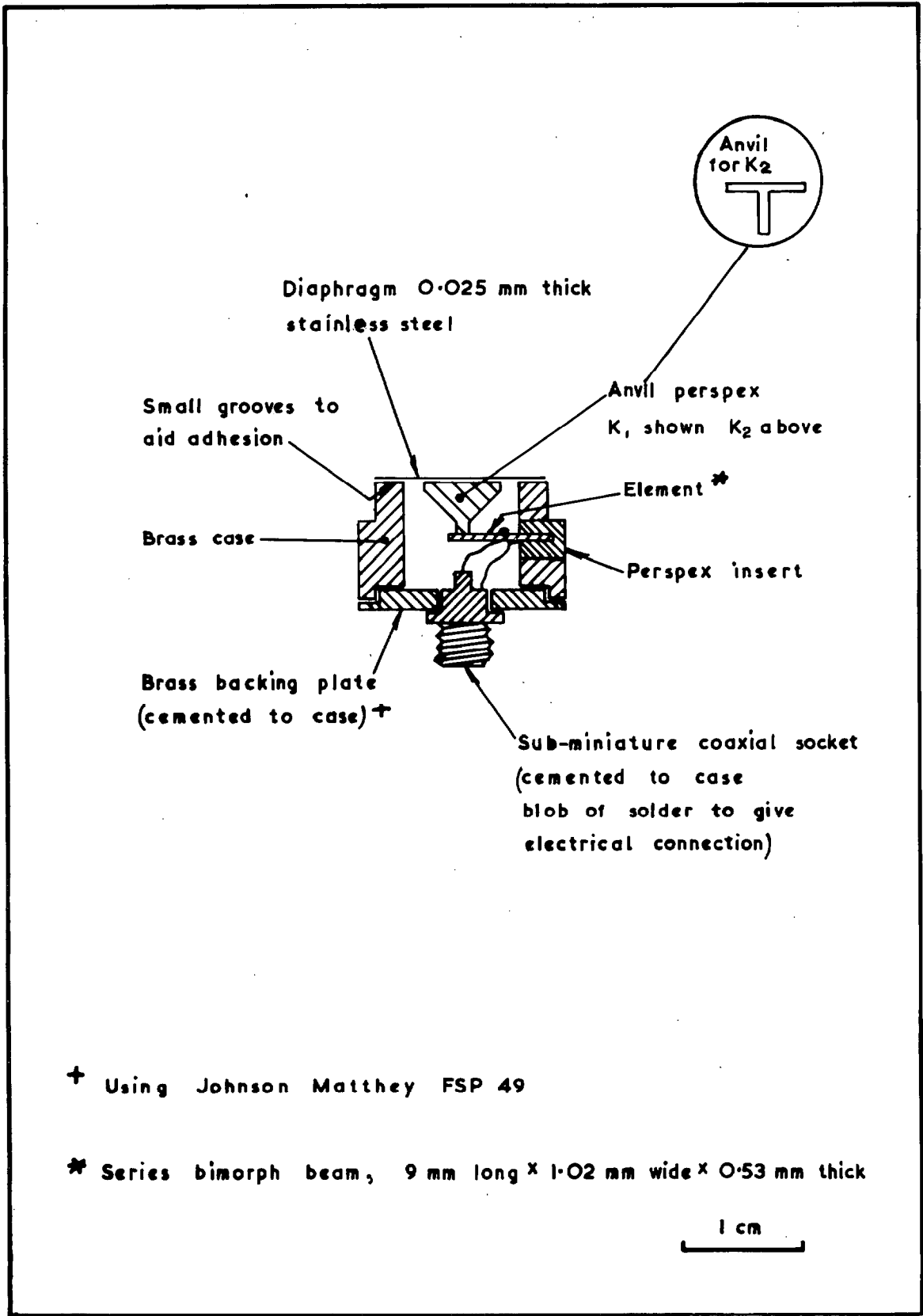
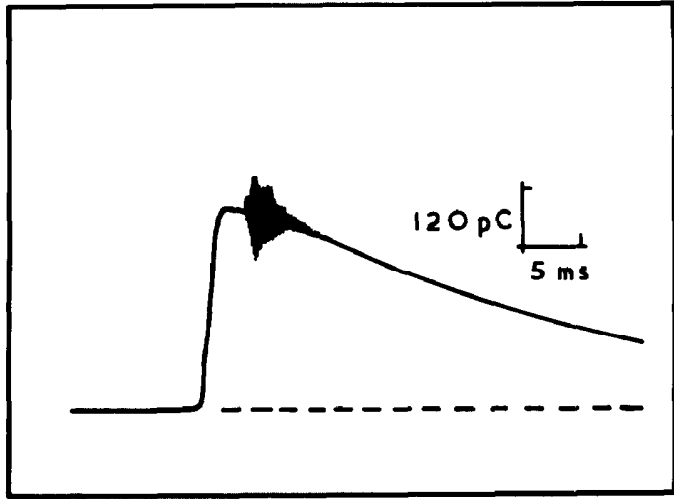
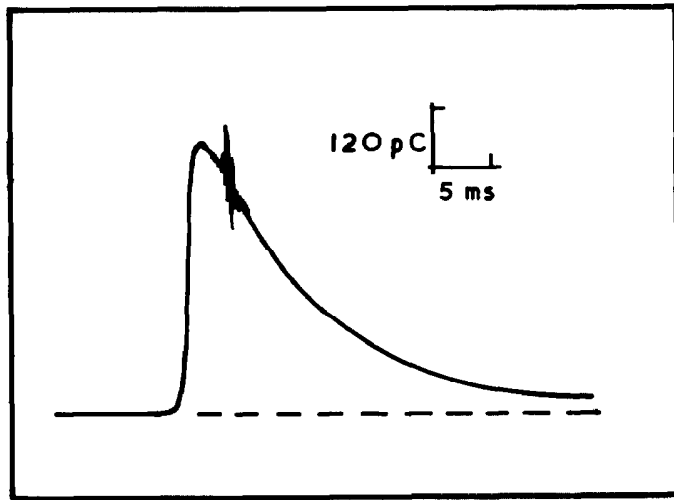


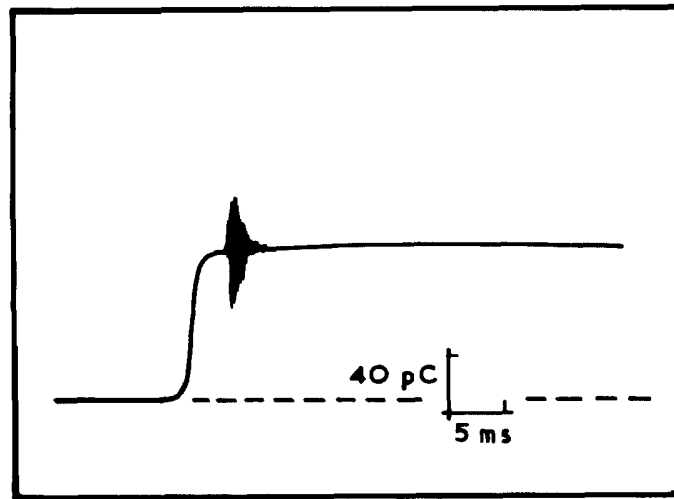
Fig. 24. The type K transducer



Type K<sub>1</sub>  
 $\Delta P = 29$  torr  
 No filter



Type K<sub>8A</sub>  
 $\Delta P = 21$  torr  
 No filter



Type K<sub>23</sub>  
 $\Delta P = 29$  torr  
 No filter

Fig. 25. Typical traces from type K transducers

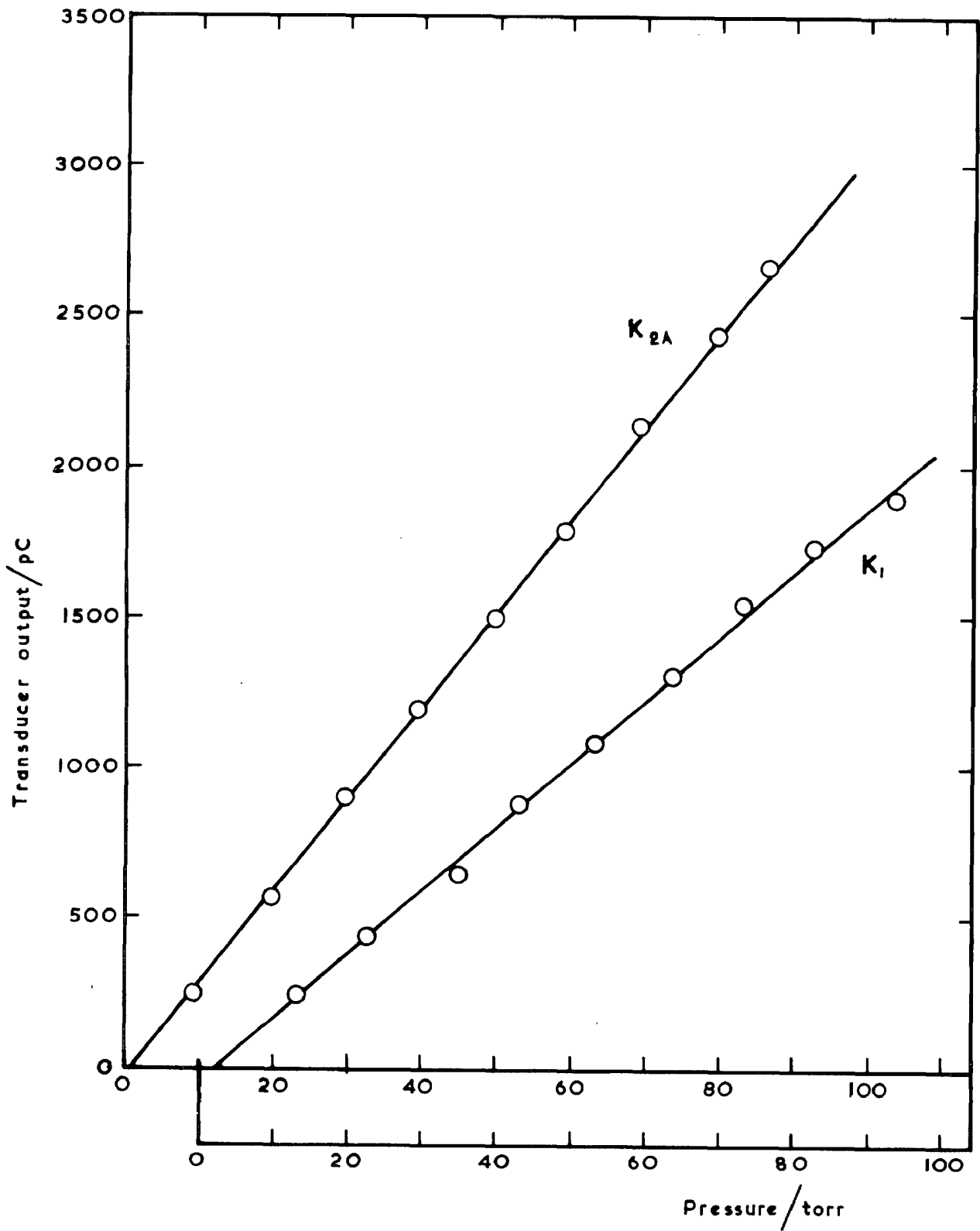


Fig. 26(a). Calibration of type K transducers

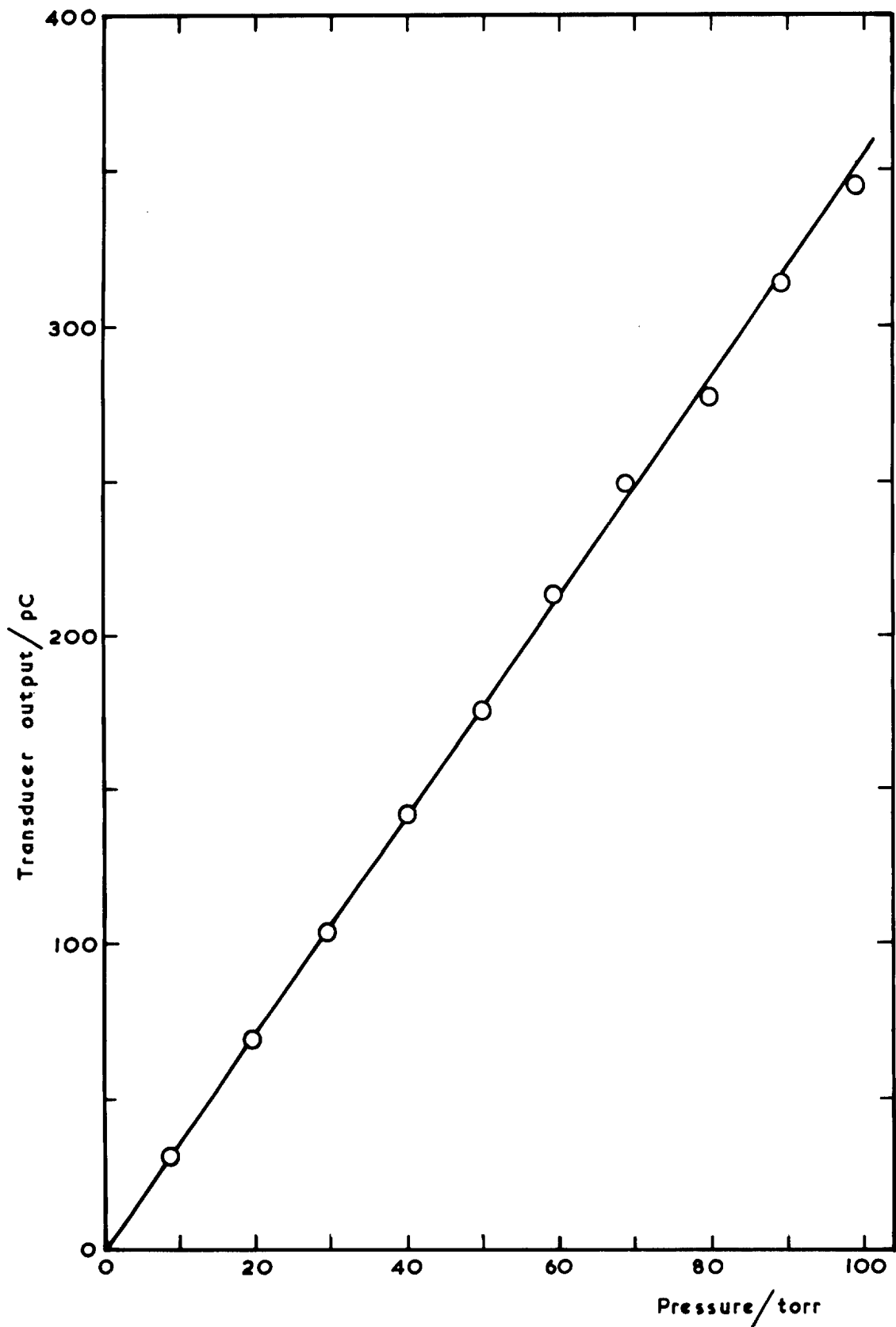
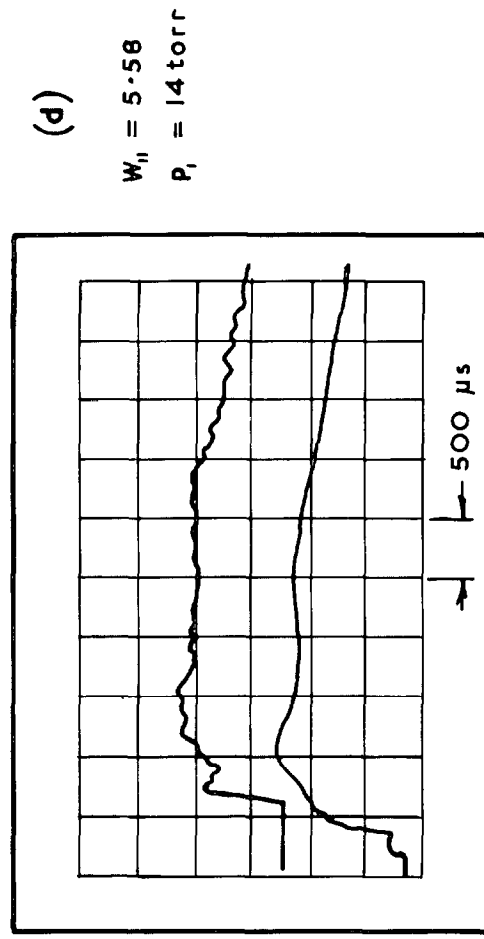
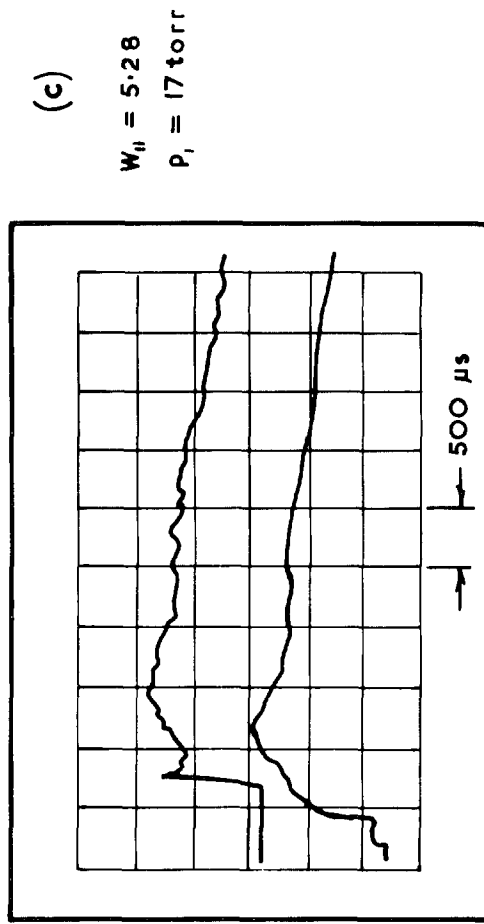
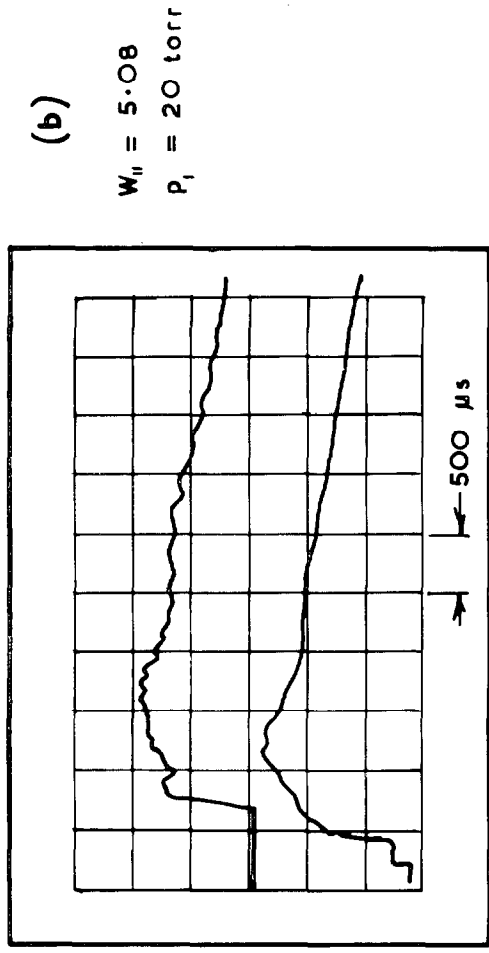
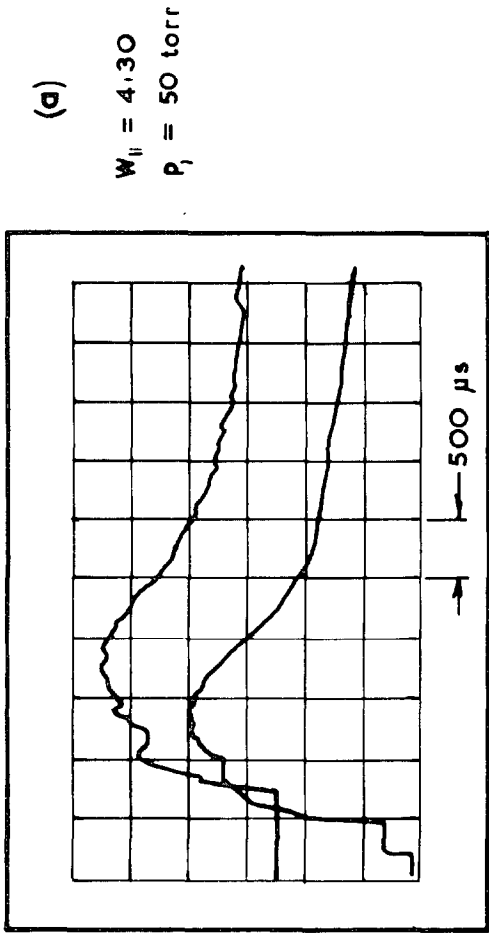
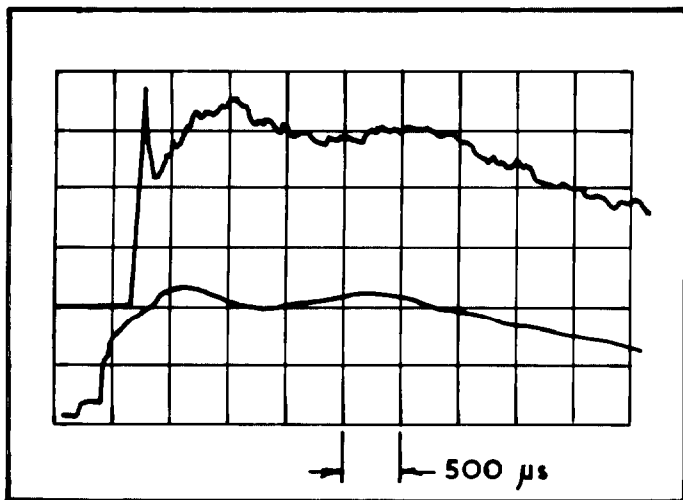


Fig. 26(b). Calibration of type K<sub>23</sub> transducer



Upper traces — pitot pressure — 6.3 torr/division  
 Lower traces — reservoir pressure — 2000 torr/division

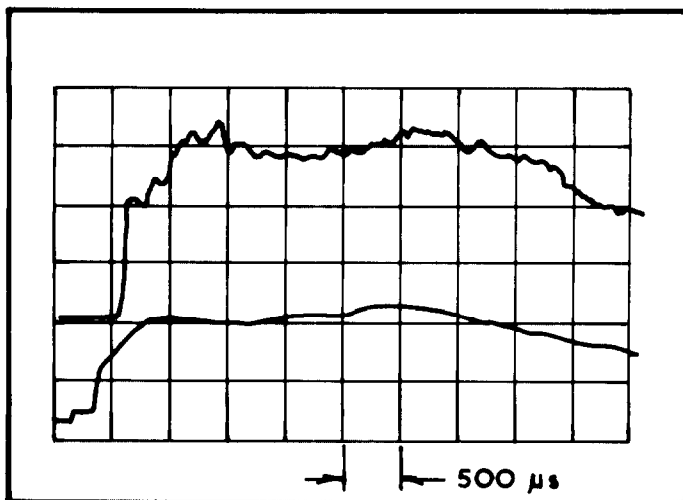
Fig. 27. Pitot pressure in working section using nozzle throat of 12.7 mm dia.



(e)

$$W_{11} = 5.83$$

$$p_1 = 12 \text{ torr}$$



(f)

$$W_{11} = 6.36$$

$$p_1 = 8 \text{ torr}$$

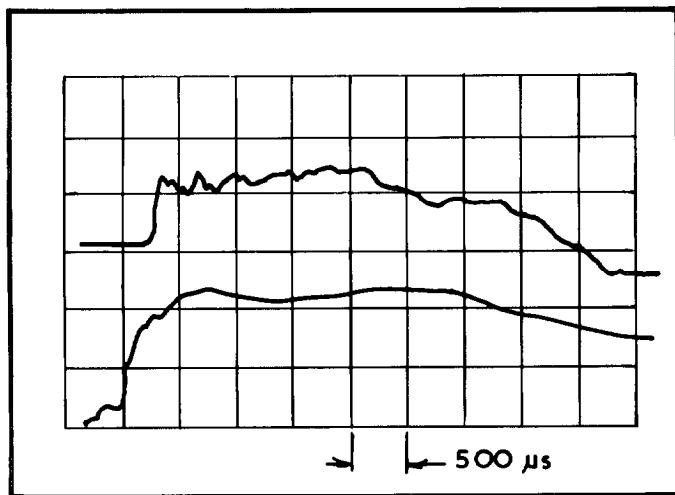
Upper traces — pitot pressure — 3.2 torr/division  
 Lower traces — reservoir pressure — 2000 torr/division

Fig. 27 (cont.).



(a)

Geom. incid. =  $-4^\circ$



(b)

Geom. incid. =  $-4^\circ$

Transducer shielded  
from flow



(c)

Geom. incid. =  $0^\circ$

Upper trace — static pressure on wedge — 0.23 torr/division  
Lower trace — nozzle reservoir pressure — 6800 torr/division

Fig. 28. Static pressure on wedge



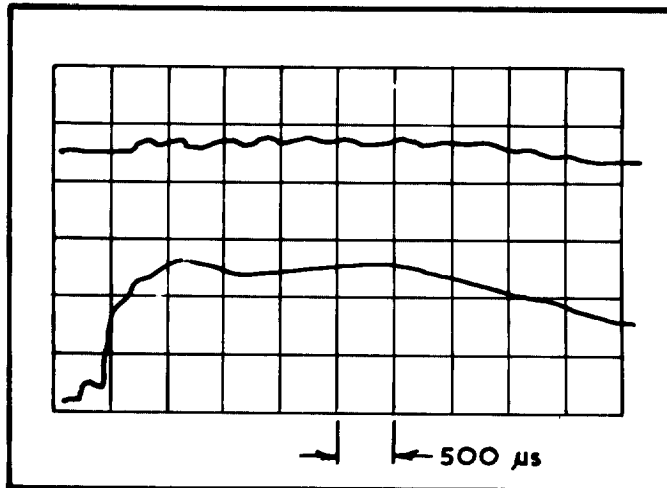
(d)

Geom. incid. =  $+4^\circ$



(e)

Geom. incid. =  $+8^\circ$



(f)

Geom. incid. =  $+8^\circ$

Transducer shielded  
from flow

Upper trace—static pressure on wedge — 0.49 torr/division  
Lower trace—nozzle reservoir pressure — 6800 torr/division

Fig. 28 (cont.).

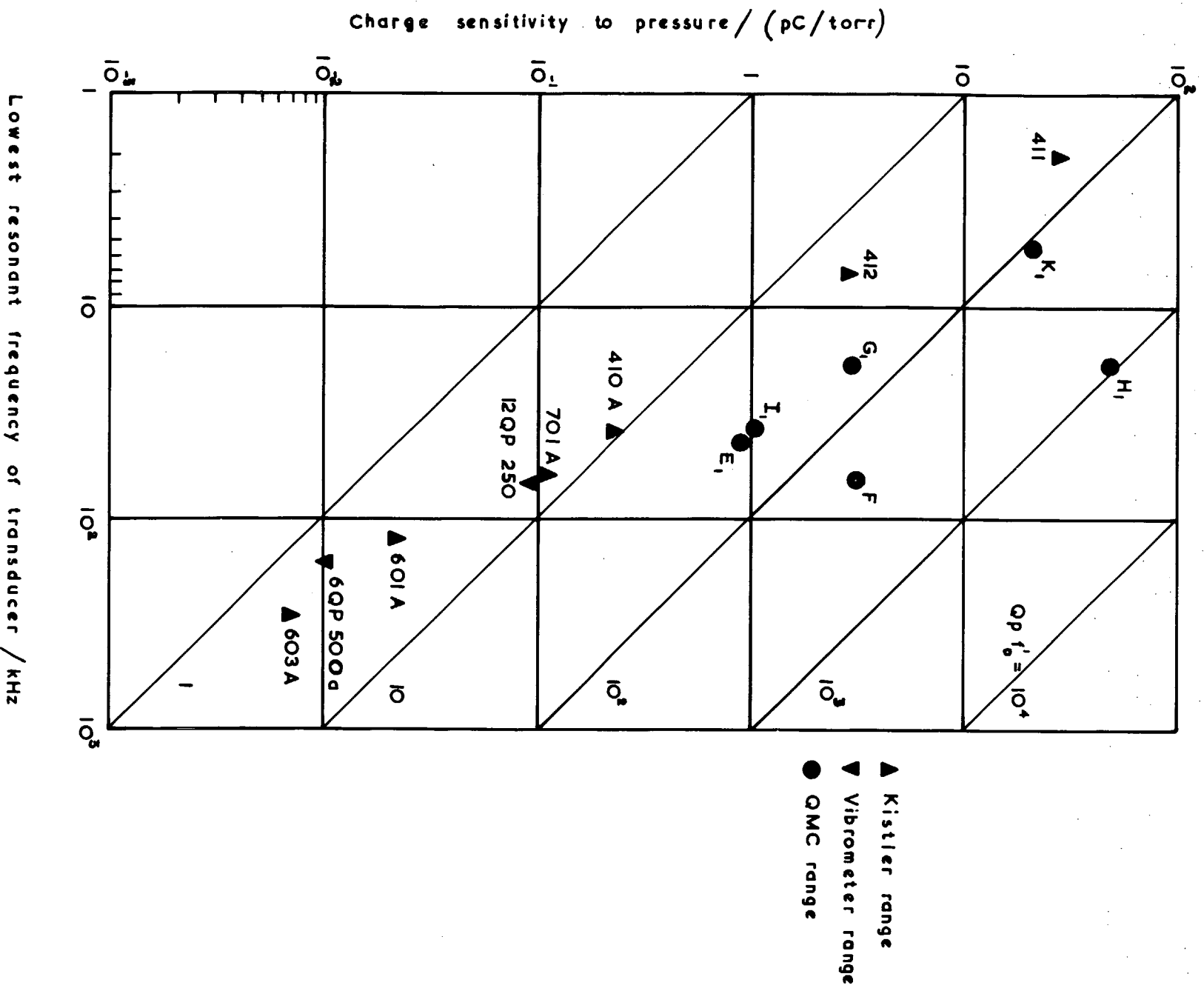


Fig. 29. Comparison of transducers on the basis of charge sensitivity  $\times$  natural frequency

RS35/502109 R4 6/72 P

A.R.C. C.P.No.1219  
September 1969

R. O. Goodchild and  
L. Bernstein

THE DESIGN OF HIGH SENSITIVITY PRESSURE TRANSDUCERS  
FOR USE IN SHOCK-TUNNELS

The theory of piezoelectricity in so far as it relates to pressure sensing elements is briefly outlined and various configurations are compared. The relative merits of charge and voltage amplifiers are discussed and a practical charge amplifier and charge calibrator are described. Both acoustic and electronic filters are considered and the extent to which a filter affects the useful rise-time of a transducer is emphasised. Several prototype transducers using sensing elements in compression, shear or bending were built and calibrated. A sensitivity of 48.9 pC/torr was achieved using a PZT bimorph disc in bending, this transducer having a natural frequency of 19 kHz. Environmental tests in a shock tube and in the hypersonic nozzle of a shock tunnel are also described.

Some brief comparisons with commercial transducers are made.

A.R.C. C.P.No.1219  
September 1969

R. O. Goodchild and  
L. Bernstein

THE DESIGN OF HIGH SENSITIVITY PRESSURE TRANSDUCERS  
FOR USE IN SHOCK-TUNNELS

The theory of piezoelectricity in so far as it relates to pressure sensing elements is briefly outlined and various configurations are compared. The relative merits of charge and voltage amplifiers are discussed and a practical charge amplifier and charge calibrator are described. Both acoustic and electronic filters are considered and the extent to which a filter affects the useful rise-time of a transducer is emphasised. Several prototype transducers using sensing elements in compression, shear or bending were built and calibrated. A sensitivity of 48.9 pC/torr was achieved using a PZT bimorph disc in bending, this transducer having a natural frequency of 19 kHz. Environmental tests in a shock tube and in the hypersonic nozzle of a shock tunnel are also described.

Some brief comparisons with commercial transducers are made.

A.R.C. C.P.No.1219  
September 1969

R. O. Goodchild and  
L. Bernstein

THE DESIGN OF HIGH SENSITIVITY PRESSURE TRANSDUCERS  
FOR USE IN SHOCK-TUNNELS

The theory of piezoelectricity in so far as it relates to pressure sensing elements is briefly outlined and various configurations are compared. The relative merits of charge and voltage amplifiers are discussed and a practical charge amplifier and charge calibrator are described. Both acoustic and electronic filters are considered and the extent to which a filter affects the useful rise-time of a transducer is emphasised. Several prototype transducers using sensing elements in compression, shear or bending were built and calibrated. A sensitivity of 48.9 pC/torr was achieved using a PZT bimorph disc in bending, this transducer having a natural frequency of 19 kHz. Environmental tests in a shock tube and in the hypersonic nozzle of a shock tunnel are also described.

Some brief comparisons with commercial transducers are made.

A.R.C. C.P.No.1219  
September 1969

R. O. Goodchild and  
L. Bernstein

THE DESIGN OF HIGH SENSITIVITY PRESSURE TRANSDUCERS  
FOR USE IN SHOCK-TUNNELS

The theory of piezoelectricity in so far as it relates to pressure sensing elements is briefly outlined and various configurations are compared. The relative merits of charge and voltage amplifiers are discussed and a practical charge amplifier and charge calibrator are described. Both acoustic and electronic filters are considered and the extent to which a filter affects the useful rise-time of a transducer is emphasised. Several prototype transducers using sensing elements in compression, shear or bending were built and calibrated. A sensitivity of 48.9 pC/torr was achieved using a PZT bimorph disc in bending, this transducer having a natural frequency of 10 kHz. Environmental tests in a shock tube and in the hypersonic nozzle of a shock tunnel are also described.

Some brief comparisons with commercial transducers are made.

DETACHABLE ABSTRACT CARDS





© Crown copyright 1972

HER MAJESTY'S STATIONERY OFFICE

*Government Bookshops*

49 High Holborn, London WC1V 6HB  
13a Castle Street, Edinburgh EH2 3AR  
109 St Mary Street, Cardiff CF1 1JW  
Brazenose Street, Manchester M60 8AS  
50 Fairfax Street, Bristol BS1 3DE  
258 Broad Street, Birmingham B1 2HE  
80 Chichester Street, Belfast BT1 4JY

*Government publications are also available  
through booksellers*